Naučnom Veću

Instituta za fiziku

Predmet: reizbor u zvanje istraživač saradnik

Molim Naučno veće da pokrene postupak za moj reizbor u zvanje istraživač saradnik.

Prilažem:

- Potpisani zahtev za pokretanje postupka
- Biografiju
- Mišljenje rukovodioca projekta sa predlogom komisije
- Kratak pregled naučne aktivnosti
- Spisak objavljenih radova
- Kopije objavljenih radova
- Potvrdu o upisanim doktorskim studijama
- Potvrdu o proseku na osnovim studijama
- Potvrdu o prihvaćenoj temi disertacije

Kosta Spasić

Biografija kandidata

Spasić Kosta rođen je u Beogradu 11.08.1984. godine. Fizički fakultet - smer Primenjena fizika i informatika završio je na Univerzitetu u Beogradu 2010. godine. Od 1.1.2011. godine je u stalnom ranom odnosu u Institutu za Fiziku u Beogradu.

Diplomski rad na temu "Aktivacija Langmuirove sonde i merenje koncentracije elektrona i jona u niskotemperaturnim plazmama u argonu" uradio je u Laboratoriji za gasnu elektroniku pod rukovodstvom prof. dr. Zorana Lj. Petrovića i dr. Nevene Puač i odbranio ga u decembru 2010. godine na Fizičkom fakultetu u Beogradu. Doktorske studije je upisao sledeće godine na Fizičkom faukultetu Univerziteta u Beogradu - smer "Fizika jonizovanog gasa, plazme i tehnologija plazme". 28.5.2013. izabran je u zvanje istraživač saradnik

Kosta Spasić ima publikovana tri rada u vrhunskim međunarodnim časopisima i dva u međunarodnom tematskom zborniku. Bio je koautor na nekoliko međunarodnih predavanja i rezultati njegovog rada su prezentovani na više međunarodnih konferencija.

Molim Naučno veće Instituta za fiziku

da pokrene postupak za reizbor Koste Spasića u zvanje istraživač saradnik. Kolega Spasić je 2010. diplomirao Primenjenu fiziku i informatiku na Fizičkom fakultetu Univerziteta u Beogradu na temu "Aktivacija Langmuirove sonde i merenje koncentracije elektrona i jona u niskotemperaturnim plazmama u argonu". Godine 2011. je upisao je doktorske studije na Fizičkom fakultetu Univerziteta u Beogradu – smer Fizika jonizovanog gasa, plazme i tehnologija plazme. Objavio je tri rada u vrhunskim međunarodnim časopisima, dva rada u međunarodnim tematskim zbornicima, njegovi rezultati su predstavljeni na više međunardonih konferencija i zadovoljio je sve zahteve za reizbor u zvanje istraživač saradnik.

Kolega Spasić je angažovan na dva projekta instituta za fiziku: III41011 „Primene niskotemperaturnih plazmi u biomedicini, zaštiti čovekove sredine i nanotehnologijama" i ON171037 „Fundamentalni procesi i primene transporta čestica u neravnotežnim plazmama, trapovima i nanostrukturama".

Njegov dosadašnji rad je pokazao da ima izvanredne sposobnosti potrebne za aktivno bavljenje naučnoistraživačkim radom.

Za komisiju predlažem:

1) Naučni savetnik Dr Nevena Puač
2) Naučni savetnik Dr Gordana Malović
3) Redovni profesor Dr Srđan Bukvić

Uz poštovanje,

Dr Nevena Puač

rukovodilac projekta III41011 MNTRS

Beograd, 21.05.2019.

Kratak pregled naučne aktivnosti kandidata Koste Spasića

Nakon diplomiranja kolega Spasić je nastavio rad u Laboratoriji za gasnu elektroniku u više pravaca. On se u okviru svog rada u ovoj Laboratoriji bavi proučavanjem i primenama radiofrekventnih pražnjenja na niskim pritiscima. Jedan od glavnih zadataka kolege Spasića je karakterizacija, optimizovanje i usavršavanje asimetričnog plazma sistema velike zapremine. Zahvaljujući stabilnosti i blagoj prirodi kapacitivno spregnute plazme, ovakva eksperimentalna postavka predstavlja prototip uređaja za industrijsko tretiranje osetljivih uzoraka koji mogu da izdrže vakuum. U tom smislu, jedan od ciljeva dijagnostikovanja ovakvog pražnjenja, sa nekoliko dijagnostičkih metoda, je bio nalaženje optimalnih parametara pogodnih za tretman različitih vrsta uzoraka.

Vršena su merenja koncentracije jona i elektrona, kao i plazma potencijala pomoću Langmuirove sonde sa mogućnošću pomeranja duž ose merenja i odgovarajućeg softvera za kontrolu uređaja i obradu podataka. Kolega Spasić je, sem Langmirove sonde, koristio derivativne sonde za proučavanje strujno naponskih karakteristika pražnjenja, kao i za određivanje snage koja je predata plazmi. Snaga predata plazmi je jedan od glavnih parametara kojim se karakterišu RF pražnjenja pošto se ona značajno razlikuje od nominalne snage date izvorom napajanja. Kao treću dijagostičku metodu kolega Spasić je koristio katalitičke sonde koje služe za određivanje koncentracije atoma (kiseonik) u plazmi i ova merenja su urađena u sklopu bilateralne saradnje sa kolegama sa Instituta Jožef Štefan iz Ljubljane. Pored već navedenih metoda kolega Spasić je radio i na ispitivanju sastava plazme maseno-energijskim spektrometrom. Ova merenja su važna jer se njima osim hemijskog sastava plazme mogu dobiti i informacije o prisustvu pobuđenih atoma i molekula koji imaju važnu ulogu u tretmanu tekstila i semena. U paraleli se radi na dijagnostici pražnjenja primenom aktinometrije pomoću iCCD kamere. Sa ciljem diversifikacije istraživanja i provere uticaja ralzičitih vrsti plazme na uzorke, konstruisana je i puštena je u rad planparalelna komora u kojoj je moguće postići nešto intenzivnije uslove pražnjenja. Sa aspekta primena ovakvih pražnjenja, rađen je tretman semena u cilju postizanja veće klijavosti i bržeg rasta biljaka, kao i sterilizacije semena. Takođe je rađen tretman tekstila radi aktivacije površine i povećanja kapaciteta za adsorpciju različitih tipova mikrokapsula koje mogu da služe za detekciju UV zračenja, osetljive su na toplotu, baktericidne ili, što je nejinteresantnije u slučaju modne industrije, imaju određenu mirisnu notu koja se oslobađa tokom vremena.

Списак референци за кандидата – Коста Спасић

М14

Монографска студија у тематском зборнику међународног значаја:

1. Z. Lj. Petrović, N. Puač, S. Lazović, D. Maletić, K. Spasić and G. Malović, *"Biomedical applications and diagnostics of atmospheric pressure plasma"*, Journal of Physics:ConferenceSeries 356 (2012) 012001, doi: 10.1088/1742-6596/356/1/012001

2. M. Dimitrova, Tsv. Popov, N. Puač, N. Škoro, K. Spasić, G. Malović, F. M. Dias and Z. Lj. Petrović, *„Radial profile of the electron energy distribution function in RF capacitive gas-discharge plasma"*, Journal of Physics: Conference Series 700 (2016) 012007 doi:10.1088/1742-6596/700/1/012007

М21

Рад у врхунском међународном часопису:

1. Saša Lazović, NevenaPuač, Kosta Spasić, Gordana Malović, Uroš Cvelbar, Miran Mozetič, Maja Radetić and Zoran Lj Petrović, "Plasma properties in a large – volume, cylindrical and asymmetric radio-frequency capacitively-coupled industrial-prototype reactor", **Journal of Physics. D: Applied Physics, 46 (7)** 075201**, 2013,** doi:10.1088/0022-3727/46/7/075201

2. Gorjanc M, Mozetič M, Primc G, Vesel A, Spasić K, Puač N, Petrović ZL, Kert M. "Plasma treated polyethylene terephthalate for increased embedment of UV-responsive microcapsules", **Applied Surface Science**. **2017** Oct 15;419:224-34., doi:10.1016/j.apsusc.2017.04.177

3. Puač N, Škoro N, Spasić K, Živković S, Milutinović M, Malović G, Petrović ZL. Activity of catalase enzyme in Paulownia tomentosa seeds during the process of germination after treatments with low pressure plasma and plasma activated water. **Plasma Processes and Polymers**. **2018** Feb;15(2):1700082.

М32

Предавање по позиву са међународног скупа штампано у изводу:

1. Diagnostics and applications of high frequency discharges, N. Puač, M. Miletić, S. Mojsilović, S. Lazović, D. Maletić, K. Spasić, G. Malović, D. Bugarski, P. Milenković and Z.Lj. Petrović 39th EPS conference on Plasma Physics, 2-6 July 2012, Stockholm, Sweden

М33

Саопштење са међународног скупа штампано у целини:

1. Z.Lj. Petrović, N. Puač, D. Marić, D. Maletić, K. Spasić, N. Škoro, J. Sivoš, S. Lazović, G. Malović, *" Development of Biomedical Applications of*

Nonequilibrium Plasmas and Possibilities for Atmospheric Pressure Nanotechnology Applications", PROC. 28th International Conference On Microelectronics (MIEL 2012), Niš, Serbia, 13-16 May, 2012

2. S. Lazović, K. Spasić, N. Puač, G. Malović, U. Cvelbar, M. Mozetič, Z. LJ. Petrović, „*Spatial profiles of atomic oxygen concentrations in a large scale CCP reactor*", ESCAMPIG XXI, Viana do Castelo, Portugal, July 10-14 2012

3. Kosta Spasić, Saša Lazović, Nevena Puač, Zoran Lj Petrović, Gordana Malović, Miran Mozetič and Uroš Cvelbar, „Catalytic probe measurements of atomic oxygen concentration in large volume oxygen CCP" 26th SPIG, Zrenjanin, Serbia, August 27-31 2012

4. Saša Lazović, Nevena Puač, Kosta Spasić, Gordana Malović, Uroš Cvelbar, Miran Mozetič and Zoran Lj. Petrović, "Diagnostics of a large scale CCP reactor suitable for textile tretments", 4th ICAPT, Strunjan, Slovenia, EU, September 9-13 2011

5. S. Lazović, N. Puač, K. Spasić, G. Malović, U. Cvelbar, M. Mozetič, Z. Lj. Petrović, „Measurements of atomic oxygen concentrations in a large scale asymmetric capacitively coupled plasma reactor by using catalytic probes", 30th ICPIG, August 28th – September 2nd 2011, Belfast, Northern Ireland, UK

6. K. Spasić, N. Škoro, N. Puač, G. Malović and Z. Lj. Petrović, „Reactive species production in oxygen low-pressure RF plasma suitable for treatment of sensitive surfaces", 3rd CEAMPP, August 25th 2013, Belgrade, Serbia

7. I. Filatova, V. Azharonok, V. Lushkevich, A. Zhukovsky, K. Spasić, S. Živković, N. Puač, S. Lazović, G. Malović and Z.Lj.Petrović, „Plasma seeds treatment as a promising technique for seed germination improvement", 31st ICPIG, 14-19 July 2013, Granada, Spain

8. N. Škoro*, K. Spasić, N. Puač, G. Malović AND Z. LJ. Petrović, „Diagnostics of low-pressure rf oxygen plasma suitable for treatment of sensitive surfaces", 20th International Conference on Gas Discharges and their Applications, 6th - 11th July 2014, Orleans, France

9. K, Spasić, N. Škoro, N. Puač, G. Malović, Z. Lj. Petrović, „Ion energy distribution and line intensities in asymmetrical oxygen rf discharge", August 26th – 29th 2014, Belgrade, Serbia

10. K. Spasić, N. Puač, N Škoro, G. Malović and Z.Lj. Petrović, „Characterization of a large volume oxygen RF discharge suitable for low-pressure treatment of sensitive samples", 32nd ICPIG, July 26th-31st, 2015, Iași, Romania

11. Spasić Kosta, Škoro Nikola, Puač Nevena, Malović Gordana, and Petrović Lj Zoran, "Production of active oxygen species in low pressure CCP used for sterilization of commercial seeds." 2015 IEEE International Conference on Plasma Sciences (ICOPS). IEEE, 2015, may 24-28, Belek, Antalya, Turkey

12.

M34
Саопштење са међународног скупа штампано у изводу:

1. Sasa Lazovic, Kosta Spasic Nevena Puac and Gordana Malovic, „Catalytic probe measurements in a large scale CCP reactor", 64th GEC, Salt Lake City, Utah, USA, November 2011

2. Saša Lazović, Nevena Puač, Kosta Spasić, Gordana Malović and Zoran Lj. Petrović, „Characterization of a large scale RF CCP reactor using Langmuir and derivative probes", 20th ISPC, Philadelphia, USA, July 24-29, 2011

3. Saša Lazović, Nevena Puač, Kosta Spasić, Gordana Malović, Zoran Lj. Petrović, Uroš Cvelbar, Miran Mozetič, „Probe diagnostics of a large scale asymmetric capacitively coupled plasma plasma reactor", 18th Inernational scientific meeting on vacuum science and techniques, Bohinjsko Jezero, Slovenia, EU, June 2-3 2011

4. S. Lazović, N. Puač, K. Spasić, G. Malović, Z. L. Petrović, „Langmuir probe measurements of a large scale RF CCP reactor", 2nd International workshop on plasma nano-interfaces and plasma characterization, Cerklje, Slovenia, EU, March 1-4, 2011

5. K. Spasić, N. Škoro, N. Puač, G. Malović and Z. Lj. Petrović, „Atomic species produced in large scale oxygen plasma used for treatments of sensitive materials", 66th Annual Gaseous Electronics Conference, Princeton, New Jersey, USA September 30 - October 4, 2013.

6. N. Puač, K. Spasić, N. Škoro, M. Gorjanc, G. Malović and Z Lj Petrović, "Optical Emission Diagnostics of N2 plasma used for textile pretreatment", ESCAMPIG XXIII, Bratislava, Slovakia, July 12-16, 2016

7. N Skoro, N Puac, K Spasic, G Malovic, M Gorjanc, Z Lj Petrovic, „Optical emission spectroscopy of OH lines in N2 and Ar plasmaduring the treatments of cotton fabric", 69th GEC, October 10-14, 2016, Bochum, Germany

8. Z.Lj. Petrović, N. Puač, G. Malović, N. Selaković, K. Spasić, D. Maletić, S. Živković, „Diagnostics of atmospheric pressure plasma jets and plasma needle and their application in biology and medicine", GEM 2016, Geelong, Australia, February 14-17, 2016.

9. N. Puač, N. Škoro, K. Spasić, S. Živković P, M. Milutinović, V. Šašić G. Malović and Z.Lj. Petrović, "Activity of catalase enzyme in *P. tomentosa* seeds after direct plasma treatments and treatments with plasma activated water", XXXIII ICPIG, July 9-14, 2017, Estoril/Lisbon, Portugal

10. Nevena Puač, Nikola Škoro, Kosta Spasić, Suzana Živković, Milica Milutinović, Gordana Malović and Zoran Lj. Petrović, "Activity of Catalase Enzyme in Paulownia Tomentosa Seeds as a Result of a Direct and Indirect Treatment by the Non-Equilibrium Plasma", JSPP2017, 4-7 december 2017, Osaka, Japan.

11. N. Škoro, N. Puač, K. Spasić, M. Gorjanc, G. Malović and Z. Lj. Petrović, "Monitoring of the cotton fabric plasma treatments by using optical emission spectroscopy", XII FLTPD, April 23th—27th 2017, Zlatibor, Serbia

12. K Spasić, N Škoro, N Puač, G Malović, Z Lj. Petrović, "Volume Scaling in Production of Active Oxygen Species in an Asymmetrical Plasma Reactor", GD2018, september 2-7, 2018, Novi Sad, Serbia
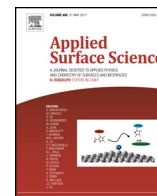
Full Length Article

Plasma treated polyethylene terephthalate for increased embedment of UV-responsive microcapsules

Marija Gorjanc [a,*], Miran Mozetič [b], Gregor Primc [b], Alenka Vesel [b], Kosta Spasić [c], Nevena Puač [c], Zoran Lj. Petrović [c], Mateja Kert [a]

[a] University of Ljubljana, Faculty of Natural Sciences and Engineering, Aškerčeva 12, SI-1000 Ljubljana, Slovenia
[b] Jozef Stefan Institute, Jamova 39, SI-1000 Ljubljana, Slovenia
[c] Institute of Physics of Belgrade, Pregrevica 118, 11080 Zemun, Serbia

ABSTRACT

Polyethylene terephthalate (PET) fabric was treated in a late afterglow of plasma created by a microwave (MW) discharge in the surfatron mode, by using oxygen (O_2) and ammonia (NH_3) gases. The series of treatments using one gas or the combination of both at different treatment times were performed in order to increase the embedment of UV-responsive microcapsules that were deposited onto PET with pad-dry-cure process. Plasma in both gases was characterized by optical emission spectroscopy (OES), which showed substantial dissociation of O_2 and NH_3 molecules as well as formation of NH_x radicals due to the partial dissociation of ammonia molecules. The chemically active species in the plasma afterglow changed the surface properties of PET that were analysed using X-ray photoelectron spectroscopy (XPS), time-of-flight secondary ion mass spectrometry (ToF–SIMS), Fourier transform infrared spectroscopy (FTIR), scanning electron microscopy (SEM) and water absorption analysis. The effectiveness of plasma treatment on embedment of UV-responsive microcapsules on PET was evaluated by UV-responsiveness, colour strength and colour depth using reflectance spectroscopy, add-on and air permeability, respectively. Treating PET by O_2 afterglow followed by a longer treatment by NH_3 afterglow increased the polymers hydrophilicity and concentration of nitrogen-rich functional groups on surface that enabled higher uptake of UV-responsive microcapsules, and consequently better responsiveness of fabric to UV radiation. The add-on of microcapsules was almost 8-times higher and the colour depth increased up to 75% for plasma treated samples.

© 2017 Elsevier B.V. All rights reserved.

1. Introduction

One of the main concerns regarding a decrease in stratospheric ozone is the consequential increase in the amount of ultraviolet (UV) radiation, which is harmful for human health and ecosystems [1–3]. Accordingly, different ultraviolet (UV) radiation sensors have been proposed with the growing interest in the research of developing flexible, textile-based UV sensors [4–6]. Due to the phase-change that photochromic dyes undergo when exposed to UV light, which is from colourless to coloured, they are considered suitable to be used as UV sensors [7–9]. When the source of UV radiation is removed, the photochromic dye reverts to its original state. Since photochromic dyes have poor stability to the environmental factors such as oxygen, pH value, light and temperature, which lead to the oxidation and deterioration, it is preferable to use them in the form of microcapsules [10,11]. One of the promising polymers that could be used as a carrier of photochromic microcapsules is polyethylene terephthalate (PET), which has high tensile strength, stability and resistance to many chemicals, environmental conditions and UV radiation [12]. PET textile with integrated UV-responsive microcapsules would be a simple and user-friendly smart protection. However, the hydrophobic nature of PET results in poor uptake and adhesion of dyes, particles and microcapsules [13–16]. The solution to the problems associated with low absorptiveness and high hydrophobicity of PET is a use of plasma [17–20] to functionalise surfaces of fibres.

Plasma technology is a dry process, which modifies the surface of polymers without changing their bulk properties. According to the desired surface properties of the polymers, it is very important to choose the right discharge parameters [21]. By changing the type of gas, gas flow, power transmitted to the plasma and treatment time one can tune the effects of plasma chemistry on the

---

* Corresponding author.
  E-mail address: marija.gorjanc@ntf.uni-lj.si (M. Gorjanc).

treated surface. For example, when hydrophilic character is desired, the polar functional groups should be introduced by oxygen, air, ammonia or nitrogen discharge gas. The nature and/or concentration of the active species created in plasma depend mostly on the chosen discharge-forming gas [22,23]. The solution to increase the hydrophilic nature of PET is to treat it with oxygen plasma [24–26]. However, for uptake of anionic dyes onto textiles it is preferable that the surface of the material contains amine-containing reactive functional groups [27–29]. Several studies on incorporation of amine-containing groups onto surface of PET by using plasma were conducted with gases such as nitrogen and ammonia, and combination of nitrogen/ammonia or ethylene/ammonia [20,30,31]. Using NH_3 plasma on PET incorporates mainly hydroxyl and amine groups, while using N_2 plasma incorporates manly carboxylic groups [31]. Treatment of PET films with a combination of N_2/H_2 plasma incorporates higher concentration of nitrogen-containing groups (4.2%) than treatment with NH_3 plasma (2.5%) [32]. However, the treatment with NH_3 plasma resulted in more stable functionalisation of the PET surface. Kolar et al. [33] treated PET films with NH_3 and N_2 plasma, combination of NH_3/Ar plasma and combination of N_2/H_2 plasma. In all cases, the surface of PET was functionalized by nitrogen, the highest when PET was treated with NH_3 plasma (10.6%) and lowest when it was treated with N_2 plasma (2.9%). The density of amino-anchor points was high enough to allow covalent bonding of heparin, an anionic anticoagulant. Salem et al. [29] tried two approaches to increase the uptake of anionic dye onto PET fabric. In the first approach, nitrogen-containing groups were incorporated using NH_3 plasma. In the second approach surface of the PET was first treated with oxygen plasma to introduce negatively charged groups as anchors for cationic polyelectrolyte. It was found that the second approach was more successful in increasing the uptake of anionic dye onto PET.

The objective of present work was to investigate combination of surface treatments of PET fabric by oxygen and ammonia plasma, with an aim to increase the uptake of anionic photochromic microcapsules onto fabric and consequently to increase its UV-responsiveness. The findings of this research could be further used for production of smart and flexible UV sensors.

2. Experimental

2.1. Materials

Polyethylene terephthalate (PET) bleached fabric, UV-responsive microcapsules containing photochromic dye ITOFINISH UV and binder ITOBINDER AG (LJ SPECIALITIES LTD.) were used. ITOFINISH UV is a light sensitive coloured dye giving reversible colour change due to the effect of the UV light. ITOBINDER AG is water based emulsion of acrylic polymer.

2.2. Surface functionalization

Polymer samples were treated in a late afterglow of plasma created by using a microwave (MW) plasma source in the surfatron mode. The plasma source was mounted onto a glass vacuum chamber 30 L in volume. The processing chamber was pumped by a two-stage rotary pump of nominal pumping speed $60\,m^3/h$. The pressure was measured with an absolute gauge attached to the processing chamber. Oxygen and ammonia of purity 99.99% were introduced separately into the processing chamber through flow controllers and the discharge tubes. Samples were placed into the center of the processing chamber, but slightly off the main stream of gas flow. After placing a sample, the processing chamber was evacuated to the ultimate pressure which was about 3 Pa. When the ultimate pressure was reached (about a minute of pumping)

the flow of gases was adjusted using a flow meter for oxygen and a precise needle valve for ammonia. We selected the flow of 220 sccm for oxygen. Continuous pumping at one side and gas inlet at the other, allowed us to for establish a constant pressure of 40 Pa in the processing chamber. The microwave discharge was ignited 8.5 cm above the chamber containing the sample. Gases were radicalized by passing through the microwave discharge. The charged particles created in plasma within the discharge zone were effectively neutralized on the way from the glowing plasma to the entrance of the processing chamber, while the neutral radicals remained fairly intact since the gas-phase recombination was negligible at the low pressure conditions and the surface effects were minimized by using the inert material (glass). The residence time of gas in the afterglow chamber is estimated from the pumping speed and geometry of the vacuum system. In a rough approximation it is 0.1 s. The life-time of oxygen atoms in the chamber at steady conditions, i.e. without continuous gas inlet and pumping the system, was estimated for the case plasma was ignited in the chamber by DC glow discharge. A catalytic probe of high temporal sensitivity was mounted into the chamber and the O-atom density was measured after turning off the discharge. The resultant life-time was about 1.5 s. The samples mounted in the processing chamber were therefore treated by neutral reactive particles formed in the gaseous plasma inside the microwave discharge – predominantly oxygen atoms in the ground state (in the case of oxygen plasma) and NH_x radicals as well as atomic hydrogen in the ground state (in the case of ammonia plasma). The applied discharge power was 150 W.

2.3. Plasma characterization

Plasma in the microwave discharge was characterized by using optical emission spectroscopy (OES). Optical emission spectra were recorded by using an Avantes Ava Spec 3648 spectrometer. The device is based on an Ava Bench 75 symmetrical Czerny Turner design with a 3648 pixel CCD detector with the focal length of 75 mm. The range of measurable wavelengths is from 200 nm–1100 nm and the wavelength resolution is 0.5 nm. The spectrometer has a USB 2.0 interface, enabling high sampling rates of up to 270 spectra per second, in which the Signal-to-noise ratio is 350:1. Integration times are adjustable from 10 μs to 10 min. At integration times below 3.7 ms, the spectrometer itself performs internal averaging of spectra before transmitting them through the USB interface. A fixed integration time of 2 s was used. Such time enabled sufficient signal intensity and enough measurement points for measuring time evolution of certain spectral features. The optical fibre was mounted 1 cm away from the discharge tube.

2.4. Residual gas analysis

A standard residual gas analyser based on mass spectrometry of the atmosphere in the reaction chamber was applied. The spectrometer was connected to the chamber via a glass capillary of low conductance allowing for appropriate pressure of the order of 10^{-3} Pa in the spectrometer. The spectrometer was pumped differentially using a turbomolecular pump of nominal pumping speed 500 l/s backed by a two-stage rotary pump.

2.5. Loading of UV-responsive microcapsules

UV-responsive microcapsules were loaded on untreated and plasma-treated PET samples using pad-dry-cure method. The PET samples were submerged in the solution containing 50 g/l of UV-responsive microcapsules and 50 g/l of binder. The excess of coating was squeezed out in the rollers of laboratory foulard, with pick-up of 100%. Afterwards the PET samples were dried for 5 min at 100 °C

and cured for 3 min at 150 °C. The add-on (Ad) of microcapsule-coated samples was calculated according to the Eq. (1):

$$Ad\,(\%) = \frac{(m_{coated} - m_{uncoated})}{m_{uncoated}} \times 100 \qquad (1)$$

2.6. X-ray photoelectron spectroscopy

The surface composition of untreated and plasma-treated samples was studied using high-resolution X-ray photoelectron spectroscopy (XPS). The samples were mounted in a TFA XPS Physical Electronics XPS instrument. The base pressure in the XPS analysis chamber was approximately 6×10^{-8} Pa. The samples were excited with X-rays over a 400 μm spot with monochromatic Al $K_{\alpha 1,2}$ radiation at 1,486.6 eV. The photoelectrons were detected with a hemispherical analyser positioned at an angle of 45° normal to the sample surface. The energy resolution was approximately 0.5 eV. Survey-scan spectra were acquired at a pass energy of 187.85 eV with a 0.1 eV energy step. An additional electron gun was used to allow for surface neutralisation during the measurements because the samples were insulating. The concentration of the different elements was determined using MultiPak v8.1c software from Physical Electronics, which was supplied with the spectrometer.

2.7. Fourier transform infrared spectroscopy (FTIR)

ATR-FTIR spectra of untreated and plasma-treated samples were acquired using FTIR spectrophotometer (Bruker IFS 66/S). The spectra were collected from samples, which were tightly pressed against a cylindrical Ge crystal. The resolution of the equipment was $4\,cm^{-1}$ with 64 scans and the spectra were obtained over the range of $4000\,cm^{-1}$–$600\,cm^{-1}$.

2.8. Time-of-flight secondary ion mass spectrometry (ToF–SIMS)

ToF–SIMS analyses were performed using a ToF–SIMS 5 instrument (ION-TOF, Münster, Germany) equipped with a bismuth liquid metal ion gun with a kinetic energy of 30 keV. The analyses were performed in an ultra-high vacuum of approximately 10^{-7} Pa. The SIMS spectra were measured by scanning a Bi_3^+ cluster ion beam with a diameter of 1 μm over a 100×100 μm² analysis area. The positive secondary ion mass spectra were calibrated using CH_2^+, CH_3^+, and $C_2H_5^+$, and the negative secondary ion mass spectra were calibrated using C^-, C_2^-, and C_3^-. An electron gun was used to enable charge compensation on the sample surfaces during the analysis.

2.9. Absorption of water

The untreated and plasma-treated PET fabrics were tested for water absorbency according to AATCC Test Method 39-1980 in order to evaluate the changes in hydrophobic character of PET samples after plasma treatment. A water droplet was carefully deposited on the surface of PET fabric and the time between the contact of the water droplet with the fabric and the disappearance of the droplet into the fabric was measured in seconds (wetting time). The average of measurements for five water drops on one substrate was calculated.

2.10. Measurements of UV-responsiveness

The untreated and plasma-treated PET samples coated with UV-responsive microcapsules were tested for their UV-responsiveness using reflectance spectrophotometer SF 600 PLUS-CT (Datacolor, Switzerland). The specular component of the spectrophotometer was included, UV filter excluded (FL40: 0% UV), measurements were performed under illumination D65 and 10° standard observer. The samples were folded twice to gain four-layered thickness of the material. The CIELAB colour values and light reflectance (R[%]) were measured prior and after 1 min irradiation with UV light source (Philips UVA type bulb, 2×18 W), at the distance of 15 cm.

The colour difference (ΔE^*_{ab}) between non-irradiated and UV irradiated sample was calculated using Eq. (2):

$$\Delta E^*_{ab} = \sqrt{\Delta L^{*2} + \Delta a^{*2} + \Delta b^{*2}}, \qquad (2)$$

where ΔL^* is a difference in lightness, Δa^* is a difference on red-green axis and Δb^* is a difference on yellow-blue axis.

2.11. Measurements of colour strength

The colour strength (K/S values) of irradiated samples was calculated from the reflectance (R) values at wavelength of visible spectra, from 400 nm to 700 nm, using the following equation:

$$\frac{K}{S} = \frac{(1-R)^2}{2R}, \qquad (3)$$

where K is absorption coefficient, S is scattering coefficient and R is reflectance factor.

The percentage of improvement in colour depth (I) was calculated according to the Eq. (4):

$$I\,(\%) = \frac{(K/S_{treated} - K/S_{untreated})}{K/S_{untreated}} \times 100, \qquad (4)$$

where $K/S_{treated}$ is a colour strength of plasma-treated microcapsule-coated PET sample and $K/S_{untreated}$ is a colour strength of untreated microcapsule-coated PET sample.

2.12. Air permeability

The air permeability of uncoated and microcapsule-coated samples was determined according to the standard ISO 9237:1999, using AirTronic 3240A air permeability tester (MESDAN), at pressure drop 100 Pa. The air permeability (mm/s) was calculated according to the Eq. (5):

$$R = \frac{q_v}{A} \times 167, \qquad (5)$$

where q_v is the arithmetic mean flow rate of air (L/min), A is the area of sample under test (cm²), 167 is the conversion factor from L/min to mm/s.

3. Results and discussion

A series of treatments in MW plasma late afterglow were performed to determine the best conditions to achieve a greater uptake of PET fabric towards microcapsules containing photochromic dye and consequently to increase the UV-responsiveness of the fabric. The parameters that were varied in the research were gases used for producing chemically reactive species in plasma afterglow or combination of gases, namely oxygen (O_2) and ammonia (NH_3), and different treatment times. Plasma was characterized by OES, while the influence of the plasma afterglow treatments on the PET fabric was evaluated using XPS, SEM and wetting time.

Figs. 1 and 2 represent optical spectra of plasma created in oxygen and ammonia, respectively. The optical spectra of plasma created in oxygen, are typical for plasma with high dissociation fraction of oxygen molecules. Almost exclusively atomic oxygen lines are observed in the spectrum presented in Fig. 1 (a small peak at 760 nm represents O_2 molecular transition). The oxygen lines arise from the transition between highly excited atoms at excitation energy above 10 eV to lower excited states. The excited
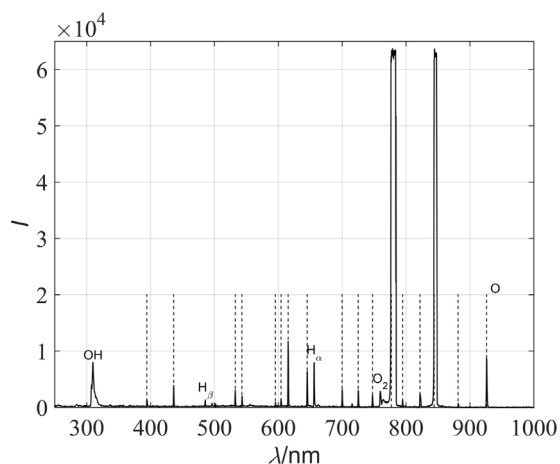
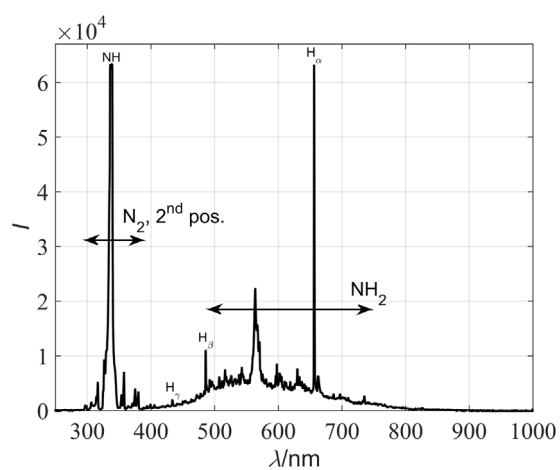**Fig. 1.** An optical spectrum of oxygen plasma acquired in the discharge tube.

Fig. 2. An optical spectrum of ammonia plasma acquired in the discharge tube.

Fig. 3. Mass spectra of residual atmosphere during base pressure (p_b), oxygen inlet (O_2) and during ammonia inlet (NH_3).

Table 1
The XPS surface composition of the untreated and plasma-treated PET fabrics (in atomic%).

Sample treatment	C	N	O	O/C	N/C
Untreated	76.3	0	23.7	0.31	–
100 s O_2	62.8	0	37.2	0.59	–
100 s NH_3	73.6	0.8	25.6	0.34	0.01
100 s O_2 + 3 s NH_3	61.1	2.5	36.4	0.60	0.04
100 s O_2 + 81 s NH_3	60.4	3.3	36.4	0.60	0.05
100 s O_2 + 243 s NH_3	59.2	4.6	36.3	0.61	0.08
200 s O_2 + 243 s NH_3	58.7	5.0	36.3	0.62	0.09

atoms mostly produced through dissociative excitation relax on the way to the processing chamber where only oxygen atoms in the ground state are present along with the molecules that might be excited to metastable states. There are also emission lines from atomic hydrogen in the visible range and the band corresponding to radiative relaxation of the OH radicals at the bandhead of 309 nm. The appearance of these spectral features is attributed to the residual atmosphere, which contains practically only water vapour in such experimental systems. As stated in subsection 2.1 the ultimate pressure is about 3 Pa what is several% of the total pressure. The water molecules diffuse also into the discharge tube and contribute to the optical spectrum presented in Fig. 1. No emission from nitrogen (ionized or neutral) is observed in the spectrum thus one can conclude the system is hermetically tight.

The samples were treated in oxygen plasma afterglow, where the main reactants are neutral atoms in the ground state, which interact chemically with polymer materials resulting in functionalisation of polymer surfaces with polar functional groups [21]. Such a treatment using only neutral reactive particles is preferred since it causes better functionalisation than conventional plasma treatment for various polymers including PET [34].

Fig. 2 represents an optical spectrum of plasma created by the microwave discharge in ammonia. The spectrum is rich in atomic hydrogen transitions that belong to the Balmer series (particularly H_α). Apart from these transitions an intensive peak is observed in the near UV range at the wavelength of 336 nm. This peak corresponds to the transition of the NH radical from $A^3\Pi$ (excited) to
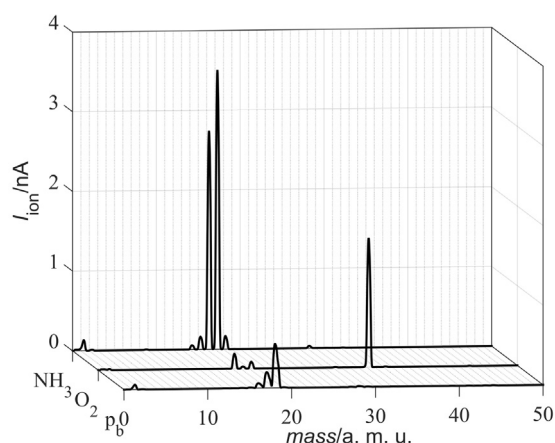
$X^3\Sigma^-$ (ground) state. Apart from these spectral features there are also broad bands in the visible range between roughly 450 and 750 nm that correspond to radiative relaxation of NH_2 radicals. The spectrum presented in Fig. 2 indicates extensive dissociation of ammonia molecules. The dissociation results in formation of atomic hydrogen and NH_x radicals. The radicals do not recombine much on the way from plasma to the processing chamber due to low pressure conditions (lack of three-body collisions which otherwise cause loss of radicals in the gas phase) and selection of the chamber material (glass is an inert material that does not allow for extensive surface recombination of H atoms to H_2 molecules [35]).

Fig. 3 represents the mass spectrum at the ultimate pressure as measured by residual gas analyser. The peak at 18 represents water vapour while the peaks at 17, 16 and 2 the dissociation products, i.e. OH, O and H_2. The water molecules partially dissociate upon interaction with the electrons used for ionization of gaseous molecules in the gas analyser. No measurable amount of other molecules is observed; therefore, the system is rather hermetically tight. Intentional introduction of oxygen is reflected in appearance of the peak at 32 (O_2) as well as relative increase of the peak at 16 (O). The relative intensity of peaks arising from water vapour decrease as shown in Fig. 3. This results are highly expecting due to high purity of oxygen. More interesting is the mass spectrum for the case when ammonia was introduced into the system, which is presented in Fig. 3. In this case we observe intensive peaks at 17 and 16 corresponding to NH_3 and NH_2, respectively, but the peak at 18 still persists indicating measurable amount of water vapour in the system during treatment of samples with ammonia afterglow. The small peak at 28 (N_2) is due to recombination of N atoms to parent molecules in the mass spectrometer rather than any inlet of air into the vacuum system.

The chemical changes on the surface of PET fabrics after plasma afterglow treatment are presented in Table 1. The untreated sample has a high concentration of carbon and low concentration of oxy-

gen as expected from the chemical composition of this polymer. The ratio between oxygen and carbon is 0.31. Treating PET sample with MW afterglow produced in oxygen gas increases the concentration of oxygen and decreases concentration of carbon on the surface of PET polymer (ratio O/C is 0.59) indicating saturation of the polymer surface with polar functional groups. Here, it is worth mentioning that the characterization depth of XPS using the classical source of X-rays is several nm so the result presented in Table 1 does not reflect the composition on the very surface but rather an average composition over the thickness of the surface film that corresponds to the escape depth of photoelectrons. Treating PET by the MW afterglow produced using only ammonia gas does not significantly change the chemical composition of the surface layer. The oxygen content is increased slightly so that the ratio O/C is 0.34 after treatment with ammonia plasma afterglow for 100 s. Such an increase could be attributed either to the experimental error or the fact that the processing chamber was not pumped down to a high-vacuum level but rather to the pressure of about 3 Pa. The residual atmosphere in the vacuum system contains predominantly water vapour (Fig. 3) whose molecules dissociate inside plasma forming OH radicals that are known to be excellent oxidants for organic materials. The optical spectrum presented in Fig. 1 clearly shows presence of such radicals. Unfortunately, in Fig. 2 the main OH band partially overlaps with the N_2 second positive band, therefore it is not as distinguished as in Fig. 1. The solid confirmation of the rather high concentration of water vapour in the experimental chamber during treatment of samples with ammonia afterglow is presented in Fig. 3. The OH radicals therefore cause some increase of the oxygen concentration on the polymer surface upon treatment with the ammonia afterglow. Appearance of nitrogen is observed on the polymer surface after treatment in ammonia plasma afterglow as the PET surface layer contains about 0.8 atomic% of nitrogen. Such a poor functionalization is explained by rather high stability of PET materials. Obviously, the atomic hydrogen created in the processing chamber is not capable to remove oxygen from the surface of polyethylene terephthalate at room temperature thus giving way to chemical bonding of nitrogen-containing groups. Such resistance of PET against atomic hydrogen at room temperature has been already observed so only application of rather dense hydrogen plasma rich in hydrogen ions as well as UV radiation allows for reducing oxygen content in the polymer surface [36]. The treatment of PET samples in late afterglow of ammonia plasma therefore does not allow for binding substantial amount of nitrogen (preferably in the form of amino groups) that would allow for appropriate surface finish prior to functionalisation with the UV-responsive microcapsules. That is why we have used a combination of oxygen and ammonia afterglows. The oxygen pre-treated sample treated with ammonia plasma afterglow for solely 3 s allowed for concentration of nitrogen in the surface film examined by XPS of about 2.5 atomic% (Table 1). Prolonged treatment causes even better functionalization since the achievable concentration of nitrogen is almost 5 atomic%. Numerous different functional groups may form upon treatment of polymers with reactive species from ammonia plasma but the afterglow of ammonia plasma is particularly suitable for formation of amino groups. The results presented in Table 1 are explained by increased affinity of pre-treated PET for binding nitrogen-containing radicals. The pre-treatment by oxygen atoms allows for saturation of PET surface with highly polar functional groups that are rather unstable Such functional groups interact with H and NH_x radicals from ammonia plasma causing partial reduction of the surface film as well as functionalization with nitrogen functional groups. The reduction probably occurs only on the very surface and not in the sub-surface layers. This could be a feasible explanation for observations presented in Table 1. Namely, the concentration of oxygen in the surface film examined by XPS is reduced only marginally even after prolonged treatment with
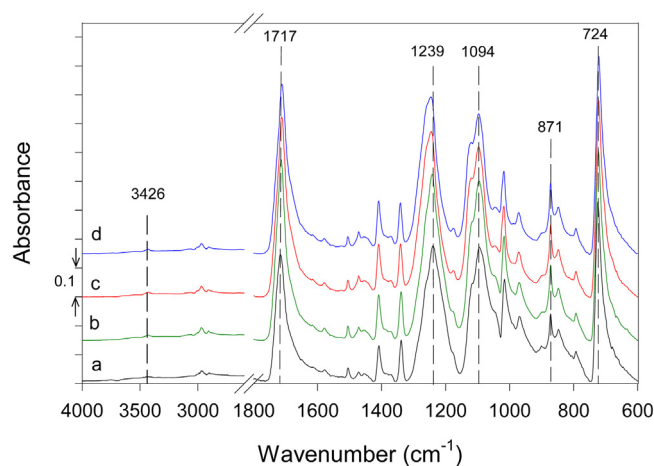

Fig. 4. FTIR spectra of untreated (a) oxygen plasma treated (b), ammonia plasma treated (c), oxygen and ammonia plasma-treated polyester (d).

late afterglow of ammonia plasma. The concentration of oxygen on samples treated by oxygen afterglow is 37 atomic% while on the samples treated first by oxygen and then ammonia afterglow is about 36 atomic% irrespective of the treatment time. Taking into account this fact one can speculate that nitrogen in the surface of our samples is bonded to carbon atoms in amide or similar oxygen-containing groups rather than amino groups. The type of the groups, however, cannot be determined by XPS due to overlapping of subpeaks in high-resolution carbon C1s peak corresponding to different surface functional groups.

To get more information about the type of nitrogen functional groups, we performed additional characterisation using Fourier transform infrared spectroscopy (FTIR) and time-of-flight secondary ion mass spectrometry (ToF-SIMS). In Fig. 4 FTIR spectra of untreated and plasma-treated PET fabric are presented. The characteristic absorption bands of PET are visible at 1717 cm^{-1} (C=O stretching of aromatic ester), 1239 cm^{-1} (asymmetric stretching of aromatic ester), 1094 cm^{-1} (aromatic ester O=C—O—C vibration), 871 cm^{-1} (vibrations of aromatic ring) and 724 cm^{-1} (C=O out-of-plane bending and ring CH out-of-plane bending), whilst the three small absorption bands between 2988 cm^{-1} and 2935 cm^{-1} belong to C—H sp^3 vibrations [37,38]. The appearance of oxygen-rich groups on PET surface such as CO, COO, OH etc. as a consequence of O_2 plasma treatment make PET surface more hydrophilic and therefore more water molecules can be absorbed. The latter can be observed in FTIR spectra of O_2 plasma-treated PET as the appearance of absorption band at 3421 cm^{-1}, assigned to intermolecular O—H bonded to C=O in the polyester chain, comparing to the untreated PET [39]. Additionally, the increase of intensity of the absorption band and its broadening at 1717 cm^{-1}, assigned to carbonyl C=O vibration is also observed after O_2 plasma treatment [40,41]. After NH_3 plasma treatment the IR spectroscopy showed no signs of amination, what is in sound with our XPS conclusions about absence of amino groups. Another reason can be also higher detection depth of FTIR and thus too low surface sensitivity. Therefore, SIMS which is a technique with very high surface sensitivity can give better information regarding surface functionalities.

In Fig. 5 are shown negative SIMS spectra of untreated PET and the one treated in combination of oxygen and ammonia plasma. In the spectrum of the untreated PET there are peaks that correspond to characteristic molecular fragments of PET material. After plasma treatment, two new peaks are observed at m/z 26 and m/z 42 that correspond to CN^- and OCN^- fragments. The ratio OCN^-/CN^- is 0.57. It was reported by Gerenser et al. [42] that OCN^-/CN^- ratio is an important indicator of the type of nitrogen-containing polymers.
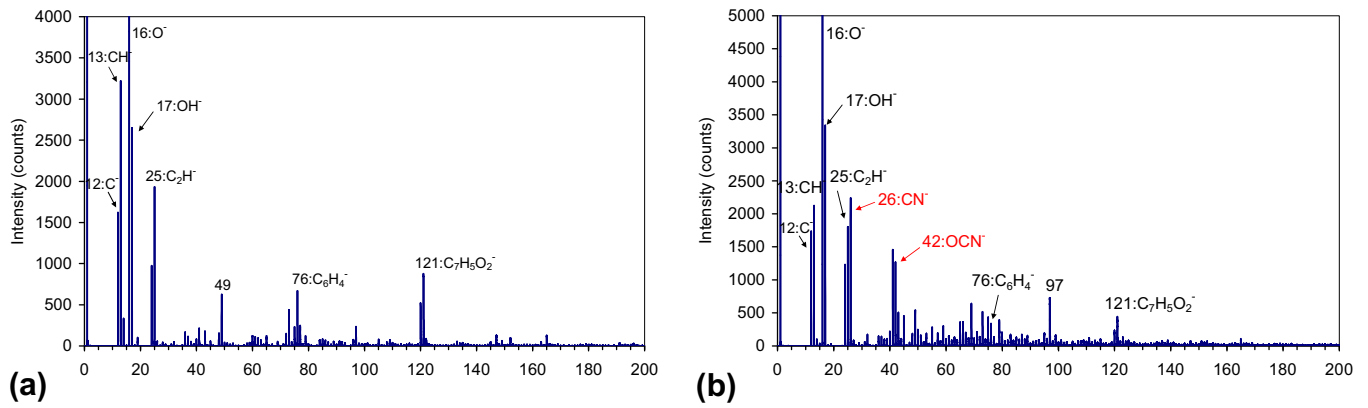
Fig. 5. Negative SIMS spectrum of: (a) untreated sample and (b) oxygen and ammonia plasma-treated sample.
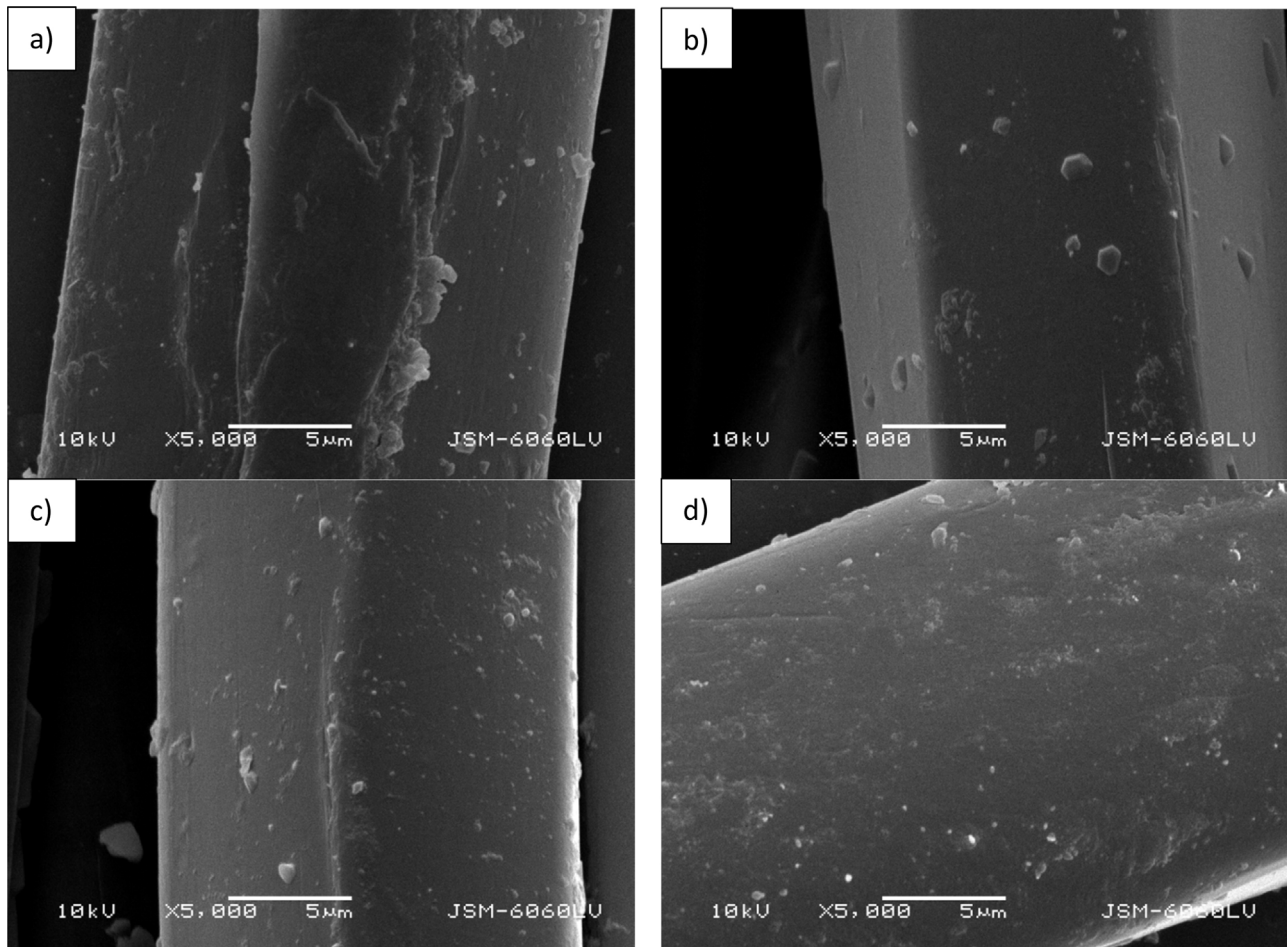

Fig. 6. The SEM images of PET samples (a) untreated, (b) treated with 100 s O_2 and 3 s NH_3 plasma afterglow, (c) treated with 100 s O_2 and 243 s NH_3 plasma afterglow, (d) treated with 200 s O_2 and 243 s NH_3 plasma afterglow.

The reported ratio for amines and imines was <0.05, for imides 0.19, for amines 0.22 and for urethanes it was 1.25. Our value of 0.57 suggests that nitrogen groups are associated with oxidized carbon and thus they support our conclusions derived from XPS results.

The water absorption analysis was performed on untreated and plasma-treated samples to evaluate the hydrophilic/hydrophobic character of PET fabric. The results summarized in Table 2 show a dramatic improvement of the water sorption after the treatments. The untreated PET fabric is moderately hydrophobic so the absorption time is almost a minute. As expected, the oxygen plasma-treated samples exhibit a hydrophilic character – the

Table 2
Water absorption of untreated and plasma-treated PET fabrics.

Sample treatment	Absorption time (s)
Untreated	54.5
100 s O_2	0.35
100 s O_2 + 100 s NH_3	0.95
100 s NH_3	28.13

absorption time is well below a second. Such a fast absorption is explained by functionalization of the polymer surface with polar oxygen-rich functional groups. Interesting enough, the absorp-

tion time remains short even after functionalization with nitrogen groups. The absorption time for the sample treated first by oxygen plasma afterglow and then by radicals from ammonia plasma is about 1 s. This is three times longer than for only oxygen-treated sample but still much shorter than for untreated sample. Such a short absorption time presented in Table 2 indicates that the sample retained hydrophilic character despite functionalization with nitrogen functional groups. Table 1 reveals that also the high concentration of oxygen on the sample treated subsequently by oxygen and ammonia plasma afterglows persists. The results presented in Tables 1 and 2 are therefore sound and just indicate that the method described in this paper allows for both functionalization with nitrogen and hydrophilic character of the sample. The combination of both is beneficial for binding the UV-responsive microcapsules.

In Fig. 6 SEM images of untreated and plasma-treated PET samples are presented, where the influence of plasma treatment on morphological changes of PET fibres is visible. On the untreated sample impurities on the surface of the fibres are present (Fig. 6a), which are removed after treatment with plasma afterglows (Fig. 6b–d). With the increasing treatment time, the cleaning of the surface is greater. In addition to the cleaning, treating PET fabric with 200s O_2 and 243s NH_3 plasma afterglow causes the surface etching effect, modifying the surface of fibres to be rougher (Fig. 6d).

The physical and chemical surface changes induced by plasma afterglow modification influence the uptake capacity of PET fabric towards microcapsules containing photochromic dye, which can be demonstrated by SEM, air permeability, add-on and colour measurements. The SEM images of microcapsule-coated PET fabrics show that treating PET fabric with plasma afterglow, regardless of the gas used, increases the uptake of microcapsules on the surface (Fig. 7). Samples modified at longer treatment time (Fig. 7c) have visibly higher amount of microcapsules embedded on the surface than samples modified at shorter treatment time (Fig. 7b) or untreated samples (Fig. 7a). The following can be expected since untreated PET fabric is hydrophobic with lower content of polar groups and does not wet in such extent as hydrophilic fabric like cotton. Also the microcapsule shell is usually not an agent that can react with the fibre, except microcapsule with reactive group in its shell which can be covalently bonded to fibre functional groups. For that reason, the binding agent is needed in the padding bath, which is responsible for the adhesion of microcapsules onto fabric. Wetting of fabric is especially important and desired at pad-dry process, because the fabric has to pick up the padding bath in a very short time in comparison with exhaust process at which the fabric is immersed in the bath during the whole process and the colorant exhausts gradually onto fabric. When the fibre hydrophilicity is increased, the wetting of fabric is faster and thus uptake of microcapsules can occur to a greater extent.

The results of SEM are in accordance to the results of air permeability (Fig. 8a) and add-on (Fig. 8b). Higher amount of the microcapsules on the plasma-treated samples lowered the permeability and increased the add-on. The air permeability of O_2 and NH_3 plasma treated microcapsule-coated sample is 2.13% and 3.21% lower than of untreated microcapsule-coated sample. As the treatment time with NH_3 plasma prolongs for the O_2+NH_3 plasma-treated PET samples, the air permeability decreases further, up to 9.56%. Higher amount of microcapsules on plasma-treated samples seal the interstices between the fibres, reducing the air permeability [43]. The sample ($200sO_2 + 243sNH_3$) with lowest air permeability had also the highest add-on (Fig. 11). The add-on on the sample $200sO_2 + 243sNH_3$ was 10.75% and on the untreated sample 1.31%, meaning that the add-on on plasma-treated sample was almost eight times higher.

The increased uptake of UV-responsive microcapsules on plasma-treated PET fabric is also determined by UV responsive-
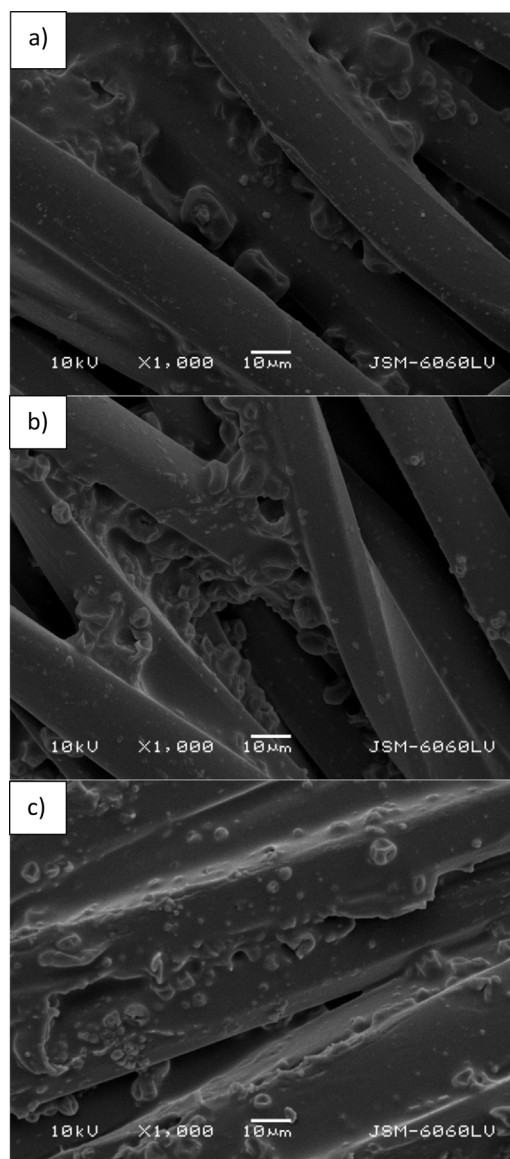
Fig. 7. The SEM images of (a) untreated, (b) treated with 100 s O_2 and 243 s NH_3 plasma afterglow, (c) treated with 200 s O_2 and 243 s NH_3 plasma afterglow microcapsule-coated PET fabric.

ness of the fabric upon UV light irradiation and colour difference (ΔE^*_{ab}) between untreated and plasma-treated sample. The UV responsiveness of microcapsule-coated PET fabric was evaluated by colour measurements (CIE $L^*a^*b^*$ values), colour strength (K/S) and percentage of improvement in colour depth (I). The CIE $L^*a^*b^*$ values (Fig. 9) are presented for microcapsule-coated PET samples before and after illumination with UV light source for 1 min. The illuminated samples are darker, bluer and greener compared to unilluminated samples. The plasma-treated samples before the illumination with UV source are slightly darker, slightly greener (moving towards negative CIE a^* axis) and yellower (moving toward the positive CIE b^* axis). The plasma-treated samples after illumination with UV source are darker (CIE L^* values decrease), slightly greener (moving towards negative CIE a^* axis) and bluer (moving towards negative CIE b^* axis). Regardless of the used gas or combination of both, the plasma treated samples are darker and bluer than untreated samples. The important indicator of photochromic performance of microcapsules on PET fabric is a photo-colouration, which is expressed as colour difference value (ΔE^*_{ab}) between non-irradiated (background colour)
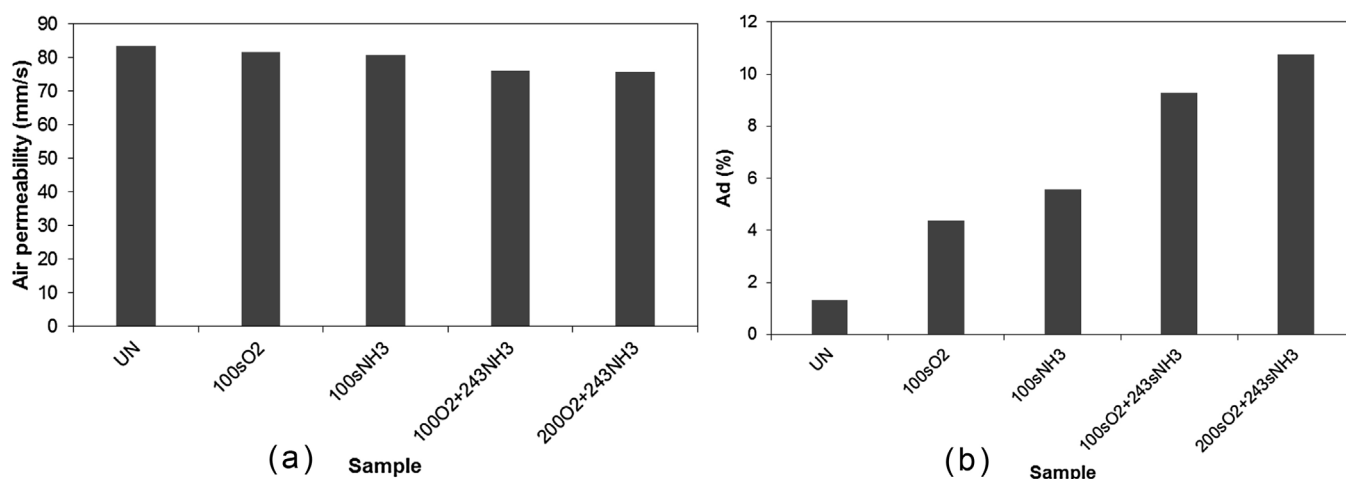
Fig. 8. Air permeability (a) and Add-on (b) of untreated and plasma-treated microcapsule-coated PET samples.
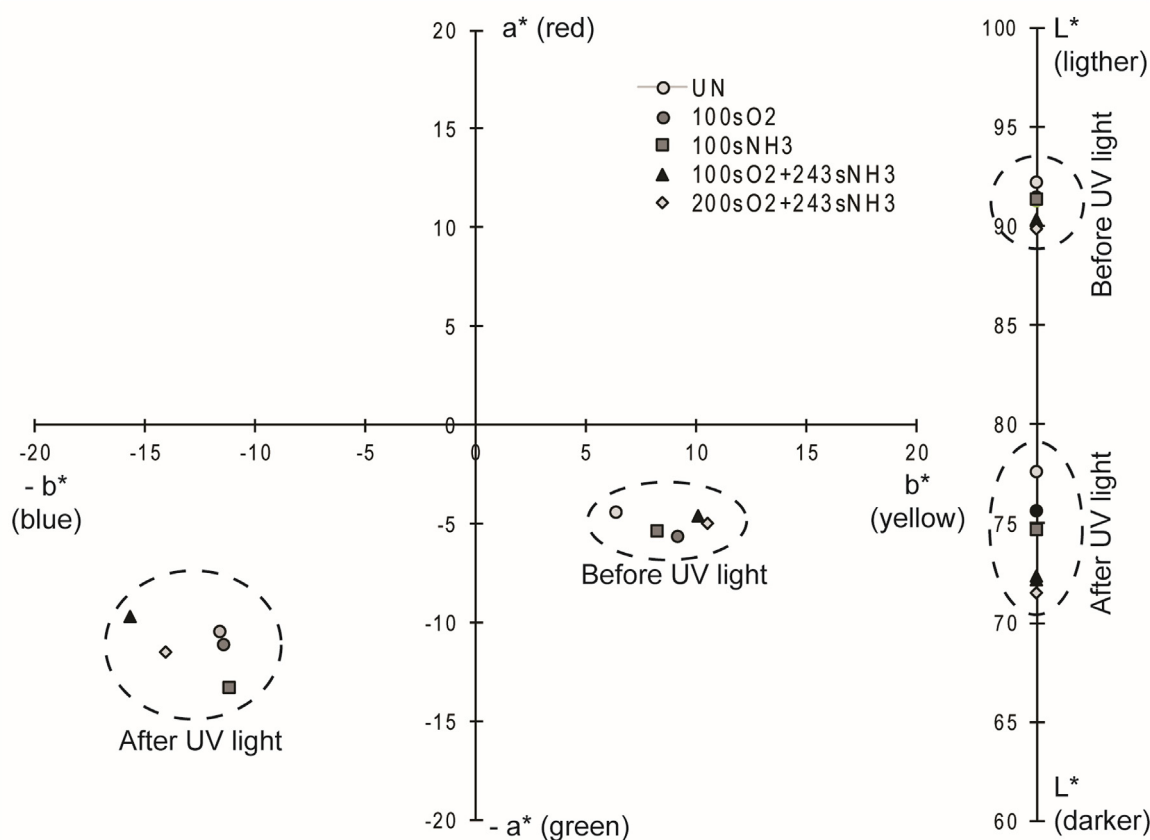

Fig. 9. CIE L*a*b* colour values of untreated and plasma-treated microcapsule-coated PET fabrics, before and after an illumination with UV light source.

and UV irradiated sample (developed colour) [44]. Higher ΔE^*_{ab} values indicate higher ability of photochromic dye to rearrange the bonding between atoms within colourless molecule creating a structure that is intensely coloured. In other words, higher ΔE^*_{ab} values represent better ability of photochromic dye to develop colour after exposure to UV radiation, or in our case higher uptake of microcapsules on PET fabric. After treating PET fabric by plasma afterglow, regardless of the gas used, the ΔE^*_{ab} values increase (Fig. 10a). The PET fabrics treated by 100 s O_2 or 100 s NH_3 afterglow have very similar ΔE^*_{ab} values, indicating that the fabrics have the same UV-responsive performance, which is in both cases higher than of the untreated sample. In Fig. 10b the values of colour differ-

ence between untreated and plasma-treated microcapsule-coated PET samples after illumination with UV source are presented. The ΔE^*_{ab} values range from 2 to 7, meaning that the difference in colour between untreated and plasma-treated sample is visible to the human eye. Highest ΔE^*_{ab} values between untreated and plasma-treated samples were calculated for samples with higher concentration of nitrogen on the surface (Table 1), which is an indication of higher uptake of microcapsules on PET fabric after longer period of treatment by NH_3 MW afterglow.

The results of CIE L*a*b* (Fig. 9) and ΔE^*_{ab} (Fig. 10) are already very good indicators for determination of the uptake capacity of PET fabric towards microcapsules containing photochromic dye. The
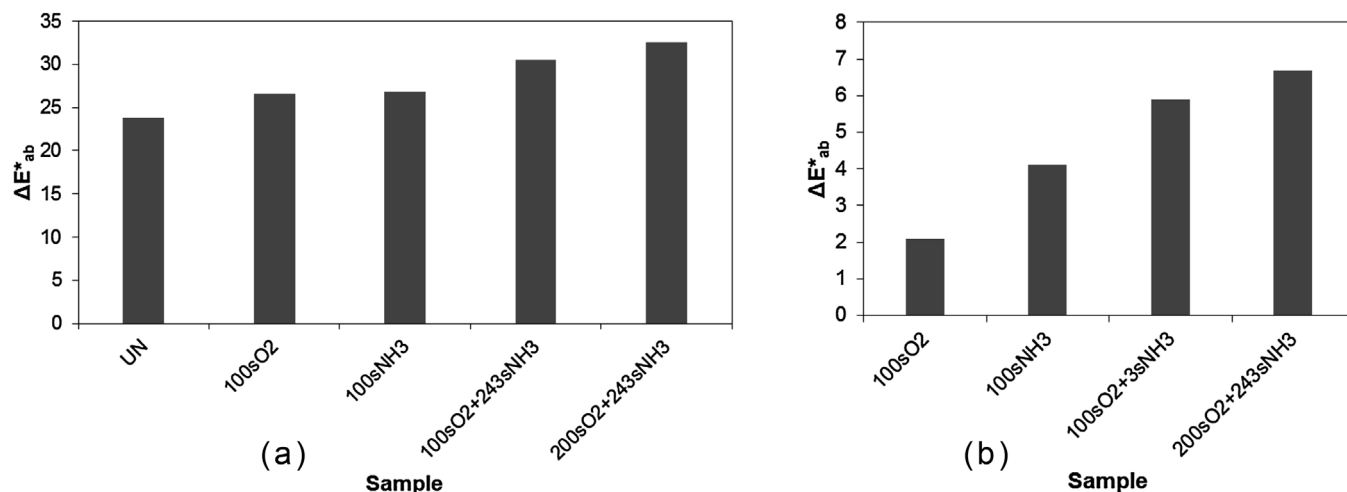
Fig. 10. The colour difference (ΔE^*_{ab}) value microcapsule-coated PET samples (a) between non-irradiated (background colour) and UV irradiated sample (developed colour) and (b) between untreated and plasma-treated UV irradiated samples.
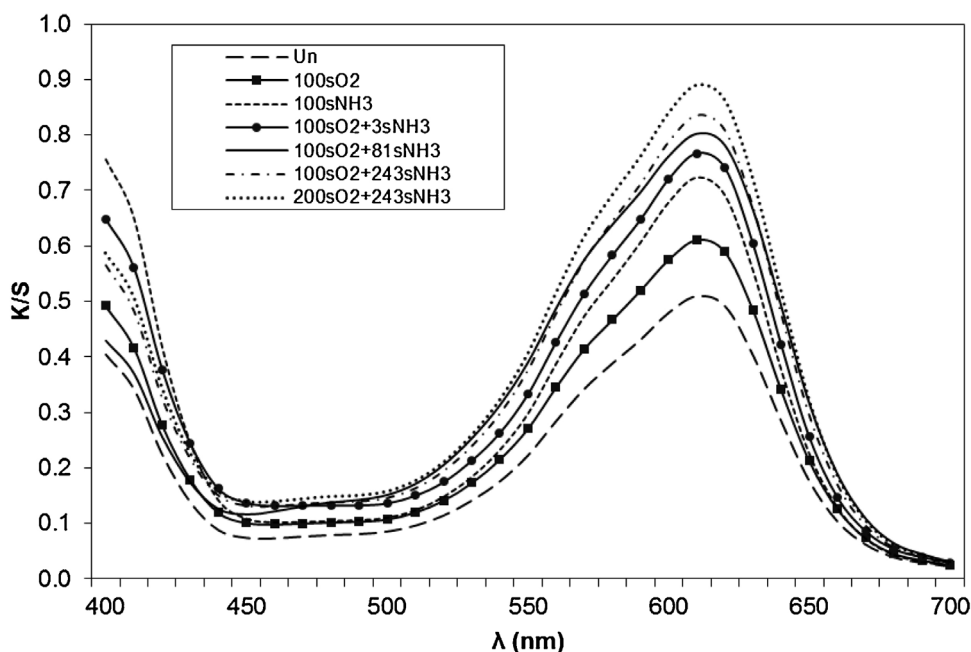

Fig. 11. Colour strength (K/S) values of untreated and plasma-treated microcapsule-coated PET samples after illumination with UV light source.

results of colour strength (K/S) values (Fig. 11) and percentage of improvement in colour depth (I) (Fig. 12) prove that MW afterglow treatment indeed increases the uptake of photochromic microcapsules onto PET fabric. The colour strength (K/S) describes the reflectance and transmittance of a translucent sample as a function of the light absorption and the light scattering in the sample [45]. The absorption of the light is proportional to the concentration of the colorant on the textile. Higher K/S value means that the sample contains higher amount of the colorant (in our case photochromic dye). The results of K/S values (Fig. 11) show that treating PET fabric with plasma increases the intensity of K/S peaks at wavelength of 610 nm. Higher peaks of K/S values are correlated with a higher quantity of UV-responsive microcapsules on the PET sample. The PET fabric treated with the NH_3 MW afterglow has higher uptake capacity towards microcapsules than PET fabric treated with O_2 MW afterglow. Also, the intensity of K/S peaks increase for samples treated by MW afterglow where a combination of gases was used. The K/S values increase with longer treatment time with NH_3
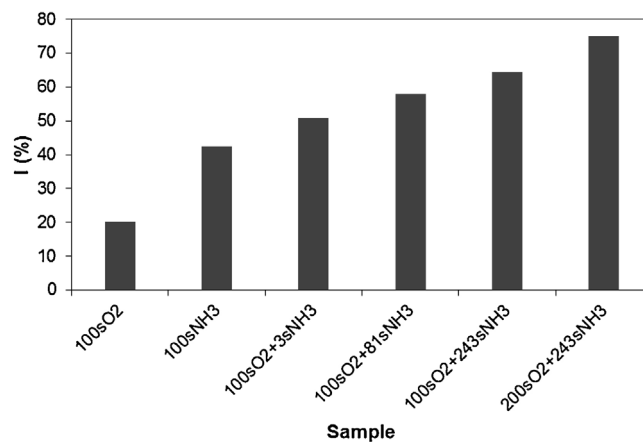

Fig. 12. The percentage of improvement in colour depth (I) between untreated and plasma-treated microcapsule-coated PET samples.

afterglow, and the highest increase of K/S values were obtained for a sample treated by 200 s O_2 and 243 s NH_3 plasma afterglow.

The results of percentage of improvement in colour depth (Fig. 12) between untreated and plasma-treated microcapsule-coated PET samples indicate that the improvement in colour strength (K/S) is almost 20% higher after treatment with O_2 plasma, and almost 75% for sample treated for 200 s with O_2 plasma and 243 s with NH_3 plasma. Again, the results prove that higher amount of nitrogen on the PET sample is favourable for higher uptake of UV-responsive microcapsules. Even short treatment with NH_3 plasma (i.e. sample *100sO2 + 3sNH3*) improves the colour depth by 50%. It was reported [46] that the pre-treatment of cotton fabric with cationic agent increased the uptake of photochromic microcapsules onto fibres during dyeing process due to incorporation of cationic charged groups onto fabric surface. The producer of microcapsules Itofinish UV blue suggests the pre-treatment of fabrics with cationic agent to enable exhaustion of negatively charged microcapsules on the fabric. In our case the incorporation of cationic groups onto PET fabric surface was obtained by NH_3 MW plasma afterglow, which caused higher uptake of microcapsules with photochromic dye at pad-dry-cure process. Therefore, the uptake of UV-responsive microcapsules is governed by two factors, one is the hydrophilic nature of substrate i.e. increased hydrophilic nature of PET fabric (Table 2), and the other is the presence of cationic functional groups on the substrate i.e. incorporation of nitrogen rich groups onto PET fabric (Table 1).

4. Conclusions

The increased embedment of UV-responsive microcapsules on hydrophobic PET fabric was successfully achieved by treating fabric in microwave discharge afterglow of oxygen and ammonia, and combination of these gases. The uptake of microcapsules was highest on sample treated with O_2 plasma afterglow for 200 s and subsequently with NH_3 plasma afterglow for 243 s. This sample had an add-on almost 8-times higher than untreated sample, which consequently led to increased colour strength (K/S values), up to 75% improvement in colour depth and the colour difference between the untreated and plasma-treated sample with a value of 7. Higher uptake of microcapsules also led to a smaller decrease of air permeability. The reasons for the higher embedment of microcapsules on plasma treated PET fabric were changes of hydrophobic character of PET, which became hydrophilic after O_2 MW plasma afterglow treatment, and functionalisation with nitrogen-rich functional groups on the surface of NH_3 plasma afterglow treated fabric. Treating PET with O_2 MW afterglow enabled better reactivity of the substrate to bond the nitrogen-rich functional groups after NH_3 afterglow treatment. The results demonstrate the positive contribution of treating PET fabric with neutral oxygen atoms, hydrogen and NH_x radicals produced in plasma to achieve higher reactivity of the substrate and consequently higher uptake of UV-responsive microcapsules.

Acknowledgements

References

[1] J.B. Kerr, V.E. Fioletov, Surface ultraviolet radiation, Atmos. Ocean 46 (2008) 159–184, http://dx.doi.org/10.3137/ao.460108.

[2] R.D. Ley, Dose response for ultraviolet radiation A–induced focal melanocytic hyperplasia and nonmelanoma skin tumors in monodelphis domestica, Photochem. Photobiol. 73 (2001) 20–23.

[3] S. Malinovic, D.T. Mihailovic, D. Kapor, Z. Mijatovic, I.D. Arsenic, NEOPLANTA: a short description of the first Serbian UV index model, J. Appl. Meteorol. Climatol. 45 (2006) 1171–1177, http://dx.doi.org/10.1175/JAM2400.1.

[4] T. Rijavec, S. Bračko, Smart dyes for medical and other textiles, in: L. van Langehove (Ed.), Smart Text. Med. Healthc. Mater. Syst. Appl., CRC press, Woodhead Publishing, Cambridge, 2007, pp. 123–149.

[5] M. Kozicki, E. Sasiadek, Textile UV detector with 2,3,5-triphenyltetrazolium chloride as an active compound, Radiat. Meas. 46 (2011) 510–526, http://dx.doi.org/10.1016/j.radmeas.2011.03.016.

[6] M. Kozicki, E. Sąsiadek, I. Karbownik, W. Maniukiewicz, Doped polyacrylonitrile fibres as UV radiation sensors, Sens. Actuators B Chem. 213 (2015) 234–243, http://dx.doi.org/10.1016/j.snb.2015.02.087.

[7] M. Aldib, R.M. Christie, Textile applications of photochromic dyes. Part 5: application of commercial photochromic dyes to polyester fabric by a solvent-based dyeing method, Color. Technol. 129 (2013) 131–143, http://dx.doi.org/10.1111/cote.12008.

[8] T.L. Dawson, Changing colours: now you see them, now you don't, Color. Technol. 126 (2010) 177–188, http://dx.doi.org/10.1111/j.1478-4408.2010.00247.x.

[9] M. Vikova, M. Vik, Colour shift photochromic pigments in colour space CIE L*a*b*, Mol. Cryst. Liq. Cryst. 431 (2005) 403–415, http://dx.doi.org/10.1080/15421400590946947.

[10] Y. Zhou, Y. Yan, Y. Du, J. Chen, X. Hou, J. Meng, Preparation and application of melamine-formaldehyde photochromic microcapsules, Sens. Actuators B Chem. 188 (2013) 502–512, http://dx.doi.org/10.1016/j.snb.2013.07.049.

[11] N. Vazquez-Mera, C. Roscini, J. Hernando, D. Ruiz-Molina, Liquid-filled capsules as fast responsive photochromic materials, Adv. Opt. Mater. 1 (2013) 631–636, http://dx.doi.org/10.1002/adom.201300121.

[12] Polyesters and Polyamides, in: B.L. Deopura, R. Alagirusamy, M. Joshi, B. Gupta (Eds.), Woodhead Publishing, Boca Raton, 2008.

[13] A. Al-Etaibi, H. Alnassar, M. El-Apasery, Dyeing of polyester with disperse dyes: Part 2. Synthesis and dyeing characteristics of some azo disperse dyes for polyester fabrics, Molecules 21 (2016) 855, http://dx.doi.org/10.3390/molecules21070855.

[14] M. Muneer, S. Adeel, S. Ayub, M. Zuber, F. Ur-Rechman, M.I. Kanjal, M. Iqbal, M. Kamran, Dyeing behaviour of microwave assisted surface modified polyester fabric using Disperse orange 25: improvement in colour strength and fastness properties, Oxid. Commun. 39 (2016) 1430–1439.

[15] B. Golja, B. Šumiga, B. Boh, J. Medved, T. Pušić, P.F. Tavčer, Application of flame retardant microcapsules to polyester and cotton fabrics, Mater. Tehnol. 48 (2014) 105–111.

[16] M. Gorenšek, M. Gorjanc, V. Bukošek, J. Kovač, P. Jovančić, D. Mihailović, Functionalization of PET fabrics by corona and nano silver, Text. Res. J. 80 (2010) 253–262, http://dx.doi.org/10.1177/0040517509105275.

[17] I.C. Gouveia, L.C. Antunes, A.P. Gomes, Low-pressure plasma treatment for hydrophilization of poly(ethylene terephthalate) fabrics, J. Text. Inst. 102 (2011) 203–213, http://dx.doi.org/10.1080/00405001003616777.

[18] M. Gorenšek, M. Gorjanc, V. Bukošek, J. Kovač, Z. Petrović, N. Puač, Functionalization of polyester fabric by Ar/N2 plasma and silver, Text. Res. J. 80 (2010) 1633–1642, http://dx.doi.org/10.1177/0040517510365951.

[19] V. Takke, N. Behary, A. Perwuelz, C. Campagne, Surface and adhesion properties of poly(ethylene glycol) on polyester(polyethylene terephthalate) fabric surface: effect of air-atmospheric plasma treatment, J. Appl. Polym. Sci. 122 (2011) 2621–2629, http://dx.doi.org/10.1002/app.34403.

[20] M.Ö. Öteyaka, P. Chevallier, S. Turgeon, L. Robitaille, G. Laroche, Low pressure radio frequency ammonia plasma surface modification on poly(ethylene terephthalate) films and fibers: effect of the polymer forming process, Plasma Chem. Plasma Process. 32 (2012) 17–33, http://dx.doi.org/10.1007/s11090-011-9330-3.

[21] M. Gorjanc, M. Mozetič, Modification of Fibrous Polymers by Gaseous Plasma: Principles, Techniques and Applications, LAP Lambert Academic Publishing, Saarbrücken, 2014.

[22] C. López-Santos, F. Yubero, J. Cotrino, A.R. González-Elipe, Surface functionalization, oxygen depth profiles, and wetting behavior of PET treated with different nitrogen plasmas, ACS Appl. Mater. Interfaces 2 (2010) 980–990, http://dx.doi.org/10.1021/am100052w.

[23] S. Babaei, P.L. Girard-Lauriault, Tuning the surface properties of oxygen-rich and nitrogen-rich plasma polymers: functional groups and surface charge, Plasma Chem. Plasma Process. 36 (2016) 651–666, http://dx.doi.org/10.1007/s11090-015-9682-1.

[24] T. Tkavc, A. Vesel, E.H. Acero, L.F. Zemljič, Comparison of oxygen plasma and cutinase effect on polyethylene terephthalate surface, J. Appl. Polym. Sci. 128 (2013) 3570–3575, http://dx.doi.org/10.1002/app.38526.

[25] I. Junkar, M. Modic, M. Mozetič, Modification of PET surface properties using extremely non-equilibrium oxygen plasma, Open Chem. 13 (2015) 490–496, http://dx.doi.org/10.1515/chem-2015-0061.

[26] J. Lv, Q. Zhou, T. Zhi, D. Gao, C. Wang, Environmentally friendly surface modification of polyethylene terephthalate (PET) fabric by low-temperature oxygen plasma and carboxymethyl chitosan, J. Clean. Prod. 118 (2016) 187–196, http://dx.doi.org/10.1016/j.jclepro.2016.01.058.

[27] M.J. Farrell, M.A. Ankeny, P.J. Hauser, Prediction of recipes for cotton cationisation and reactive dyeing to shade match conventionally dyed cotton, Color. Technol. 130 (2014) 363–367, http://dx.doi.org/10.1111/cote.12101.

[28] F.R. Oliveira, M. Fernandes, N. Carneiro, A. Pedro Souto, Functionalization of wool fabric with phase-change materials microcapsules after plasma surface

modification, J. Appl. Polym. Sci. 128 (2013) 2638–2647, http://dx.doi.org/10.1002/app.38325.

[29] T. Salem, D. Pleul, M. Nitschke, M. Müller, F. Simon, Different plasma-based strategies to improve the interaction of anionic dyes with polyester fabrics surface, Appl. Surf. Sci. 264 (2013) 286–296, http://dx.doi.org/10.1016/j.apsusc.2012.10.014.

[30] Q. Zheng, J. Huang, S. Cao, H. Gao, A flexible ultraviolet photodetector based on single crystalline MoO3 nanosheets, J. Mater. Chem. C 3 (2015) 7469–7475, http://dx.doi.org/10.1039/C5TC00850F.

[31] T.K. Markkula, J.A. Hunt, F.R. Pu, R.L. Williams, Surface chemical derivatization of plasma-treated PET and PTFE, Surf. Interface Anal. 34 (2002) 583–587, http://dx.doi.org/10.1002/sia.1365.

[32] J. Casimiro, B. Lepoittevin, C. Boisse-Laporte, M.G. Barthés-Labrousse, P. Jegou, F. Brisset, P. Roger, Introduction of primary amino groups on poly(ethylene terephthalate) surfaces by ammonia and a mix of nitrogen and hydrogen plasma, Plasma Chem. Plasma Process. 32 (2012) 305–323, http://dx.doi.org/10.1007/s11090-011-9345-9.

[33] M. Kolar, M. Mozetič, K. Stana-Kleinschek, M. Fröhlich, B. Turk, A. Vesel, Covalent binding of heparin to functionalized PET materials for improved haemocompatibility, Materials (Basel) 8 (2015) 1526–1544, http://dx.doi.org/10.3390/ma8041526.

[34] A. Vesel, M. Mozetič, Low-pressure plasma-assisted polymer surface modifications, in: J. Izdebska, S. Thomas (Eds.), Print. Polym. Fundam. Appl., Elsevier, Amsterdam, 2016, pp. 101–121.

[35] M. Mozetič, A. Vesel, V. Monna, A. Ricard, H density in a hydrogen plasma post-glow reactor, User Model. User-Adapt. Interact. 71 (2003) 201–205, http://dx.doi.org/10.1016/S0042-207X(02)00737-6.

[36] N. Recek, A. Vesel, Surface modification of polymer polyethylene terephthalate with plasmas created in different gases, Mater. Technol. 48 (2014) 893–897.

[37] Z. Omerogullari, D. Kut, Application of low-frequency oxygen plasma treatment to polyester fabric to reduce the amount of flame retardant agent,

Text. Res. J. 82 (2012) 613–621, http://dx.doi.org/10.1177/0040517511420758.

[38] H. Dave, L. Ledwaini, N. Chandwani, K. Puravi, B. Desai, S.K. Nema, Surface modification of polyester fabric by non-thermal plasma treatment and its effect on coloration using natural dye surface modification of polyester fabric by non-thermal plasma treatment and its effect on, J. Polym. Mater. 30 (2013) 291–304.

[39] P. Mazeyar, E. Izadyar, Influence of atmospheric-air plasma on the coating of a nonionic lubricating agent on polyester fiber, Radiat. Eff. Defects Solids 166 (2011) 408–416, http://dx.doi.org/10.1080/10420150.2011.553230.

[40] I. Novák, I. Chodák, J.Á.N. Sedliačik, J. Prachár, Pre-treatment of polyester-based veneers, Ann. Warsaw Univ. Life Sci. For. Wood Technol. 92 (2015) 312–316.

[41] M.M. Kamel, M.M. El Zawahry, H. Helmy, M.A. Eid, Improvements in the dyeability of polyester fabrics by atmospheric pressure oxygen plasma treatment, J. Text. Inst. 102 (2011) 220–231, http://dx.doi.org/10.1080/00405001003672366.

[42] L.J. Gerenser, J.M. Grace, G. Apai, P.M. Thompson, Surface chemistry of nitrogen plasma-treated poly(ethylene-2,6-naphthalate): XPS HREELS and static SIMS analysis, Surf. Interface Anal. 29 (2000) 12–22, http://dx.doi.org/10.1002/(SICI)1096-9918(200001)29:1<12::AID-SIA687>3.0.CO;2-7.

[43] M.I. Guignard, C. Campagne, S. Giraud, M. Brebu, N. Vrinceanu, L.I. Cioca, Functionalization of a bamboo knitted fabric using air plasma treatment for the improvement of microcapsules embedding, J. Text. Inst. 106 (2015) 119–132, http://dx.doi.org/10.1080/00405000.2014.942115.

[44] M.A. Chowdhury, M. Joshi, B.S. Butola, Photochromic and thermochromic colorants in textile applications, J. Eng. Fibres Fabr. 9 (2014) 107–123.

[45] A. Berger-Schunn, Practical Color Measurement, John Wiley & Sons, Inc, New York, 1994.

[46] M. Kamata, S. Osamu, S. Suefuku, S. Ohtsu-shi, T. Maeda, Dyeing method and dyed product, EP0480162 (A1) – 1992-04-15 (1991).

Plasma properties in a large-volume, cylindrical and asymmetric radio-frequency capacitively coupled industrial-prototype reactor

You may also be interested in:

Characterization and global modelling of low-pressure hydrogen-based RF plasmas suitable for surface cleaning processes
Nikola Škoro, Nevena Pua, Saša Lazovi et al.

Diagnostics and biomedical applications of radiofrequency plasmas
Saša Lazovi

Extremely non-equilibrium oxygen plasma for direct synthesis of metal oxide nanowires on metallic substrates
Miran Mozetic

Determination of the neutral oxygen atom density in a plasma reactor loaded with metal samples
Miran Mozetic and Uros Cvelbar

Characterization of an asymmetric parallel plate radio-frequency discharge using a retarding field energy analyzer
D Gahan, S Daniels, C Hayden et al.

Ion energy distribution measurements in rf and pulsed dc plasma discharges
D Gahan, S Daniels, C Hayden et al.

Application of extremely non-equilibrium plasmas in the processing of nano and biomedical materials
Miran Mozeti, Gregor Primc, Alenka Vesel et al.

Catalytic probes with nanostructured surface for gas/discharge diagnostics
A Drenik, U Cvelbar, K Ostrikov et al.

Plasma properties in a large-volume, cylindrical and asymmetric radio-frequency capacitively coupled industrial-prototype reactor

Saša Lazović[1,2], Nevena Puač[1], Kosta Spasić[1], Gordana Malović[1], Uroš Cvelbar[2], Miran Mozetič[2], Maja Radetić[3] and Zoran Lj Petrović[1]

[1] Institute of Physics, University of Belgrade, Pregrevica 118, Belgrade, Serbia
[2] Jožef Stefan Institute, Jamova cesta 39, 1000 Ljubljana, Slovenia
[3] Faculty of Technology and Metallurgy, University of Belgrade, Karnegijeva 4, 11000 Belgrade, Serbia

E-mail: lazovic@ipb.ac.rs

Abstract

We have developed a large-volume low-pressure cylindrical plasma reactor with a size that matches industrial reactors for treatment of textiles. It was shown that it efficiently produces plasmas with only a small increase in power as compared with a similar reactor with 50 times smaller volume. Plasma generated at 13.56 MHz was stable from transition to streamers and capable of long-term continuous operation. An industrial-scale asymmetric cylindrical reactor of simple design and construction enabled good control over a wide range of active plasma species and ion concentrations. Detailed characterization of the discharge was performed using derivative, Langmuir and catalytic probes which enabled determination of the optimal sets of plasma parameters necessary for successful industry implementation and process control. Since neutral atomic oxygen plays a major role in many of the material processing applications, its spatial profile was measured using nickel catalytic probe over a wide range of plasma parameters. The spatial profiles show diffusion profiles with particle production close to the powered electrode and significant wall losses due to surface recombination. Oxygen atom densities range from $10^{19}\,\text{m}^{-3}$ near the powered electrode to $10^{17}\,\text{m}^{-3}$ near the wall. The concentrations of ions at the same time are changing from 10^{16} to the $10^{15}\,\text{m}^{-3}$ at the grounded chamber wall.

(Some figures may appear in colour only in the online journal)

1. Introduction

Low-temperature plasmas represent an irreplaceable tool for many industrial processes due to a variety of chemical reactions that can be induced and controlled, even at low gas temperatures. Most of the energy delivered to non-equilibrium plasmas is transferred to electrons and not to the heating of the background gas or walls of the vessel. Therefore, the electrons are determining the nature of chemical processes in the plasma as well as at the plasma–sample interfaces. Energetic electrons in plasma can produce active species (ions, radicals, metastables and new electrons) in very high concentrations that can hardly be matched by traditional chemical or other methods. In addition, non-equilibrium plasmas may be easily modified and controlled by changing the composition, pressure, current density and flow, thus allowing a wide range of variation of a number of parameters and allowing optimization and even on-line control of some technological plasma based processes.

However, the interaction between the plasma created active species and the substrate is also depending on the material properties of the substrate. Intrinsic surface properties

and desired treatment effects are setting the requirements for the plasma source design, defining the range of applicable internal and external plasma parameters. From the point of practical use, the crucial aim is to determine the optimal range of applicable plasma parameters and proper plasma operating regime [1–5]. Controllable plasma chemical reactions are widely used in the processing of materials of different origins and properties [6, 7]. For example, field of microelectronics is strongly influenced by the development of plasma devices, i.e. by improved results on plasma deposition, etching, ashing, implantation, surface cleaning and other surface modification processes [8, 9]. Another rapidly growing research field is biomedical plasma applications [10–13]. Related to this, low-pressure plasmas also find their place in the sterilization of medical instruments, processing of biocompatible materials and, for example, in increasing antibacterial properties of textiles later used in medical, military or food preparation purposes. While it was expected that atmospheric pressure plasmas would replace the low-pressure reactors, the complexity of vacuum system is replaced by other complexities, such as small gap, instability of operation and usage of helium as a buffer gas [14, 15]. Thus, low pressure plasmas are still an option for applications of materials and samples that can be placed in vacuum.

In order to measure plasma parameters and effectively control the plasma process, we need to apply different diagnostic techniques. Typically, we are looking for quantitative results which can be monitored as an indication of the plasma processing and also in order to compare with models that are required to understand plasmas, to optimize the equipment and even to control processing in real time.

Several methods have been developed for measurement of neutral atom density. The mass spectroscopy is suitable as long as plasma is created at low pressures; however, in many plasmas partial pressure may be as high as 100 Pa [16, 17]. For these cases and the cases of atmospheric pressure discharges, differential pumping of the mass spectrometer is obligatory, which significantly increases the cost of the technique and introduces some problems [18]. A similar problem occurs when measuring plasma ions. In any case, mass spectrometry, while providing detailed results, has a limitation due to difficulty in making absolute calibration. Chemical titration using NO is a reliable method, but it tends to be time consuming and destructive so it is not suitable for real time measurements [19, 20]. Laser absorption spectroscopy such as laser-induced fluorescence (LIF), two-photon laser-induced fluorescence (TALIF) [21] or cavity ring-down spectroscopy (CRDS) [22] are reliable methods, but require expensive equipment and are therefore of little interest for industry. On the other hand, optical emission spectroscopy (OES) is easy to use; it requires inexpensive equipment and allows real time measurements. Nevertheless it is still nowadays regarded as semi-qualitative since quantification of the results is difficult (see [23]).

Catalytic probes are simple, easy to use and allow real-time monitoring of the neutral atom density as long as the neutral gas temperature is close to the room temperature, and the dissociation fraction is many orders of magnitude larger than the ionization fraction [24]. Until now, catalytic probes were used to measure atomic oxygen species in inductively coupled radiofrequency and microwave discharges [25, 26]. Some measurements were also performed in capacitively coupled radiofrequency plan parallel reactors [27–29]. Reports show that atomic oxygen concentrations are of the order of 10^{21} m^{-3} except for the capacitively coupled plasma (CCP) reactor where densities are lower, 10^{19} m^{-3}.

In this paper we apply several diagnostic techniques to study plasma of a large-scale asymmetric capacitive plasma reactor. We have developed an industrial reactor of a simple design where homogeneous, stable plasma capable of long term operation is generated. The main objective was to limit the energy of the ions bombarding the sample surfaces while still having sufficient densities of active plasma species.

The large size reactor was built to demonstrate the properties of plasma of a large size that can reasonably handle on-line textile treatment. This would require an additional differential pumping stage so that the textile would be introduced through a slit at one side of the reactor wall, continuously moved through the plasma and finally the treated textile would be rolled after exiting. Additionally, the intensity of the treatment can also be controlled by adjusting the distance between the power electrode and the samples. Our previous studies of plasma treatment of textile [30] were carried out in a similar asymmetric reactor of a much smaller volume. In this paper, we present results on characterization of the large volume plasma. Langmuir and catalytic probes were used to measure spatial profiles of concentration of ions and of atomic oxygen. Detailed electrical characterization of the reactor was performed using home-made derivative probes which proved to be superior to commercial probes and power meters, overcoming problems with operating frequency ranges and calibration. The current–voltage characteristics of the discharge, as well as, the real power delivered to the plasma by the generator will be presented. All measurements were carried out in air plasma for several different pressures and powers.

The ion energies and concentrations can be independently controlled using two RF sources operating at different frequencies [31, 32], but due to simplicity and reduced cost, we have chosen asymmetrical (cylindrical) geometry of the reactor [33]. This asymmetry provides a very large ratio of areas of the grounded to the powered electrode and consequently pronounced differences between voltage drops in the sheaths. This leads to differences in energies of ions bombarding the two electrodes. In addition, relatively large atomic oxygen densities are present. Oxygen atoms are necessary for plasma modification of seeds, polymers and textiles [34–37] for which the reactor was already used, as well as, many other treatments. However, a detailed characterization of plasma species, especially of ions, neutral atoms as well as proper input powers, is not yet available including correlations between those species and plasma properties. One of the most common problems in microelectronic manufacturing [38] is temporal variation of plasma properties due to modification of surfaces of the vessel. We have thus developed a simple real time monitoring plasma processes based on the catalytic probes that may be easily applied in large-scale industrial processes.
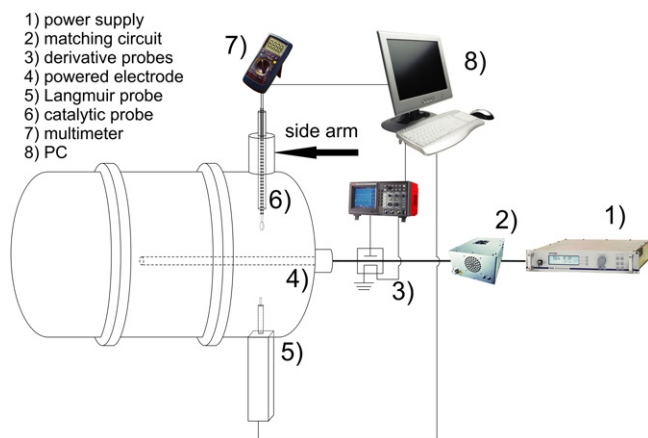
Figure 1. Schematics of the experimental setup.

2. Experimental setup

A CCP reactor powered at 13.56 MHz and operated at low pressures with a large volume in which uniform plasma can be created was used for experiments. The discharge chamber made of stainless steel was 2.5 m long and 1.17 m in diameter. The powered electrode was 1.5 m long (and could be extended to fully 2.5 m), 3 cm in diameter and made of aluminum. It is placed axially at the centre of the chamber. The chamber has a platform at the bottom where samples can be placed. The distance between the platform and the powered electrode is adjustable by moving the platform. The outer chamber wall is the grounded electrode and the sample platform is grounded as well.

The electrical circuit consists of an RF power generator Dressler Cesar 1310 in combination with Variomatch matching network. Derivative probes were placed as close as possible to the powered electrode. Langmuir and catalytic probe were placed side-on to the reactor wall (as presented in figure 1). The reduced pressure is maintained using a two-stage rotary pump ($60 \, \text{m}^3 \, \text{h}^{-1}$). Ambient air is introduced into the chamber through a needle valve.

In the regime with flowing working gas, the pumping system can also affect the way atomic oxygen recombines at the catalytic probe surface [39]. Due to this reason, we measured densities in both fluent and stationary regime, with and without pumping. Our results showed that in the present setup the effect of pumping on results was negligible.

Knowledge of power introduced into the plasma is essential in characterizing plasmas and controlling operating conditions in plasma processing. Non-linear impedance of the plasma imposes harmonics of the drive frequency. Asymmetry of the discharge chamber also affects the way harmonics are generated. Due to this non-linearity, the change in external circuitry leads to unpredictable variation of the plasma properties. For example, the auto-tune feature on the matching network can result in different reflected power minima for several apparently identical measurements which will result in different values of power deposited into the plasma [40]. Therefore, the power measured at the RF generator is not the best parameter.

Disadvantages of using commercial power meters lie in the fact that the power is usually measured only at a single frequency or in a very narrow range of frequencies, thus leaving out the information about power delivered to the load at the frequencies of the higher harmonics. There are also commercial probes available for current and voltage measurements at radio frequencies but their disadvantage is that in most of the cases their frequency response is not characterized properly. Derivative probes which are calibrated in a wide range of frequencies (from an order of magnitude lower to an order of magnitude higher) overcome these problems. Such probes can be placed close to the powered electrode reducing the error introduced by the losses in the part of external electrical circuit from the probes to the powered electrode. We have used previously described derivative probes [41] in order to measure the power transmitted to the plasma and analyse harmonic composition of the signals.

Both probes were placed into a stainless steel box opposite each other and as close as possible to the powered electrode. Instantaneous voltages and currents were monitored using derivative probes which were connected to the oscilloscope with cables of identical length (so there would be no additional phase differences between current and voltage signals introduced). All waveforms were collected by the computer for further analysis. Numerical processing of the acquired data consists of a fast Fourier transform (FFT), calibration in the frequency domain of both amplitude and phase and inverse fast Fourier transform (IFFT) after which the real calibrated waveforms are obtained. Measurements using derivative probes were carried out for the whole range of powers delivered by the RF generator. Before every measurement reflected power was checked and, if needed, adjusted to be less than 1% of the forward power.

Spatial profiles of the ion concentrations were measured using Hiden Analytical ESPION advanced Langmuir probe system which was placed side-on. The system has a linear motion drive which enables probe positioning with the minimal spatial resolution of 0.1 mm. Measurements were made in air at 100 mTorr. We have used a platinum probe tip, 5 mm long and 0.15 mm in diameter. Linear motion drive was used to position the probe at distances from 50.5 to 20.5 cm measured from the powered electrode. Measurements of $V–I$ curves were made for all those positions of the Langmuir probe. At every position 50 measurements were made each consisting on average of 10 scans with pre-cleaning for each measurement. Afterwards, the $V–I$ curves were smoothed and data were processed using HidenESPSoft. Orbit motion-limited theory implemented in the standard HIDEN ESPion software was applied. Mass of N_2^+ ion was assumed in the analysis thus giving an effective density where contributions of other ions are projected onto that of N_2^+.

Spatial profiles of the neutral oxygen atoms were measured using nickel catalytic probe (polycrystalline nickel disc with purity $\sim$99.8%). The probe covered the same distances from the powered electrode where the ion concentrations were measured. The catalytic probe was moved even further away from the powered electrode than the reactor
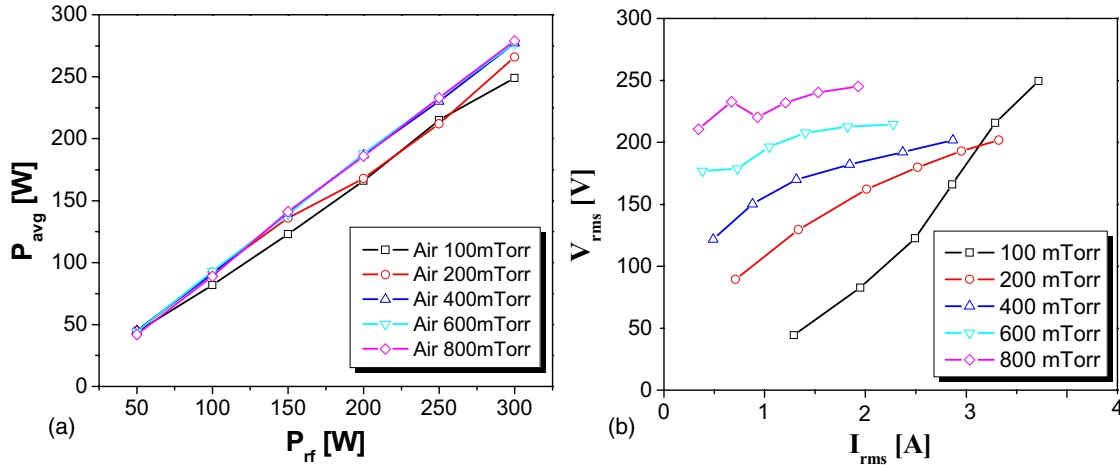
Figure 2. (*a*) Average power delivered to the plasma measured by derivative probes (P_{avg}) as a function of power given by the RF generator (P_{rf}). (*b*) Volt–ampere characteristics of the discharge measured by derivative probes. Gas was air at 100, 200, 400, 600 and 800 mTorr.

walls. Namely, it was necessary to mount a cylindrical, stainless steel, side chamber (arm) which is perpendicular to the chamber wall in order to mount the probe and allow its movement. The chamber wall is 57.5 cm away from the electrode, and the catalytic probe was moved up to 6 cm inside the side tube. Measurements of oxygen concentrations were extended into the reactor side arm.

The asymmetry of the reactor introduces large differences in ion energies and fluxes near the powered electrode and near the grounded chamber wall due to different values of sheath potential drops:

$$\left(\frac{U_p}{U_g}\right) = \left(\frac{A_g}{A_p}\right)^k, \tag{1}$$

where U_p and U_g are sheath voltages and A_p and A_g are the areas of powered and grounded electrodes, respectively. Theoretically, k ranges from 1.25 to 4, and experimentally it is less than 2.5 [42]. The smaller the electrode area, the smaller is its capacitance, and therefore the corresponding potential drop is larger. On the other hand, the sheath thickness, which will also affect the capacitance and the voltage drops, may depend on the voltage across it, through Child's law. The problem needs to be solved self-consistently to obtain the voltages [43]. Pronounced gradients of ion energies and concentration appear at different distances from the powered electrode in our reactor. Therefore, the position of the substrate or the measuring probe will strongly affect the intensity of the positive ion bombardment of the substrate surface. The highest flux of ions and the highest energies will be associated with the bombardment of the smaller electrode (1) [42, 44].

3. Results and discussion

3.1. Electrical characterization of the reactor: power measurements and current–voltage characteristics

We first recorded current and voltage waveforms and then calculated the mean power as the time integral of their product. Dependence of the average power, measured by the derivative probes, on the power produced by the RF generator in air

for several pressures is given in figure 2(*a*). We can see that the dependence is linear and that most of the power is indeed delivered to the reactor. With the changing of pressure, the delivered power does not change significantly. The discrepancy increases with an increase in the power.

From the volt–ampere (V–A) characteristics shown in figure 2(*b*) we can conclude that the plasma is operating in the α regime judged by the almost linear V–A dependence. The differential impedance magnitude is decreasing with an increase in pressure (from 100 Ω down to 30 Ω). We can also see that the root mean square values (rms) of voltage are ranging from about 50 up to 250 V and that working voltages are increased with an increase in pressure of the working gas. On the other hand, rms values of current are decreased with an increase in the pressure, remaining in the range from 0.2 to 3.8 A.

As mentioned above, the dimensions of the reactor were selected to be such that it could accommodate processing of a standard width of the textile as used in the industry. It turned out that it was possible to achieve uniformity over the entire width of the textile and stable operation for hours without any sparking that often occurs at atmospheric pressure. Our experimental device that was used in our previous studies of textile treatment [30, 34, 35, 45] had 0.37 m diameter and length of 0.5 m. Thus, its volume is about 50 times smaller than the volume of the large size reactor. Nevertheless the large volume reactor was able to provide the same level of treatment of the surface with only an increase in 30–50% in power.

3.2. Influence of ion bombardment on heating of the catalytic probe and samples

There are two major reasons for performing Langmuir probe measurements in the main reactor chamber. The first one is to establish the flux of ions which determines the basic effect but if allowed to be excessive may damage the sample. Secondly, we need to estimate the contribution of ion bombardment to the heating of the catalytic probe. For that purpose we have measured spatial profiles in air at 100 mTorr at different

distances from the powered electrode. Ion bombardment, light quanta, radiation, accommodation of gaseous molecules, relaxation of metastable oxygen and ion recombination can significantly contribute to the heating of the probe, depending on the type of the discharge and operating conditions.

If we assume that the heating of the probe is only due to recombination of atomic oxygen and ion bombardment, then the heat dissipated at the probe surface is given by

$$P_{\text{heat}} = P_O + P_i = j_O \gamma W_d \pi r^2 + j_i W_i \pi r^2 \quad (2)$$

where P_O is the contribution due to the neutral oxygen atom recombination, P_i is the ion bombardment term, j_O is the neutral oxygen atom flux and j_i is the ion flux, γ is the coefficient for heterogeneous surface recombination of O atoms on the nickel surface with the value of 0.27 [46], W_d and W_i are the dissociation and first ionization energy of oxygen molecules and r is the nickel probe disc radius. Here, it is worth noting that our discharge is created in air, which can also produce neutral nitrogen atoms and other species including metastables. However, one should have in mind that the dissociation energy of N_2 is 9.75 eV, as compared with 5.12 eV for O_2. Additionally, the recombination coefficient for N atoms is also lower and is 0.1. Due to this reason, the dissociation of O molecules with dissociation energy of 5.12 eV is the most probable channel, and contributions of N atoms can be neglected in first approximation.

Neutral oxygen atom flux and ion flux are then given by

$$j_O = \tfrac{1}{4} n_O v_O; \qquad j_i = n_i v_i, \quad (3)$$

where n_O and n_i are the O atom and ion density, in the probe vicinity, respectively. v_O is the average of the absolute value of thermal velocity of O atoms, v_i is the Bohm velocity. The probe is being heated until the temperature saturates and then the discharge is turned off. At this moment heating and cooling rates of the probe are equal. The cooling rate is given by

$$P = mc_p \frac{\Delta T}{\Delta t}, \quad (4)$$

where m is the nickel disc mass, c_p its specific thermal capacity and $\Delta T / \Delta t$ is the absolute value of the temperature derivative just after turning off the discharge. It is important to note that by equating the heating and the cooling terms and taking into account only the neutral atom contribution, the concentrations are calculated as follows:

$$n = \frac{4mC_p}{v \gamma W_d \pi r^2} \frac{\Delta T}{\Delta t}. \quad (5)$$

Another important fact is that from the ratio of $j_i W_i / j_O \gamma W_d$ we can calculate the upper limit for the ion contribution to the heating of the electrode. The ion contribution to the energy of the electrode W_i is the sum of the kinetic energy which is gained in the sheaths and the ionization energy (the first ionization energy for O_2 molecule is 12 eV) [27]. Obviously, the ion kinetic energy in a strongly asymmetric discharge of this kind is going to be significantly different at different distances from the powered electrode, as mentioned before (1). From figures 3 and 4, we can see that the
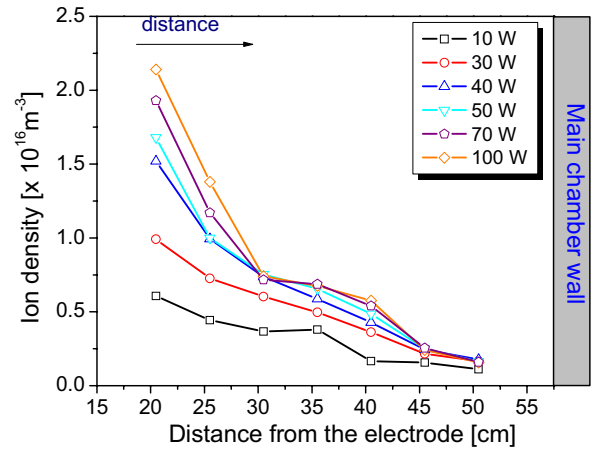

Figure 3. Spatial profiles of ions measured by the Langmuir probe in air at 100 mTorr and at different powers.
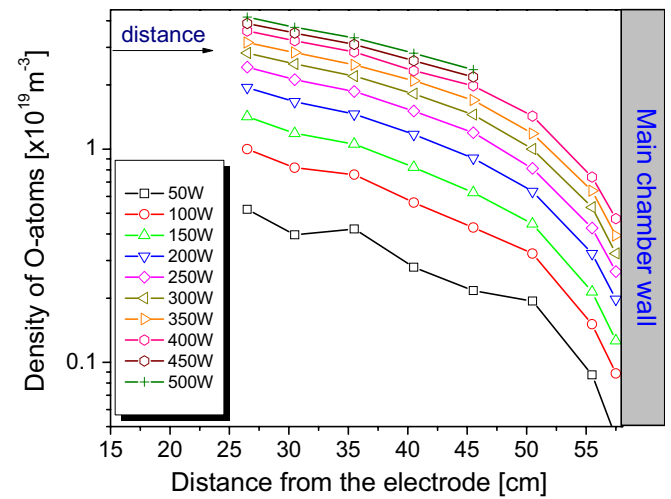

Figure 4. Concentrations of oxygen atoms measured by the catalytic probe in air at 100 mTorr at different powers.

ion concentrations are three orders of magnitude lower than the measured neutral atomic oxygen concentrations for low generator powers up to 100 W. We were not able to conduct proper Langmuir probe measurements for higher powers due to additional secondary discharge developing at the tip of the probe influencing our results, but we expect the same ratio to be maintained for powers higher than 100 W.

Ion measurements were performed in air plasma at 100 mTorr and at distances from the powered electrode of 20.5 cm up to 50.5 cm. Measured ion densities are between 10^{15} and 10^{16} m^{-3} (figure 3), whereas concentrations of neutral oxygen atoms were of the order of 10^{18}–10^{19} m^{-3} (figure 4). Ion and atomic oxygen concentrations are typically decreasing with the distance from the powered electrode, and increasing with the power.

Recombination coefficient of nickel is 0.27 for neutral atomic oxygen recombination while almost every ion (for example O^+, N^+, N_2^+, O_2^+, NO^+) reaching the probe surface recombines with probability 100% and contributes to the probe's heating. In the case of the symmetric CCP, the authors report that the ion contribution is about 2%, when

taking W_i to be 12 eV + 18 eV [26]. Having in mind that in the region close to the grounded electrode of the asymmetric CCP, the ion energies are lower than 18 eV [30], we can conclude that the contribution to heating of the catalytic probe due to ions is even lower than for the symmetric CCP. More precisely, the upper limit to the contribution to heating of the catalytic probe surface due to ions in our case ranges from 1.2% to 2%, as previously estimated. Unfortunately, due to the limited length of the catalytic probe we were not able to go very close to the powered electrode.

From the above results we can conclude that in our experiments the ion contribution to the heating of the catalytic probe surface is not substantial. In the same light, we can see that close to the main chamber wall neither ion energies (1) nor ion concentrations (see figure 3) are high and that the wall represents a drain for both species.

3.3. Radial dependence of atomic oxygen in cylindrical chamber and chamber extension

The dependence of oxygen atom densities with the distance from the powered electrode is influenced by the balance of production and losses. Having in mind cylindrical geometry of the reactor, atomic oxygen is produced in the plasma at close proximity to the powered electrode, while on the other hand recombination takes place predominantly at the surface of reactor walls. Atom recombination at the probe surface may, amongst other things, be affected by the vicinity and area of the reactor walls in the main chamber and the side tube.

The spatial profiles of oxygen atom densities in the main reactor and in the side arm are shown in figure 5. We cannot guarantee whether the reading of the atom density at the position of the chamber wall is the same as it is at the wall where there is neither side arm nor catalytic probe. Nevertheless the profiles are consistent with diffusion profiles with a small but appreciable reflection. As expected, at lower pressures the density is lower which is consistent with a longer mean free path.

The densities in the small tube continue decreasing but faster than in the main chamber. This is consistent with increased losses due to smaller size vessel and larger probability of reaching the walls. The observed profiles offer a possibility to control fluxes of reactive particles by placing samples at different distances from the powered electrode, even placing them inside the sidearm.

4. Conclusion

Plasma behaviour was studied in a large-volume (2.6 m^3) asymmetric CCP (industrial prototype) reactor of a simple design (with a side arm that is needed to mount probes). Two key properties of plasma for application in textile treatment, densities of ions (physical sputtering and damage to the surface) and oxygen atoms (chemical functionalization of surfaces) and electrical characteristics were measured. The wetting time achieved by this system was dramatically reduced. Since the wetting time after plasma treatment is extremely short and difficult to measure, we could not quantify these results,
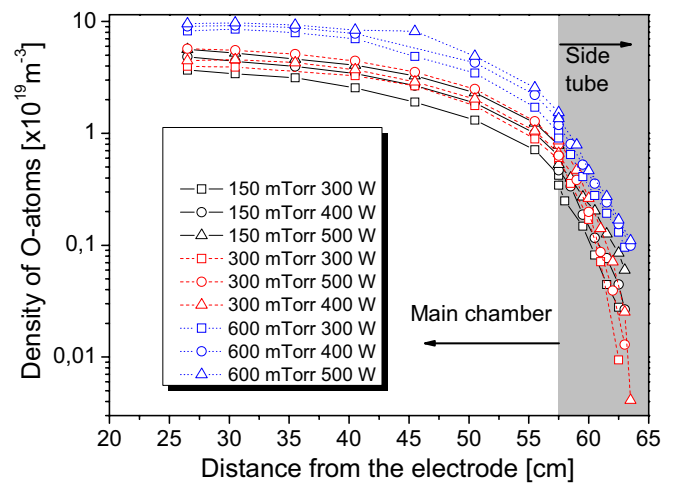
Figure 5. Spatial profiles of oxygen atoms measured by the catalytic probe in air in the main reactor vessel and in the side arm (tube positioned perpendicular to the chamber wall) in which the probe is mounted (the main chamber wall distance from the powered electrode is 57.5 cm). Measurements were made at different powers and gas pressures.

i.e. we could not compare the two treated samples. Although, we can state that the reduction in wetting time is similar and causes very fast wetting of the samples whereas plasma non-treated samples are very hydrophobic and water as well as dye solution does not penetrate the textile. Size of the reactor would allow continuous treatment of textile from the rolls of the standard width used in the industry.

Derivative probes used for electrical characterization of the reactor and plasma power measurement proved to provide reliable results. We found that our plasma operates in alpha mode and most of the generated power is dissipated inside the plasma [47]. Due to reactor design and its cylindrical asymmetric geometry, spatial distributions of ions and atomic oxygen are changing significantly as we move away from the powered electrode. Langmuir probe was used to measure the spatial profiles of ion densities in order to make sure that samples will not be damaged by ion bombardment and to calculate the ion contribution to the heating of the catalytic probe. Ion densities were of the order of 10^{16} m^{-3}. A nickel catalytic probe was used to measure the spatial profiles of atomic oxygen in air for a wide range of pressures. It is determined that in the main reactor vessel the atomic oxygen densities are of the order of 10^{19} m^{-3} and are almost linearly decreasing as we move away from the powered electrode. In the small side reactor the densities are 10^{18} m^{-3} or even 10^{17} m^{-3} depending on the proximity to the walls and pressure. Therefore, there is a wide range of atomic oxygen concentrations which can be delivered to the samples based on the position of treated material, inside the main vessel or perpendicular side arm. The results indicate that the diffusion is the mechanism governing profiles of neutral atoms. Atomic oxygen loss processes are dominantly affected by the recombination of atoms at the vessel/tube walls. Taking into account the power measured by the derivative probes, spatial profiles of ion densities measured by the Langmuir probe and spatial profiles of atomic oxygen optimal set of

J. Phys. D: Appl. Phys. **46** (2013) 075201

S Lazović *et al*

important plasma parameters can be obtained for optimization of sensitive material treatment according to required flux of ions or atoms to its surface. It is shown that high atomic density can be achieved even for lower powers, and therefore lower processing costs, by placing the sample close to the powered electrode but in that case one has to deal with somewhat higher ion energies.

Compared with other plasma sources investigated by the catalytic probes (MW and ICP for example) here we have two to four orders of magnitude lower oxygen atom densities due to its large size and smaller volume where the atoms are produced [48]. This property makes the cylindrical reactor appropriate for treatment of sensitive samples such as seeds, polymers and textile. The primary reason for the low measured densities is the distance from the powered electrode and a very large volume. At the same time one may select the geometry and position of the sample to control the fluxes. The energy of ions may also be controlled by selecting position (1) and also by biasing.

Acknowledgments

References

[1] Fridman A and Kennedy L A 2004 *Plasma Physics and Engineering* (New York: Taylor and Francis)

[2] Mahony C M O, Maguire P D and Graham W G 2005 Electrical characterization of radio frequency discharges *Plasma Sources Sci. Technol.* **14** S60–7

[3] Godyak V A 2011 Electrical and plasma parameters of ICP with high coupling efficiency *Plasma Sources Sci. Technol.* **20** 025004

[4] Kieft I E, Laan E P v d and Stoffels E 2004 Electrical and optical characterization of the plasma needle *New J. Phys.* **6** 149–63

[5] Gahan D, Daniels S, Hayden C, Scullin P, O'Sullivan D, Pei Y T and Hopkins M B 2012 Ion energy distribution measurements in rf and pulsed dc plasma discharges *Plasma Sources Sci. Technol.* **21** 024004

[6] Makabe T and Yagisawa T 2011 Low-pressure nonequilibrium plasma for a top-down nanoprocess *Plasma Sources Sci. Technol.* **20** 024011

[7] Roth C, Oberbossel G and Rudolf von Rohr P 2012 Electron temperature, ion density and energy influx measurements in a tubular plasma reactor for powder surface modification *J. Phys. D: Appl. Phys.* **45** 355202

[8] Chen F F and Chang J P 2003 *Lecture Notes on Principles of Plasma Processing* (Dordrecht/New York: Kluwer/Plenum)

[9] Makabe T and Petrović Z L 2006 *Plasma Electronics: Applications in Microelectronic Device Fabrication* (New York: Taylor and Francis)

[10] Dobrynin D, Fridman G, Friedman G and Fridman A 2009 Physical and biological mechanisms of direct plasma interaction with living tissue *New J. Phys.* **11** 115020

[11] Kong M G, Kroesen G, Morfill G, Nosenko T, Shimizu T, van Dijk J and Zimmermann J L 2009 Plasma medicine: an introductory review *New J. Phys.* **11** 115012

[12] Lazović S *et al* 2010 The effect of a plasma needle on bacteria in planktonic samples and on peripheral blood mesenchymal stem cells *New J. Phys.* **12** 083037

[13] Petrović Z L, Puač N, Lazović S, Maletić D, Spasić K and Malović G 2012 Biomedical applications and diagnostics of atmospheric pressure plasma *J. Phys.: Conf. Ser.* **356** 012001

[14] Puač N, Maletić D, Lazović S, Malović G, Đorđević A and Petrović Z L 2012 Time resolved optical emission images of an atmospheric pressure plasma jet with transparent electrodes *Appl. Phys. Lett.* **101** 024103

[15] Stefanović I, Kuschel T, Škoro N, Marić D, Petrović Z L and Winter J 2011 Oscillation modes of direct current microdischarges with parallel-plate geometry *J. Appl. Phys.* **110** 083310

[16] Ferreira J A and Tabarés F L 2007 Cryotrapping assisted mass spectrometry for the analysis of complex gas mixtures *J. Vac. Sci. Technol.* A **25** 246

[17] Gaboriau F, Cartry G, Peignon M-C and Cardinaud C 2006 Etching mechanisms of Si and SiO$_2$ in fluorocarbon ICP plasmas: analysis of the plasma by mass spectrometry, Langmuir probe and optical emission spectroscopy *J. Phys. D: Appl. Phys.* **39** 1830–45

[18] Malović G, Puač N, Lazović S and Petrović Z 2010 Mass analysis of an atmospheric pressure plasma needle discharge *Plasma Sources Sci. Technol.* **19** 034014

[19] Mozetić M, Ricard A, Babić D, Poberaj I, Levaton J, Monna V and Cvelbar U 2003 Comparison of NO titration and fiber optics catalytic probes for determination of neutral oxygen atom concentration in plasmas and postglows *J. Vac. Sci. Technol.* A **21** 369

[20] Mozetič M, Cvelbar U, Vesel A, Ricard A, Babic D and Poberaj I 2005 A diagnostic method for real-time measurements of the density of nitrogen atoms in the postglow of an Ar–N$_2$ discharge using a catalytic probe *J. Appl. Phys.* **97** 103308

[21] Gaboriau F, Cvelbar U, Mozetic M, Erradi A and Rouffet B 2009 Comparison of TALIF and catalytic probes for the determination of nitrogen atom density in a nitrogen plasma afterglow *J. Phys. D: Appl. Phys.* **42** 055204

[22] Labazan I and Milošević S 2004 Determination of electron density in a laser-induced lithium plume using cavity ring-down spectroscopy *J. Phys. D: Appl. Phys.* **37** 2975–80

[23] Makabe T and Petrović Z L 2002 Development of optical computerized tomography in capacitively coupled plasmas and inductively coupled plasmas for plasma etching *Appl. Surf. Sci.* **192** 88–114

[24] Drenik A C U, Vesel A and Mozetič M 2005 *Inform. MIDEM* **35** 85

[25] Mozetič M, Vesel A, Cvelbar U and Ricard A 2006 An iron catalytic probe for determination of the O-atom density in an Ar/O$_2$ afterglow *Plasma Chem. Plasma Process.* **26** 103–17

[26] Primc G, Zaplotnik R, Vesel A and Mozetič M 2011 Microwave discharge as a remote source of neutral oxygen atoms *AIP Adv.* **1** 022129

[27] Vrlinic T, Mille C, Debarnot D and Poncin-Epaillard F 2009 Oxygen atom density in capacitively coupled RF oxygen plasma *Vacuum* **83** 792–6

[28] Gomez S, Steen P G and Graham W G 2002 Atomic oxygen surface loss coefficient measurements in a capacitive/inductive radio-frequency plasma *Appl. Phys. Lett.* **81** 19

[29] Kitajima T, Noro K, Nakano T and Makabe T 2004 Influence of driving frequency on oxygen atom density in O$_2$ radio frequency capacitively coupled plasma *J. Phys. D: Appl. Phys.* **37** 2670–6

[30] Puač N, Petrović Z L, Radetić M and Djordjevic A 2005 Low pressure RF capacitively coupled plasma reactor for modification of seeds, polymers and textile fabrics *Mater. Sci. Forum* **494** 291–6

[31] Kitajima T, Takeo Y, Nakano N and Makabe T 1998 Effects of frequency on the two-dimensional structure of capacitively coupled plasma in Ar *J. Appl. Phys.* **84** 5928

[32] Kitajima T, Takeo Y, Petrović Z L and Makabe T 2000 Functional separation of biasing and sustaining voltages in two-frequency capacitively coupled plasma *Appl. Phys. Lett.* **77** 489

[33] Gahan D, Daniels S, Hayden C, Sullivan D O and Hopkins M B 2012 Characterization of an asymmetric parallel plate radio-frequency discharge using a retarding field energy analyzer *Plasma Sources Sci. Technol.* **21** 015002

[34] Ilić V, Šaponjić Z, Vodnik V, Lazović S, Dimitrijević S, Jovančić P, Nedeljković J M and Radetić M 2010 Bactericidal efficiency of silver nanoparticles deposited onto radio frequency plasma pretreated polyester fabrics *Indust. Eng. Chem. Res.* **49** 7287–93

[35] Mihailović D, Šaponjić Z, Radoičić M, Lazović S, Baily C J, Jovančić P, Nedeljković J and Radetić M 2011 Functionalization of cotton fabrics with corona/air RF plasma and colloidal TiO(2) nanoparticles *Cellulose* **18** 811–25

[36] Živković S, Puač N, Giba Z, Grubišić D and Petrović Z L 2004 The stimulatory effect of non-equilibrium (low temperature) air plasma pretreatment on light-induced germination of *Paulownia tomentosa* seeds *Seed Sci. Technol.* **32** 693–701

[37] Morent R, De Geyter N, Verschuren J, De Clerck K, Kiekens P and Leys C 2008 Non-thermal plasma treatment of textiles *Surf. Coat. Technol.* **202** 3427–49

[38] Hrunski D, Grählert W, Beese H, Kilper T, Gordijn a and Appenzeller W 2009 Control of plasma process instabilities during thin silicon film deposition *Thin Solid Films* **517** 4188–91

[39] Cvelbar U, Mozetič M, Babič D, Poberaj I and Ricard A 2006 Influence of effective pumping speed on oxygen atom density in a plasma post-glow reactor *Vacuum* **80** 904–7

[40] Miller P A, Anderson H and Splichal M P 1992 Electrical isolation of radiofrequency plasma discharges *J. Appl. Phys.* **71** 1171–6

[41] Puač N, Petrović Z, Živković S, Giba Z, Grubišić D and Đorđević A 2005 *Plasma Processes and Polymers* ed R d'Agostino *et al* (Weinheim: Wiley)

[42] Koenig H R and Maissel L I 1970 Application of Rf discharges to sputtering *IBM J. Res. Dev.* **14** 168–71

[43] Lieberman M A and Lichtenberg A J 2005 *Principles of Plasma Discharge and Materials Processing* (Hoboken, NJ: Wiley)

[44] d'Agostino R, Favia P and Fracassi F 1997 *Plasma Processing and Polymers* vol 346 (Dordrecht: Kluwer)

[45] Gorenšek M, Gorjanc M, Bukošek V, Kovač J, Petrović Z and Puač N 2010 Functionalization of Polyester Fabric by Ar/N$_2$ Plasma and Silver *Textile Res. J.* **80** 1633–42

[46] Šorli I and Ročak R 2000 Determination of atomic oxygen density with a nickel catalytic probe *J. Vac. Sci. Technol.* A **18** 338

[47] Savić M, Radmilović Radenović M, Šuvakov M, Marjanović S, Marić D and Petrović Z L 2011 On explanation of the double-valued Paschen-like curve for RF breakdown in argon *IEEE Trans. Plasma Sci.* **39** 2556–7

[48] Balat-Pichelin M and Vesel A 2006 Neutral oxygen atom density in the MESOX air plasma solar furnace facility *Chem. Phys.* **327** 112–8

FULL PAPER

Activity of catalase enzyme in *Paulownia tomentosa* seeds during the process of germination after treatments with low pressure plasma and plasma activated water

Nevena Puač[1] (ORCID) | **Nikola Škoro**[1] | **Kosta Spasić**[1] | **Suzana Živković**[2] |
Milica Milutinović[2] | **Gordana Malović**[1] | **Zoran Lj. Petrović**[1,3]

[1] Institute of Physics, University of Belgrade, Pregrevica 118, 11080 Belgrade, Serbia

[2] Institute for Biological Research "Siniša Stanković", University of Belgrade, Bulevar despota Stefana 142, 11060 Belgrade, Serbia

[3] Serbian Academy of Sciences and Arts, Knez Mihailova 35, 11000 Belgrade, Serbia

Correspondence
Institute of Physics, University of Belgrade, Pregrevica 118, 11080 Belgrade, Serbia.
Email: nevena@ipb.ac.rs

In this work we present results of two significantly different types of plasma treatment on *Paulownia tomentosa* Steud. seeds. In the first type, seeds were directly treated in low-pressure plasma and then imbibed with distilled water. In the second type, an atmospheric pressure plasma was used for obtaining plasma activated water (PAW) which is then used for imbibition of seeds. The CAT activity and protein content is evaluated during 4 d following the imbibition process, i.e., immediately after the phytochrome activation and in the 3 subsequent days. Comparison of results of treated seeds to the control group allows to correlate the enzyme activity and protein content during the initial stages of germination with plasma treatment types and treatment conditions.
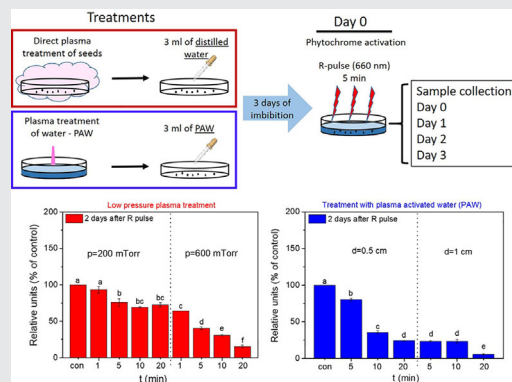
KEYWORDS

catalase, non-equilibrium plasma, plasma activated water, seed germination

1 | INTRODUCTION

Non-equilibrium plasmas for decades played an important role in treatments of various types of materials in order to modify roughness, hydrophobicity, produce coatings, polymerization, nanostructuring, increase the active area for absorbed dyes on textile surface, etc.[1–6] The choice which plasma system will be used is determined mainly by the type of the sample and the effect that plasma needs to achieve.

Another very important point in favor of plasmas is that they are environmentally friendly and, in most cases, cost efficient solutions that can supplement or replace in total classical treatments. Lately, the driving force for development of plasma sources, especially those that operate at atmospheric pressure, is the expansion of biomedical applications of plasmas. Low temperature plasmas so far have been successfully used for sterilization, wound healing, blood coagulation, cancer treatment, increasing of differentiation,

and proliferation of normal and human stem cells, stomatology, dermatology, and treatment/production of biocompatible materials.[7–14] Applications of these devices is accompanied by their detailed characterization by various diagnostic techniques[5,15,16] as well as comprehensive modeling that describe plasma behavior and chemistry, especially chemistry of reactive oxygen and nitrogen species (RONS) production that have key importance in biomedical applications.[4,17–24]

In recent times, new and fast developing field of low temperature plasma applications is plasma agriculture (application of plasmas for different aspects of agriculture and food industry). It was shown that both low pressure and atmospheric pressure plasmas can be successfully used in stimulation of seed growth, increase of germination percentage and decontamination, breaking of dormancy or increase in the length of seed sprout.[25–34] Plasma treatment of seeds became one of the starting points in opening of a wide area of applications of plasmas in agriculture and related biotechnologies. Nowadays, this list is much wider including treatments of seeds, soil, usage of plasma activated water, etc.[35–41]

In direct plasma treatments, i.e. where seeds are in direct contact with plasma or afterglow, the surface of seeds undergoes a variety of changes. During the plasma treatment, depending on the plasma conditions, the surface is activated so other functional groups can be attached (-COOH, -COH, -COO, -NH$_2$, -OH, -NO, etc.). Also, during the treatment seed surface is etched and, at the same time, decontaminated from various types of microbes. As a result the surface contact angle is reduced and seeds' surface changes from hydrophobic to hydrophilic.[42,43] The main species responsible for this type of changes are neutrals and ions of nitrogen and oxygen, especially O(^{3}P), O$_2$($^1\Delta_g$), O$_3$, NO, N, O(^{1}D) and O$_2^-$ ion, which is signaling molecule in most of the cell processes. Lately, as an alternative to the direct plasma treatment of seeds and plants, application of water treated by plasma, the plasma activated water (PAW), gives similar results in the increase of germination percentage, decontamination of both seeds and plants and faster growth.[44–46] The reason for these enhancement lies in the fact that in comparison to regular water PAW contains large amounts of chemically active species produced in plasma and at the plasma-liquid interface. These species are transferred from the interface volume to the liquid bulk and are able to trigger desired responses in biological samples. Some of the most important species appearing in the liquid bulk of PAW that are involved in triggering cell mechanisms are OH, O, NO, H, H$_2$O$_2$, NO$_2^-$, O$_2^-$, NO$_3^-$, OH$^-$.[47–50] In this paper, we want to compare the effects of these two significantly different types of treatments on the seeds of model plant *P. tomentosa* Steud. To accomplish this we have used a low pressure radio-frequency (RF) plasma system for direct treatment of seeds and an atmospheric pressure plasma jet (APPJ)[51] for treatment of distilled water in order to obtain PAW which is then used for imbibition of the seeds. In addition to being a model plant *P. tomentosa* is a viable agricultural product often used in medical supplements and as addition to alcoholic drinks.

Seeds of *P. tomentosa* are positively photoblastic and their germination is phytochrome-controlled. The light requirement for maximum germination may vary from brief exposure to several hours of red light, depending on seed maturation conditions.[52] A large number of RONS are continuously produced during seed and plant development, from embryogenesis to germination.[53] However, cells have evolved protective mechanisms in order to control free radical-induced cellular damage.[54]

Process of *P. tomentosa* seeds germination consists of three phases: imbibition, the phase of phytochrome activity and the phase of radicle protrusion and elongation. The optimum imbibition time is 3 d. Previous findings showed that a 5 min illumination with red light (660 nm) is sufficient for the phytochrome activation, the phase that lasts from 48 to 72 h. The processes following, including radicle protrusion, require several days after which germination is completed.[52,55,56]

In the experiments that will be presented in this paper we have investigated the early phase of germination, preferentially immediately after the light treatment and up to 3 d after the phytochrome activation, through CAT enzyme protein content and activity. Catalase (CAT, EC 1.11.1.6) is a tetrameric protein found in all aerobic organisms that catalyzes the dismutation of H$_2$O$_2$ into water and oxygen.[57] CAT represents one of the several cellular antioxidant defenses that play an important role in scavenging reactive oxygen species (ROS).[58] It was shown that, particularly in oily seeds, CAT is very important in the early germination events because it removes H$_2$O$_2$ produced during β-oxidation of the fatty acids.[59]

Increased generation of ROS seems to be a common feature of the early germination phase, which is the critical step of the process, since it involves activation of a regulatory system controlled by intrinsic (i.e., dormancy) and extrinsic (i.e., environmental conditions, such as temperature, oxygen, and water availability) factors.[53]

Plasma treatment has been found to promote seedling growth, increase proline concentration as well as activities of superoxide dismutase (SOD) and peroxidase (POD) in wheat seedlings under drought stress.[60] Similar observations have been made for oilseed rape seedlings, confirming that SOD and CAT activities were significantly increased after cold plasma treatment. Jiang et al.[61] reported that cold plasma treatment increases activities of POD, phenylalanine ammonia lyase (PAL), and polyphenol oxidase (PPO) of tomato under disease stress.[62] In spite of these studies of antioxidant enzymes activity in plasma treated seedlings and plants, evaluation of cold plasma effect on seeds during germination has not been investigated. Having in mind that plasma treatment of seed induces a significant increase in germination, it is of particular interest to study the effect of plasma on seeds.

Hydrogen peroxide is widely generated in plants and mediates various physiological and biochemical processes. As a signaling molecule, it can activate proteins/genes related to plant growth and development. Accumulation of hydrogen peroxide can reinforce cell walls through lignification. CAT activity is essential for the removal of the potentially toxic hydrogen peroxide produced under various stress conditions and then for the avoidance of oxidative-stress-related damage.[63] CAT is also important in fine-tuning the cellular H_2O_2 and then in modulating the related signaling pathways.[64,65]

In order to investigate the correlation between the plasma effects and CAT activity and protein content during the initial stages of germination process we performed direct treatment of *P. tomentosa* seeds in an asymmetrical capacitively coupled plasma (CCP) reactor under two different pressures and several treatment times. Apart from direct plasma treatment of seeds, an indirect treatment method was used where we treated distilled water by using APPJ in order to obtain PAW. After the treatment, PAW was used for imbibition of *P. tomentosa* seeds. In both cases, the CAT activity and protein content was evaluated during 4 d following the imbibition process, i.e., immediately after the phytochrome activation and in the 3 subsequent days.

2 | EXPERIMENTAL SECTION

2.1 | Low pressure plasma treatments

Low pressure treatments of seeds were performed in the cylindrically shaped capacitively coupled plasma (CCP) reactor with a powered electrode centrally positioned along the axis (see Figure 1). This asymmetrical system has ability to produce large volume of homogeneous plasma performing mild treatments of many seeds at the same time. Until now it was successfully used for different types of textile treatments[66,67] and in treatments of seeds and commercial grains for disinfection and to increase the germination percentage.[26,27,68] It was previously characterized in more detail and also the PIC model was used to estimate the main parameters of plasma treatments.

Main goal in construction of this RF plasma system was to achieve homogeneous plasma in large volume with the low energy of ions that bombard the grounded electrode that serves as sample holder. This was achieved by using large surface ratio between the powered and grounded electrode ($A_{pow}/A_{gnd} = 700$). The results obtained from the PIC simulation show us that the energy of ions impinging the grounded electrode and the samples are around 1–2 eV. The samples are positioned on the grounded electrode and due to their small size we can say that they are positioned in the plasma sheath. The estimation of the sheath thickness obtained from the PIC simulation is around 2 cm at the
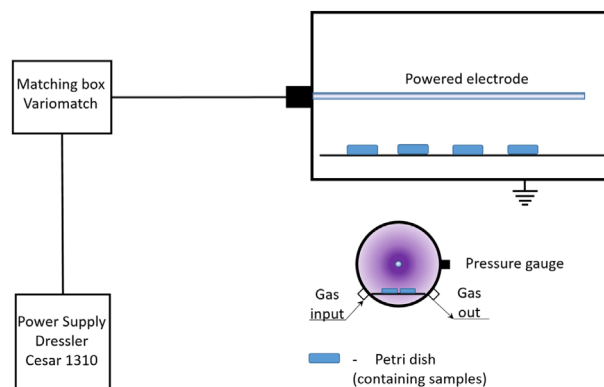
FIGURE 1 Schematics of the experimental set-up

grounded electrode. At the same time the electrical field at this electrode does not exceeds 75 V/cm. The averaged concentration of oxygen ions given by PIC analysis is $\sim 10^{15}$ m^{-3}.[69,70] The concentration of neutral oxygen atoms obtained by using catalytic probe in the same chamber geometry, but larger in scale, is of the order of 10^{19} m^{-3}. It was shown that the concentration of ions coincides with the results obtained by PIC simulation ($\sim 10^{15}$ m^{-3}). Mass spectrometry measurement revealed that the main ions in the discharge are O^-, O_2^-, O_2^+, and O^+. But the most important is the presence of the atomic and molecular oxygen metastables, especially $O_2(^1\Delta_g)$. As with other species that concentration of excited and metastable increases with the increase of working pressure.[71]

The length and diameter of the chamber are 46 and 37.5 cm, respectively. Chamber wall, which serves as the grounded electrode, is made of stainless steel while the powered electrode is made of aluminum. The powered electrode is axially placed, with length of 40 cm and diameter of 1.4 cm. The electrode is powered by RF signal at 13.56 MHz through automatically adjusting matching network. The power during the treatments was kept constant at 100 W given by RF power supply (Dressler Cesar 1310).

The platform for holding samples is positioned 13 cm bellow powered electrode. Since it is connected to the chamber wall it is also electrically grounded. A door mounted on one side of the cylindrical chamber provides an easy access and allows positioning of samples on the holder.

During all treatments flow of the gas was controlled by a flow controller connected to the gas inlet of the chamber while the exhaust line was connected to the mechanical pump. Here we need to emphasize that only mechanical pump was used. Therefore, the baseline pressure that could be reached was 20 mTorr which implies that certain amount of impurities (air, in particular) were present. Pressure in the chamber was measured by a capacitive gauge attached to one of the chamber ports.
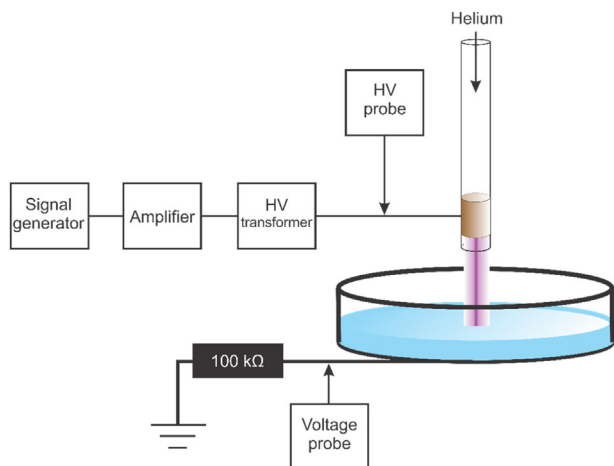
Treatments were performed in oxygen at pressures of 200 and 600 mTorr which, with a constant pumping speed,

corresponded to gas flows of 80 and 435 sccm. For each pressure four different treatment times were engaged: 1, 5, 10, and 20 min. During the treatments four Petri dishes (6 cm in diameter), each containing 100 seeds, were positioned on the platform inside the chamber. After the end of the treatment, the seeds were immediately taken out of the chamber and transferred to other sterile Petri dishes. The imbibition of the treated seeds was performed by using 3 ml of distilled water.

2.2 | Atmospheric pressure plasma treatments – Plasma Activated Water

We have used a standard atmospheric pressure plasma jet (APPJ)[51,72,73] for treatments of distilled water (see Figure 2). After the treatments, the obtained plasma activated water (PAW) was used for imbibing the *P. tomentosa* seeds. The design of the APPJ used in the experiments is simple and it consists of a glass tube with the electrode made of copper tape wrapped around the tube 5 mm from its end. The outer and inner diameters of the glass tube were 6 and 4 mm, respectively. The electrode was connected to a high voltage sinusoidal signal of 50 kHz that allows plasma to ignite immediately after the signal is turned on. The high voltage signal is obtained by home-made power supply system consisting of a function generator (PeakTech DDS Function Generator 4025), a home-made amplifier, and a high-voltage transformer.

To allow operation of plasma in glow regime,[16,74] He gas was flown through the tube with the rate of four slm. For treatments of water, the jet was positioned vertically with a glass Petri dish underneath. At the bottom of the dish we placed copper tape that was connected to the ground through a 100 kΩ resistance. This electrical circuit permits monitoring of the discharge current going to the ground by measuring the voltage drop on the resistor. At the same time, high-voltage probe connected to the powered electrode measures voltage supplied to the plasma jet. To produce plasma activated water we placed 12 ml of distilled water into the Petri dish (6 cm in diameter). The distances between the end of the glass tube of the jet and the water surface used in treatments were 0.5 and 1 cm. For both distances the applied voltage was kept constant at $6\,kV_{Peak-to-Peak}$. and measured current was $6\,mA_{Peak-to-Peak}$ for 0.5 cm distance and $4\,mA_{Peak-to-Peak}$ for the distance of 1 cm. The water volume after treatments was checked and found to be the same as the initial. Treatment times were 5, 10, and 20 min.

In order to characterize PAW we have measured pH and dissolved oxygen content immediately after the treatment. Dissolved oxygen content analysis measures the amount of gaseous oxygen (O_2) dissolved in an aqueous solution. For the pH measurements we have used Hanna Instruments HI1131B pH electrode with HI5522 controller and for the percentage of dissolved oxygen in water Hanna Instruments DO electrode HI764080 powered by HI2004 unit.

2.3 | Plant material and seed treatment

Seeds of the empress tree (*P. tomentosa* Steud.) were collected during 2015 in the Garden of the Institute for Biological Research "Siniša Stanković," University of Belgrade, and stored at room temperature until use. Batches of 100 seeds (plasma pre-treated or not) or 200 seeds (PAW treated or not) were placed in Petri dishes (6 cm in diameter) and imbibed with 3 ml of distilled water or plasma treated water, respectively. Germination was performed at $25 \pm 2\,°C$, in darkness. Seeds were induced to germinate with a 5 min red light pulse (660 nm, Philips TL 20/15 fluorescent tubes with 3 mm plastic Röhm & Haas filters, No. 501; fluence rate $3.54\,\mu mol\,m^{-2}\,s^{-1}$) applied after 3 d of imbibition.[52] Seed samples were taken subsequently during next 4 d, in 24 h intervals, weighted and stored at $-70\,°C$ until further analysis. A weak green safelight was used for manipulations in the dark. All experiments were repeated twice, with 3–5 replicates each. The schematics of the procedure for the sample collection is given in Figure 3.

2.4 | Protein extraction

P. tomentosa seeds (about 0.025 g FW) were grounded in liquid nitrogen with a mortar and pestle and homogenized in 1 ml of potassium phosphate buffer (100 mM, pH 7.5) containing 2 mM PMSF, 0.5 mM EDTA, 0.5% Triton X–100, and 2% (w/v) polyvinylpolypyrrolidone (PVPP). The homogenates were centrifuged at $14000 \times g$ for 20 min, at $+4\,°C$. The supernatant was used for assays. Protein content in seed extracts was determined according to Bradford[75] using bovine serum albumin as a standard.

FIGURE 2 Experimental set-up for treatment of distilled water
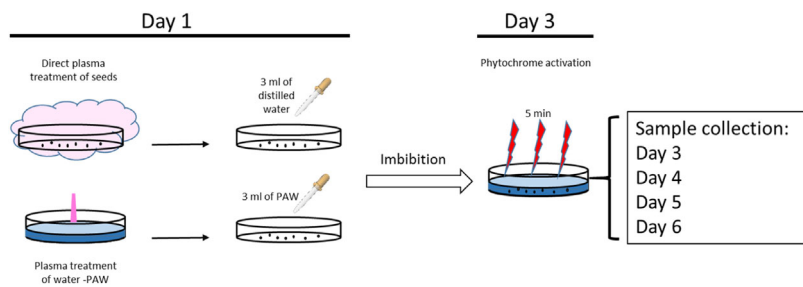
FIGURE 3 The experimental procedure for collecting the samples for enzyme analysis

2.5 | Native polyacrylamide gel electrophoresis and enzyme activity staining

Proteins were separated on the 10% non-denaturing poly-acrylamide gel. Electrophoresis was performed at +4 °C for 2.5 h, at constant current of 120 V using Mini-Protein II system (Bio-Rad, Richmond, CA). Equal amounts of proteins (30 µg) were loaded on gels. Gels were stained for CAT activity according to Woodbury et al.[76]

2.6 | SDS-PAGE and immunoblotting

Samples for sodium dodecyl sulfate polyacrylamide gel electrophoresis (SDS-PAGE) were dissolved in the equal volume of Laemmli buffer.[77] Separation of proteins was performed at room temperature using Mini-Protein II system (Bio-Rad, Richmond, CA) for 50 min at 200 V. Equal amounts of proteins (15 µg) were loaded on 10% SDS polyacrylamide gels. For detecting molecular weight of separated proteins, colored molecular weight markers 10–260 kDa (SpectraTM Multicolor Broad Range Protein Ladder, Fermentas GmbH, Germany) were used. After separation, proteins were transferred electrophoretically (60 V for 1.5 h, at 4 °C) onto PVDF membranes (Bio-Rad, SAD) using Mini Trans-Blot Module (Bio-Rad, SAD). Membranes were blocked overnight at 4 °C in a solution of 10% (w/v) non-fat dry milk (NFDM; Nestle, USA) and probed with anti-catalase antibody (1:1000, AS09501; Agrisera Antibodies, Sweden), and goat HRP conjugated anti-rabbit IgG secondary antibody (1:20000, Ao545, Sigma Aldrich, St. Louis, USA). Secondary antibodies were visualized using an enhanced chemiluminescence detection system (ECL) and densitometrically quantified using ImageJ 1.32j software (W. Rasband, National Institute of Health, USA).

2.7 | Statistical analysis

Densitometry was performed on scanned gel and immunoblot images using the ImageJ gel analysis tool.[78] Statistical analysis was performed using Stagraphics software, version 4.2 (StatPoint, Inc. 1982–2006, USA). Differences among different treatments were tested using standard analysis of variance (ANOVA). The means were separated using Fisher's Least Significant Difference (LSD) post hoc test for $p \leq 0.05$. Treatments denoted by the same letter are not significantly different ($p \leq 0.05$).

3 | RESULTS AND DISCUSSION

3.1 | Low pressure plasma treatments

It was previously shown that asymmetrical CCP system described above can be successfully used in treatments of *P. tomentosa* seeds in order to increase percentage of germination. However, the effect of plasma on germination is affected by plasma parameters like electric field, power, time, pressure, and type of gas used in treatments.

It is well documented that electric field can positively influence germination.[79,80] On the other hand, detrimental effect can appear if seeds are exposed to electric field for a very long time or if the field is very strong.[79] In our case electric field (75 V cm^{-1}) influencing the samples is quite low comparing to the electric fields (up to several kV cm^{-1}) used in literature. We believe that influence of electric field is not significant and main effect is obtained through bombardment of the seed surface by reactive chemical species created in the plasma and accelerated by the electric field in the sheath.

Regarding the plasma power, it was shown that higher powers can induce damage to the seeds due to increased thermal effects and destruction of seed wall by particle bombardment. Therefore, for our chamber it was found that optimal treatment times are up to 10 min for power of 100 W.[26,27,66] Concerning the pressure, its changes affect densities and energies of particles present in plasma (the most important are reactive species such are O^-, O_2^-, O_2^+, O^+, and $O_2(^1\Delta_g)$). At lower pressures, densities of particles produced in plasma are lower, but they have higher energies due to fewer number of collisions, i.e., longer mean free paths.[4] Energies of ions are directly influenced by the pressure through the balance of energy gained from the field and dissipated in collisions. Fast neutral particles can be affected indirectly as those may be created by the charge exchange collisions with ions.[81]

In our case, we performed treatment at two pressures which are not far apart: 200 and 600 mTorr. Thus, the main difference between two pressures would be in higher particle densities (neutrals, radicals, and ions) that reach surface of treated seeds at 600 mTorr in comparison to the case of 200 mTorr. Taking into account all this, a set of plasma parameters close to the optimal for germination has been chosen in order to investigate the response of the CAT enzyme to the plasma treatments.
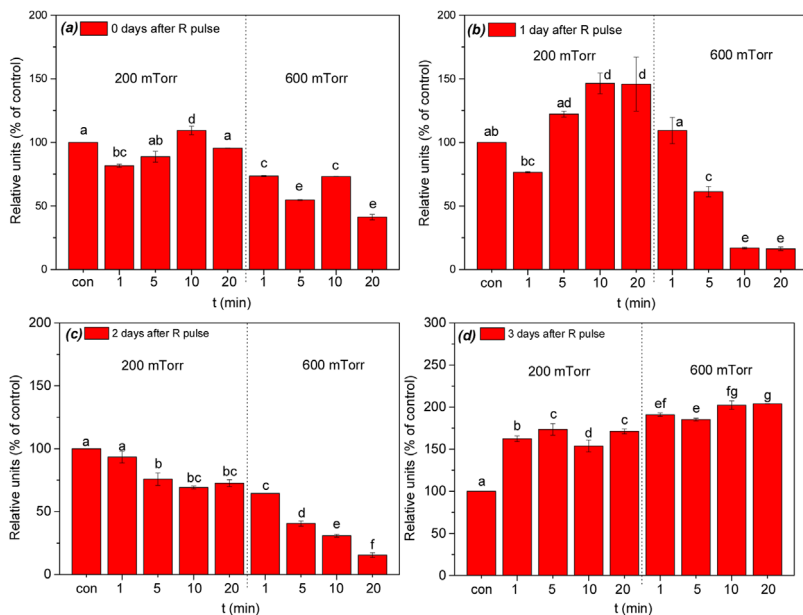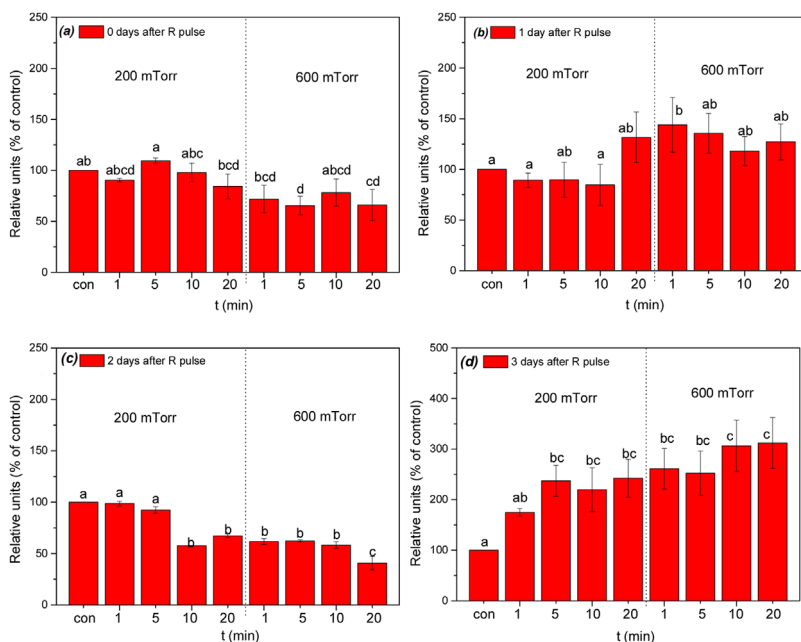
FIGURE 4 Catalase activity in plasma treated *P. tomentosa* seeds measured immediately (a), 1 d (b), 2 d (c), or 3 d after R light pulse (d). Results for different treatment times (t) and two pressures are shown. The band volume was recorded by using densitometric analysis. Data were normalized using control signal. Values are means obtained from three independent experiments shown with standard error. Treatments denoted by the same letter are not significantly different ($p \leq 0.05$) according to the Fisher's LSD test

As for the effect of the pressure on the seeds and their germination, the selected seeds do not have a hydrophobic protective seed coat so oxidization of the protective layer to allow water to penetrate the seed is not an issue. It has been postulated[26,27] that a deposition of different active molecules and radicals may promote germination and growth of these seeds mainly through their signaling functions in the cell. Thus the explanation of the effect must be sought in plasma chemistry leading to production of active species. Understanding, control, and optimization of the effects of plasmas depends on being able to connect the plasma chemical processes to the processes inside the cells of the seed. The effect of plasma should be small enough to promote the germination and not too large to have detrimental effect on the living cells.

We have measured both CAT protein content and CAT enzyme activity at the beginning of the germination process (immediately after activation of phytochrome) and in 3 subsequent days. The activity of CAT for samples treated for different times is shown in Figure 4. Relative intensity for each experimental band was calculated by normalizing the experimental absolute intensity to the corresponding control absolute intensity. One should bear in mind that the control group follows the entire process as other seeds with the exception of plasma treatment (see Figure 3). In other words, control groups have passed imbibition (3 d) then they were initiated by the R pulse and then subsequently taken for analysis in 4 subsequent days. Standard behavior of CAT enzyme activity in control samples of

P. tomentosa is observed and it increases after R light pulse. CAT is only one of the relevant enzymes that is responsible in early stages of germination and later on peroxidase becomes even more important. Both of these enzymes together with the related radicals play their part in a complex mechanism of germination that is being triggered by plasma. Thus, one cannot easily correlate activity of one enzyme to the efficiency of germination. While effects of plasma are similar and in the same direction as those reported earlier[26,27] results will strongly depend on the season, duration of storage, and other parameters. Thus we have to find optimal conditions for each batch. In addition we have improved performance of our plasma source in the meantime.

When comparing the effects of pressures on the enzyme activity measured immediately after the activation of the phytochrome (day 0), the samples treated in plasma at 600 mTorr of oxygen exhibit a higher reduction in CAT activity if compared to 200 mTorr treatments (see Figure 4(a)). On the contrary, for the treatment at 200 mTorr changes in the activity are small, seeds treated for 1 min show slightly lower activity, while the others show either similar (5 and 20 min) or slightly higher (10 min) CAT activity. Similar trends can be observed in the samples collected on day 1 (see Figure 4(b)) with a much larger increase of the activity at 200 mTorr. The treatments with higher pressure (600 mTorr) and longer treatment times (10 and 20 min) induce four times lower CAT activity compared to the untreated sample. At the same time for pressure of 200 mTorr we can see increase in the CAT activity as the treatment time increases. Two days after the R pulse the enzyme activity declines more or less linearly with increment of pressure and treatment time (see Figure 4(c)). Thus, CAT activity in seeds after 20 min treatment at 600 mTorr was nearly four times lower in comparison with control samples. However, 3 d after the R pulse the activity of CAT increased for both treatments, exhibiting 1.5–2 fold higher values in comparison with CAT activity measured in control samples (Figure 4(d)). *P. tomentosa* seeds are positively photoblastic, meaning that their germination is stimulated by light. After the imbibition (rapid initial water uptake) seeds were induced to germinate by red light pulse, and entered the next-plateau phase.[82] Plateau phase involves the reactivation of metabolism, including the resumption of cellular respiration, the biogenesis of mitochondria, DNA repair, the translation and/or degradation of stored mRNAs, the transcription and translation of new mRNAs, and the activation of antioxidant enzymes at the appropriate time.[83,84,85] Therefore, sequential expression of antioxidant enzymes has been considered to

FIGURE 5 Immunoblot analysis of catalase in *P. tomentosa* seeds, measured immediately (a), 1 d (b), 2 d (c), or 3 d after R light pulse (d). Results for different treatment times (t) and two pressures are shown. The band volume was recorded by using densitometric analysis. Data were normalized using control signal. Values are means obtained from three independent experiments shown with standard error. Treatments denoted by the same letter are not significantly different ($p \leq 0.05$) according to the Fisher's LSD test

be of particular importance for the completion of germination.[86,87] It is possible that a renewal of antioxidant system may be initiated with the repair of cell membranes and organelle development, which are required for complete germination and growth demands by the seedlings.[88] Increased CAT activity could be an indication of the cellular evaluated ROS, since the amount of CAT present in aerobic cells is directly proportional to the oxidative state of the cells.[89] Measurement of CAT activity may be a parameter to determine seed viability and germination as observed by Baily et al.[90]

With few exceptions, radicle extension through the structures surrounding the embryo is the event that terminates germination and marks the commencement of the seedling growth.[91] The time for this event to be completed varies from several hours to many weeks, depending on the plant species and the germination conditions. The present study shows a significant increase in the enzyme activity 3 d after R pulse (see Figure 4(d)), which can be associated with metabolic switch occurring in seeds between germination and subsequent post-germination phase. Apart from CAT, it was shown previously that another antioxidant enzyme peroxidase (POD) also has very important role in germination. In *P. tomentosa* seeds activity of POD is very low before the process of radicle protrusion begins, i.e., the activity is increased during later phases of germination. On the other hand, in germinated seeds and seedlings, POD activity

increases significantly.[92] Final result of seed germination process (measured as percent of germinated seeds) will be reflection of overall metabolic activity in seeds and young seedlings, including antioxidant enzymes activity (e.g., CAT, but also the activity of other enzymes).

Immunoblot analysis showed that only one isoform of 50 kDa is detected in all the samples and in Figure 5 we present the results of CAT protein content obtained for the same set of parameters as CAT activity. Germination process immediately and 1 d after the R light pulse resulted in an increase in CAT protein content, but with slight difference in comparison to the control seeds (Figure 5(a, b)).

Significant reduction in CAT content was observed 2 d after the phytochrome activation (see Figure 5(c)). Here we can observe a reduction in CAT protein content for longer treatment times at 200 mTorr and for all treatment times at 600 mTorr. Similar behavior was observed in the CAT activity (Figure 1(c)). It should be noted that enzyme content was by far the highest in treated seeds 3 d after the activation of phytochrome (about 2.5 fold greater then control samples) and remained more or less constant regardless of experimental conditions used in this study. Enhanced CAT protein content is in accordance with the increment in enzyme activity in germinating seeds showed in Figure 4(d). It must be remembered that immunoblot analysis gives indications about the synthesis of CAT subunits and does not necessarily reflect the enzyme activity.[93] This may explain why the slight apparent decrease or increase in protein content (Figure 5) was not correlated with the changes of CAT activity in the same batch of *P. tomentosa* seeds (Figure 4).
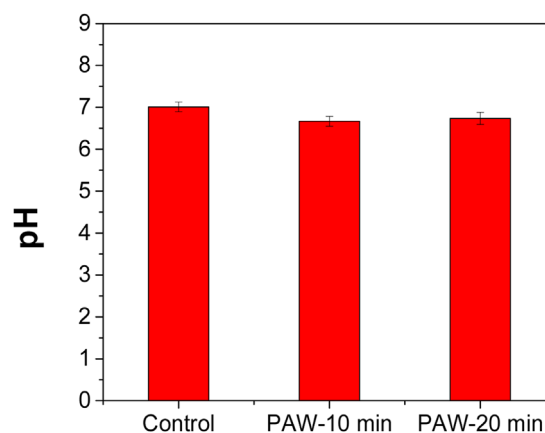
FIGURE 6 pH values of plasma treated water for two different treatment times. Distance from the edge of the glass tube of the plasma jet and water surface was 1 cm
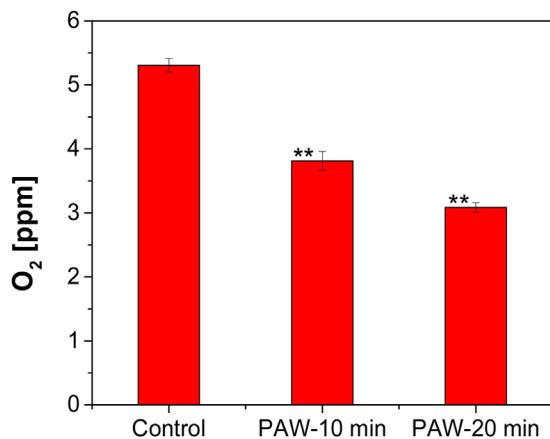
FIGURE 7 Dissolved oxygen content in treated water in the control sample and after the treatments. Distance from the edge of the glass tube of the plasma jet and water surface was 1 cm

3.2 | Atmospheric pressure plasma treatment of distilled water - PAW

Unlike the case of low pressure treatments where seeds were in direct contact with plasma, when it comes to APP treatments the seeds are only indirectly influenced by plasma through the imbibition with plasma activated water. CAT activity and protein content are more affected when plasma is

further away from the liquid for all durations. While this may be counter intuitive it could be the result of the liquid interrupting the plasma at closer proximities or it may result from the greater obstruction to the gas flow including more likely turbulence for smaller proximity. During the water treatment reactive species produced in the plasma are transported to the gas-liquid interface from where they can penetrate and/or induce chemical reactions and creation of new species in the bulk liquid.[47,94] Some of these species, like H_2O_2, O_2^-, NO_2^-, NO_3^-, have direct influence on processes in biological systems so changes in their concentration should affect enzyme activity. Before using PAW for imbibition of seeds, we have measured pH of treated water and amount of dissolved oxygen (DO) after plasma treatments. Measurements of pH were performed as described in experimental section and the results are presented in Figure 6.

In Figure 6 we can see that plasma does not change significantly the pH value of treated water. In other words, we kept plasma treatment within the limits of only small variations of pH value in order to avoid detrimental effect due to a significantly changed pH factor. Its value is slightly decreased, from $pH_{Ctrl} = 7$ to $pH_{treat} = 6.7$, after the treatments (regardless of treatment time). Gregory D. et al. showed that process of germination and seedling growth of *P. tomentosa* seeds is influenced if the pH values of the environment are below $pH = 5$.[95] If the pH values are in the range 6–7, the germination process and development of the seedling is not influenced. Similarly, the CAT activity in plants is pH-dependent.[96] Arabaci and Usluoglu showed that the CAT activity is significantly influenced if the pH value drops below 4.[97] Therefore, taking into account measured pH, our PAW used for imbibition of *P. tomentosa* seeds should have negligible influence on the enzyme activity and germination of seeds due to the change in pH.

Another parameter that was measured was oxygen content in the water before and after the treatment. The results are shown in Figure 7. We can see that plasma treatment reduces the oxygen content in water. The reduction of the oxygen content can be assigned to the presence of the helium flow.[98] The presence of He flow above the water surface reduces the partial pressure of O_2 and therefore reducing the solubility of oxygen in the water. The He flow used in the experiment is sufficient to create sparging effect and cause decrease of oxygen content.[99] With an increase of the treatment times at distance of 1 cm oxygen content is reduced by 40%. Similar result is observed at
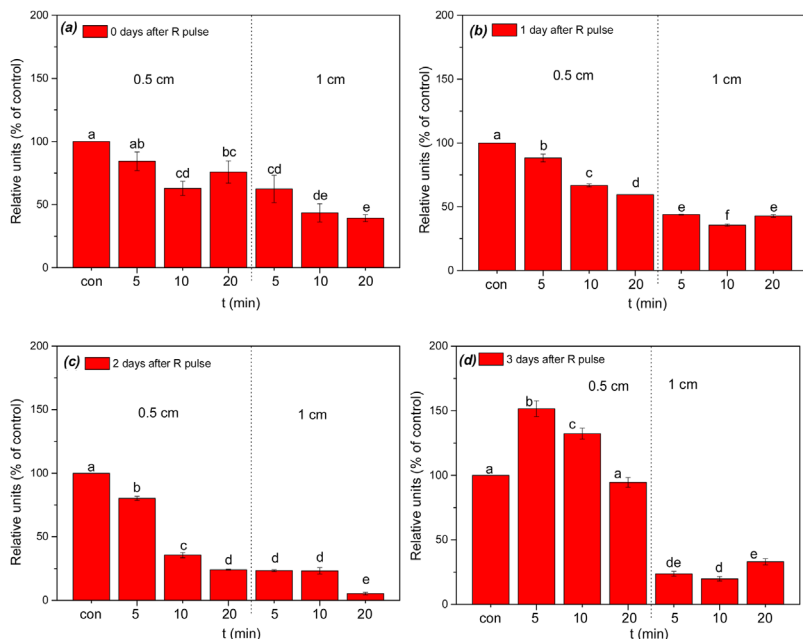
FIGURE 8 Catalase activity of *P. tomentosa* seeds germinated in plasma treated water, measured immediately (a), 1 d (b), 2 d (c), or 3 d after R light pulse (d). Results for different treatment times (t) to obtain PAW and two distances are shown. The band volume was recorded by using densitometric analysis. Data were normalized using control signal. Values are means obtained from three independent experiments shown with standard error. The values with the same letter indicate statistically homogenous groups ($p \leq 0.05$), as per Fisher's LSD test
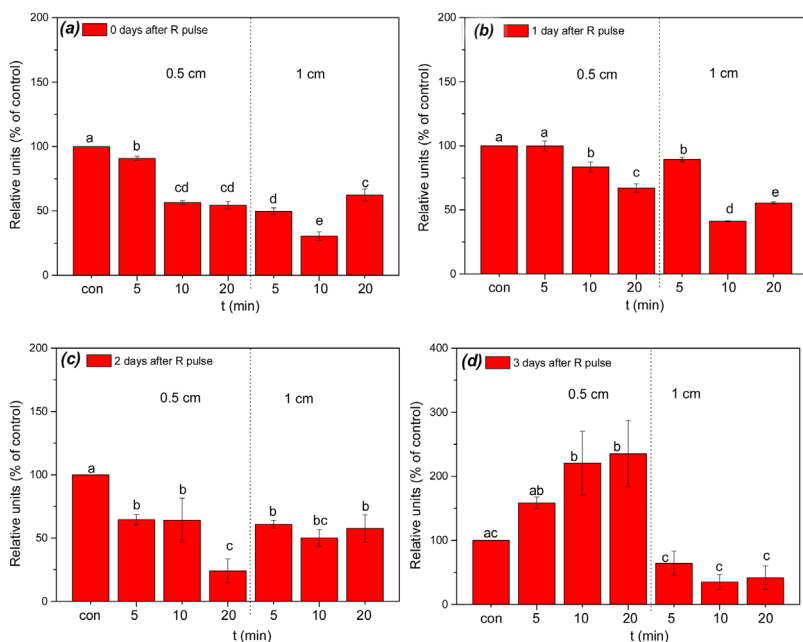
FIGURE 9 Immunoblot analysis of catalase in *P. tomentosa* seeds germinated in plasma treated water, measured immediately (a), 1 d (b), 2 d (c), or 3 d after R light pulse (d). Results for different treatment times (t) to obtain PAW and two distances are shown. The band volume was recorded by using densitometric analysis. Data were normalized using control signal. Values are means obtained from three independent experiments shown with standard error. Treatments denoted by the same letter are not significantly different ($p \leq 0.05$) according to the Fisher's LSD test

both distances. One has to bear in mind that oxygen content cannot be directly correlated with CAT activity due to the complexity of mechanisms involved.

Nevertheless, the seed germination is particularly sensitive to oxygen deficiency. The oxygen requirement for seeds typically varies depending on the species and their dormancy status.[100] During early phase of imbibition, seeds consume oxygen at slower rates, but at a much higher rate during radicle protrusion and hypocotyl growth. For example, Rajashekar and Baek show that oxygen limitation during imbibition can produce adverse effects which may last during early seedling growth and development. On the other hand, adding of the hydrogen peroxide reversed the effect of hypoxia resulting in normal hypocotyl elongation and stem growth.[101]

CAT enzyme activity obtained after the imbibition with PAW is shown in Figure 8. The samples were collected and the CAT activity is measured in the same manner as in the case of low pressure plasma treatments. As in the low-pressure case, the data were normalized to signal of the control group of the corresponding day. We can see that CAT activity in samples that were imbibed with PAW is lower than in the untreated samples immediately after the phytochrome activation and in 2 subsequent days (see Figure 8(a–c)). Also, the activity does not change significantly between day 0 and day 1 (see Figure 8(a, b)). In both cases it is decreased

maximally 2.5–3 times if compared with control samples. At day 2 we have even more reduction in CAT activity, going up to 10 times lower than untreated samples (see Figure 8(c)). In all cases, the reduction in the activity is higher for PAW treated with 1 cm distance between the plasma jet tube and water surface than for the case of 0.5 cm distance. The decrease in CAT activity within 3 d after R light pulse (Figure 8(d)) can be to some extent correlated to the decreased level of dissolved oxygen.

Significant increase in CAT activity occurred 3 d after the R light pulse at 0.5 cm treatment (Figure 8(d)), and it appears that this increment corresponds to the initial phase of post germination process, designated as phase of radicle protrusion and elongation, as already mentioned above.

Most likely CAT reserves are broken down during early stages of germination and de novo synthesis is occurring along with the radicle protrusion. It should be noted that ROS produced in PAW, especially hydrogen peroxide, could mitigate the adverse effects of hypoxia, both during imbibition and germination, as it can generate free oxygen and water by CAT and other catalysts including many transition metal ions present in the seeds.[102] When density of radicals increases it is likely that it would stimulate a greater production of CAT. If that production is insufficient to keep up with radicals, then depletion may occur. In addition, several radicals and other active species may participate in the kinetics of a particular enzyme. Active species produced in PAW, such as nitrate (NO_3^-) and nitrite (NO_2^-) ions most likely deposit on the seed surface, having an influence on seed germination as well as on the CAT activity. The same is true for hydrogen peroxide (H_2O_2). Although it could be expected that H_2O_2 concentration increases with treatment time, which would result in higher CAT activity, Figure 8 shows the opposite results (lower CAT values for longer treatment time of PAW), particularly for 0.5 cm treatment. Most likely higher content of ROS produced in the case of 0.5 cm treatment contributes to the higher levels of active species that could impair the enzyme activity. Precise regulation of H_2O_2 accumulation by cell antioxidant machinery is crucial to achieve a balance between oxidative signaling that promotes germination and oxidative damage that prevents or delays germination. According to "oxidative window" hypothesis proposed by Bailly et al.,[103] both lower and higher levels of ROS impair seed germination, and it is only possible within a critical range of concentrations.

One subunit of 50 kDa was present in *P. tomentosa* seeds in all treatments (Figure 9). The intensity of the band

corresponding to the CAT subunit appeared to decrease significantly for both treatment distances in comparison to the control sample, up to 3rd day after the R light pulse. A sharp decline in CAT protein content (1.5–2 fold) was noticed immediately after the R light pulse, for longer exposure treatments at 0.5 cm distance (10 and 20 min) and for all treatments at 1 cm distance between the jet and water surface, respectively (Figure 9(a)). CAT content in PAW treated seeds showed similar pattern on the 1st and 2nd day after the phytochrome activation (Figure 9(b, c)). Subsequent germination process (3 d after R pulse) resulted in an increase in CAT protein content in seeds after the 0.5 cm distance PAW treatment, but after the 1 cm PAW treatment it showed no significant difference compared to control seeds (Figure 9(d)).

One should bear in mind that different levels of enzymatic activity are not exclusively dependent on enzyme synthesis, but on various other factors as well. Thus, in future studies it would be advisable to take into account the differences between the effect of plasma treatment on germination and subsequent post-germination process of *P. tomentosa* seeds, suggesting that CAT activity at these stages may be subject to post-translational regulation.

4 | CONCLUSION

In this paper we have presented results of CAT enzyme activity and protein content obtained during the second phase of germination of *P. tomentosa* seeds (phase of phytochrome activity). Two significantly different types of plasma treatments were used. In the first type, the seeds were in direct contact with plasma and, in the second, atmospheric pressure plasma was used for obtaining PAW which is then applied to the seeds. In the former case, for direct plasma treatments, we have used low pressure RF discharge that was previously shown to be a good solution for increasing germination percentage of *P. tomentosa* seeds.[26,27] In the latter case, an APPJ was used in order to obtain PAW and immediately after the plasma treatment of water pH and dissolved oxygen content were measured. In our case the pH does not change significantly and stays in the range 6.5–7. Therefore, the processes related to germination and protrusion of radicle are not influenced by change in pH. On the other hand, the percentage of dissolved oxygen in the PAW is decreased to up to 40% compared to untreated water. This can influence the germination process in negative way by reducing the germination percentage, radicle protrusion, and slow early seedling growth and development. However, PAW contains H_2O_2 produced during plasma treatments which could substitute for O_2 deficiency and activate CAT genes for synthesis of new proteins.

We have observed standard behavior of CAT enzyme activity in control samples of *P. tomentosa* seeds. In these samples the CAT enzyme activity increases in the first 3 d after R light pulse. However, both plasma treatments used in this study, low-pressure plasma seed treatment and PAW, cause decrease in CAT activity/protein content in seeds compared to the control samples in time period up to 2 d after R light pulse. For low-pressure direct treatments decayed levels of CAT activity and protein content are correlated to the treatment times and pressures with the biggest change for 600 mTorr and longest treatment time. In the case of indirect PAW treatment we observed similar behavior at the longest distance and for the longest treatment time of PAW.

Differences in CAT activity/content noticed 3 d after the inductive light pulse strongly suggest that approximately 48 h after the R pulse *P. tomentosa* seeds enter the 3rd phase of germination process-phase of radicle protrusion and elongation, i.e., germination *sensu stricto* is terminated and post germination processes take place.[52] Moreover, discrete differences on the level of CAT content could be distinguished between the treatments used in this study.

REFERENCES

[1] P. Favia, G. Cicala, A. Milella, F. Palumbo, P. Rossini, R. d'Agostino, *Surf. Coat. Tech.* **2003**, *169*, 609.

[2] D. Mihailovic, Z. Saponjic, R. Molina, N. Puac, P. Jovancic, J. Nedeljkovic, M. Radetic, *ACS Appl. Mater. Interfaces.* **2010**, *2*, 1700.

[3] S. Vizireanu, S. D. Stoica, C. Luculescu, L. C. Nistor, B. Mitu, G. Dinescu, *Plasma Sources Sci. Technol.* **2010**, *19*, 034016.

[4] T. Makabe, Z. L. Petrovic, *Plasma Electronics: Applications in Microelectronic Device Fabrication.* CRC Press, Boca Raton, Florida, USA **2014**.

[5] J. Vasiljević, M. Gorjanc, B. Tomšič, B. Orel, I. Jerman, M. Mozetič, A. Vesel, B. Simončič, *Cellulose* **2013**, *20*, 277.

[6] D. Kontziampasis, G. Boulousis, A. Smyrnakis, K. Ellinas, A. Tserepi, E. Gogolides, *Microel. Eng.* **2014**, *121*, 33.

[7] D. Dobrynin, G. Fridman, G. Friedman, A. Fridman, *New J. Phys.* **2009**, *11*, 115020.

[8] M. Gherardi, E. Turrini, R. Laurita, E. De Gianni, L. Ferruzzi, A. Liguori, A. Stancampiano, V. Colombo, C. Fimognari, *Plasma Process. Polym.* **2015**, *12*, 1354.

[9] E. Sardella, R. Gristina, G. S. Senesi, R. d'Agostino, P. Favia, *Plasma Processes Polym.* **2004**, *1*, 63.

[10] M. Vandamme, E. Robert, S. Lerondel, V. Sarron, D. Ries, S. Dozias, J. Sobilo, D. Gosset, C. Kieda, B. Legrain, J. M. Pouvesle, *Int. J. Cancer* **2012**, *130*, 2185.

[11] R. Matthes, C. Bender, R Schlüter, I. Koban, R. Bussiahn, S. Reuter, J. Lademann, K. D. Weltmann, A. Kramer, *PLoS ONE* **2013**, *8*, 70462.

[12] Z. Machala, K. Hensel, Y. Akishev, *Plasma for Bio-Decontamination, BT Medicine and Food Security*. Springer Science & Business Media, Demanovska Dolina, Slovakia **2011**.

[13] S. Lazović, N. Puač, M. Miletić, D. Pavlica, M. Jovanović, D. Bugarski, S. Mojsilović, D. Maletić, G. Malović, P. Milenković, Z. Petrović, *New J. Phys.* **2010**, *12*, 083037.

[14] H. Tanaka, M. Mizuno, F. Kikkawa, M. Hori, *Plasma Med.* **2016**, *6*, 101.

[15] S. Große-Kreul, S. Hübner, S. Schneider, D. Ellerweg, A Von Keudell, S. Matejčík, J. Benedikt, *PSST* **2015**, *24*, 044008.

[16] M. Gherardi, N. Puač, D. Marić, A. Stancampiano, G. Malović, V. Colombo, Z. L. Petrović, *Plasma Sources Sci. Technol.* **2015**, *24*, 064004.

[17] A. Bogaerts, Z. Donko, K. Kutasi, G. Bano, N. Pinhao, M. Pinheiro, *Spectrochim. Acta B*. **2000**, *55*, 1465.

[18] K. Kutasi, B. Saoudi, C. D. Pintassilgo, J. Loureiro, M. Moisan, *Plasma Process. Polym.* **2008**, *5*, 840.

[19] M. J. Kushner, *J. Phys. D* **2005**, *38*, 1633.

[20] M. S. Benilov, G. V. Naidis, *IEEE Trans. Plasma Sci.* **2003**, *4*, 488.

[21] N. Škoro, N. Puač, S. Lazović, U. Cvelbar, G. Kokkoris, E. Gogolides, *J. Phys. D* **2013**, *46*, 475206.

[22] Z. L. Petrović, S. Dujko, D. Marić, G. Malović, Ž. Nikitović, O. Šašić, J. Jovanović, V. Stojanović, M. Radmilović-Radenovic, *J. Phys. D* **2009**, *42*, 194002.

[23] R. D. White, R. E. Robson, S. Dujko, P. Nicoletopoulos, B. Li, *J. Phys. D* **2009**, *42*, 194001.

[24] M. Savic, M. Radmilovic-Radjenovic, M. Suvakov, S. Marjanovic, D. Maric, Z. L. Petrovic, *IEEE Trans. Plasma Sci.* **2011**, *39*, 2556.

[25] B. Šerá, V. Straňák, M. Šerý, M. Tichý, P. Špatenka, *Plasma Sci. Technol.* **2008**, *10*, 506.

[26] S. Živković, N. Puač, Z. Giba, D. Grubišić, Z. LJ. Petrović, *Seed Sci. Technol.* **2004**, *32*, 693.

[27] N. Puač, Z. Lj, Petrović, S. Živković, Z. Giba, D. Grubišić, A. R. Đorđević, *Plasma Processes and Polymers*, Weinheim, Germany **2005**, Ch. 15.

[28] E. Bormashenko, R. Grynyov, Y. Bormashenko, E. Drori, *Sci. Rep.* **2012**, *2*, 3.

[29] L. K. Randeniya, G. J. J. B. de Groot, *Plasma Process. Polym.* **2015**, *12*, 608.

[30] B. Šerá, P. Špatenka, M. Šerý, N. Vrchotová, I. Hrušková, *IEEE Trans. Plasma Sci.* **2010**, *38*, 2963.

[31] Z. Zhou, Y. Huang, S. Yang, W. Chen, *Agricultural Sciences* **2011**, *2*, 23.

[32] B. Peethambaran, J. Han, K. Kermalli, J. Jiaxing, G Fridman, R Balsamo, A. Fridman, V. Miller, *Plasma Medicine* **2015**, *5*, 87.

[33] L. Sivachandiran, A. Khacef, *RSC Adv*. **2016**, *7*, 1822.

[34] S. Ikawa, A. Tani, Y. Nakashima, K. Kitano, *J. Phys. D*. **2016**, *49*, 425401.

[35] M. Hijosa-Valsero, R. Molina, H. Schikora, M. Müller, J. M. Bayona, *J. Hazard. Mater.* **2013**, *262*, 664.

[36] V. I. Parvulescu, M Magureanu, P. Lukes, *Plasma Chemistry and Catalysis in Gases and Liquids*. John Wiley & Sons, Weinheim, Germany **2012**.

[37] N. Hayashi, A. Nakahigashi, M. Goto, S. Kitazaki, K. Koga, M. Shiratani, *Jpn. J. Appl. Phys.* **2011**, *50*, 08JF04.

[38] G. Kamgang-Youbi, J. M. Herry, T. Meylheuc, J. L. Brisset, M. N. Bellon-Fontaine, A. Doubla, M. Naitali, *Lett. Appl. Microbiol.* **2009**, *48*, 13.

[39] M. J. Traylor, M. J. Pavlovich, S. Karim, P. Hait, Y. Sakiyama, D. S. Clark, D. B. Graves, *J. Phys. D*. **2011**, *44*, 472001.

[40] L. Sivachandiran, A. Khacef, *RSC Adv*. **2017**, *7*, 1822.

[41] H. D. Stryczewska, K. Ebihara, M. Takayama, Y. Gyoutoku, M. Tachibana, *Plasma Process. Polym.* **2005**, *2*, 238.

[42] L. Ling, J. Jiafeng, L. Jiangang, S. Minchong, H. Xin, S. Hanliang, D. Yuanhua, *Sci. Rep.* **2014**, *4*, 1.

[43] L. K. Randeniya, G. J. J. N. de Groot, *Plasma Process. Polym.* **2015**, *12*, 608.

[44] R. Ma, G. Wang, Y. Tian, K. Wang, J. Zhang, J. Fang, *J. Hazard. Mater.* **2015**, *300*, 643.

[45] A. Bertaccini, A. Canel, V. Colombo, N. Contaldo, M. Gherardi, L. Laurita, A. Stancampiano, Y. Zambon, Presented at 6th ICPM, Bratislava, Slovakia, September, **2016**.

[46] A. Bertaccini, E. Biondi, V. Colombo, M. Gherardi, L. Laurita, C. Lucchese, S. Perez, A. Stancampiano, Presented at 6th ICPM, Bratislava, Slovakia, September, **2016**.

[47] P. J. Bruggeman, M. J. Kushner, B. R. Locke, J. G. E. Gardeniers, W. G. Graham, D. B. Graves, R. C. H. M. Hofman-Caris, D. Maric, J. P. Reid, E. Ceriani, D. Fernandez, Rivas, J. E. Foster, S. C. Garrick, Y. Gorbanev, S. Hamaguchi, F. Iza, H. Jablonowski, E. Klimova, J. Kolb, F. Krcma, P. Lukes, Z. Machala, I. Marinov, D. Mariotti, S. Mededovic, Thagard, D. Minakata, E. C. Neyts, J. Pawlat, Z. L. Petrovic, R. Pflieger, S. Reuter, D. C. Schram, S. Schröter, M. Shiraiwa, B. Tarabová, P. A. Tsai, J. R. R. Verlet, T. von Woedtke, K. R. Wilson, K. Yasui and, G. Zvereva, *Plasma Sources Sci. Technol*. **2016**, *25*, 53002.

[48] M. M. Hefny, C. Pattyn, P. Lukes and, J. Benedikt, *J. Phys. D. Appl. Phys.* **2016**, *49*, 404002.

[49] S. Samukawa, M. Hori, S. Rauf, K. Tachibana, P. Bruggeman, G. Kroesen, J. C. Whitehead, A. B. Murphy, A. F. Gutsol, S. Starikovskaia, U. Kortshagen, J. P. Boeuf, T. J. Sommerer, M. J. Kushner, U. Czarnetzki and, N. Mason, *J. Phys. D. Appl. Phys.* **2012**, *45*, 253001.

[50] I. Adamovich, S. D. Baalrud, A. Bogaerts, P. J. Bruggeman, M. Cappelli, V. Colombo, U. Czarnetzki, U. Ebert, J. G. Eden, P. Favia, D. B. Graves, S. Hamaguchi, G. Hieftje, M. Hori, I. D. Kaganovich, U. Kortshagen, M. J. Kushner, N. J. Mason, S. Mazouffre, S. M. Thagard, H. R. Metelmann, A. Mizuno, E. Moreau, A. B. Murphy, B. A. Niemira, G. S. Oehrlein, Z. L. Petrovic, L. C. Pitchford, Y. K. Pu, S. Rauf, O. Sakai, S. Samukawa, S. Starikovskaia, J. Tennyson, K. Terashima, M. M. Turner, M. C. M. v. d. Sanden, A. Vardelle, *J. Physics D: Appl. Phys.* **2017**, *50*, 323001.

[51] N. Puač, D. Maletić, S. Lazović, G. Malović, A. Đorđević, Z. L. Petrović, *Appl. Phys. Lett.* **2012**, *101*, 024103.

[52] D. Grubišić, M. Nešković, R. Konjević, *Plant Sci*. **1985**, *39*, 13.

[53] C. Bailly, H. El-Maarouf-Bouteau, F. Corbineau, *C. R. Biol*. **2008**, *331*, 806.

[54] L. Rajjou, I. Debeaujon, *C. R. Biol*. **2008**, *331*, 796.

[55] D. Grubišić, R. Konjević, *Planta* **1990**, *181*, 239.

[56] D. Grubišić, Z. Giba, and, R. Konjević, *Photochem. Photobiol*. **1992**, *56*, 629.

[57] J. G. Scandalios, L. Guan, A. N. Polidoros, *Cold Spring Harbor Monograph Series* **1997**, *34*, 343.

[58] W. F. Beyer, Jr, I. Fridovich, *Oxygen Radicals in Biology and Medicine*, Springer, Boston, MA, USA **1988**, Ch. 49, p. 651.

[59] J. D. Bewley, M. Black, *Seeds*, Springer, Boston, MA, USA **1994**, Ch. 1.

[60] HU Ming-jing, *J. Shanxi Agricultural Sci*. **2010**, *11*, 9.

[61] L. Ling, L. Jiangang, S. Minchong, Z. Chunlei, D. Yuanhua, *Sci. Rep.* **2015**, *5*, 13033.

[62] J. Jiang, Y. Lu, J. Li, L. Li, X. He, H. Shao, Y. Dong, *PloS ONE* **2014**, *9*, e97753.

[63] H. Willekens, D Inzé, M. Van Montagu, W. Van Camp, *Mol. Breeding* **1995**, *1*, 207.

[64] R. Mittler, *Trends Plant Sci.* **2002**, *7*, 405.

[65] S. O. Neill, K. S. Gould, P. A. Kilmartin, K. A. Mitchell, K. R. Markham, *Funct. Plant Biol.* **2002**, *29*, 1437.

[66] M. Gorenšek, M. Gorjanc, V. Bukošek, J. Kovač, Z. Petrović, N. Puač, *Text. Res. J.* **2010**, *80*, 1633.

[67] D. Mihailović, Z. Šaponjić, R. Molina, N. Puač, P. Jovančić, J. Nedeljković, M. Radetić, *ACS Appl. Mater. Interfaces* **2010**, *2*, 1700.

[68] I. Filatova, V. Azharonok, V. Lushkevich, A. Zhukovsky, K. Spasić, S. Živković, N. Puač, S. Lazović, G. Malović, Z. Lj. Petrović, Presented at 31st ICPIG, Granada, Spain, July, **2013**.

[69] N. Puač, Z. Raspopović, Z. Lj. Petrović, Presented at 22nd SPIG, Tara, Serbia, August, **2004**.

[70] N. Puač, Z. LJ. Petrović, M. Radetić, A. Djordjević, *Mater. Sci. Forum* **2005**, *494*, 291.

[71] K. Spasić, N. Škoro, N. Puač, G. Malović, Z.LJ. Petrović, Presented at ICOPS, Antalya, Turkey, May, **2015**.

[72] D. Maletić, N. Puač, N. Selaković, S. Lazović, G. Malović, A. Đorđević, Z. Lj. Petrović, *Plasma Sources Sci. Technol.* **2015**, *24*, 025006.

[73] D. Maletić, N. Puač, G. Malović, A. Đorđević, Z. L. Petrović, *J. Phys. D: App Phys.* **2017**, *50*, 145202.

[74] J. Benedikt, S. Hofmann, N. Knake, H. Boettner, R. Reuter, A. von Keudell, V. Schulz-von der Gathen, *Eur. Phys. J. D.* **2010**, *60*, 539.

[75] M. M. Bradford, *Anal. Biochem.* **1976**, *72*, 248.

[76] W. Woodbury, A. K. Spencer, M. A. Stahmann, *Anal. Biochem.* **1971**, *44*, 301.

[77] U. K. Laemmli, *Nature* **1970**, *227*, 680.

[78] M. D. Abramoff, P. J. Magelhaes, S. J. Ram, *Biophoton. Int.* **2004**, *11*, 36.

[79] J. D. Moon, H. S. Chung, *J. Electrostat.* **2000**, *48*, 103.

[80] S. Lynikiene, A. Pozeliene, G. Rutkauskas, *Int. Agrophys.* **2006**, *20*, 195.

[81] D. Marić, P. Hartmann, G. Malović, Z. Donkó, Z. LJ. Petrović, *J. Phys. D: Appl. Phys.* **2003**, *36*, 2639.

[82] Z. Giba, D. Grubišić, R. Konjević, in *Nitric Oxide Signaling in Higher Plants*, J. R. Magalhaes, R. P. Singh, L. P. Pasos, (Eds.), Studium Press, LLC, Houston, USA **2004**.

[83] Ł. Wojtyla, K. Lechowska, S. Kubala, M. Garnczarska, *Front. Plant Sci.* **2016**, *7*, 66.

[84] H. Nonogaki, G. W. Bassel, J. D. Bewley, *Plant Sci.* **2010**, *179*, 574.

[85] J. D. Bewley, K. J. Bradford, H. W. Hilhorst, H. Nonogaki, *Seeds*. Springer, New York, USA **2013**.

[86] C. Bailly, A. Benamar, F. Corbineau, D. Côme, *Seed Sci. Res.* **2000**, *10*, 35.

[87] J. Bogdanović, K. Radotić, A. Mitrović, *Biologia Plantarum* **2008**, *52*, 396.

[88] K. Chen, R. Arora, *Plant Sci.* **2011**, *180*, 212.

[89] K. Apel, H. Hirt, *Annu. Rev. Plant Biol.* **2004**, *55*, 373.

[90] C. Bailly, A. Benamar, F. Corbineau, D. Come, *Physiol. Plant.* **1998**, *104*, 646.

[91] J. D. Bewley, *The plant cell* **1997**, 9, 7, 1055.

[92] B. Živković, *Master Thesis*, University of Belgrade, Serbia, September, **2006**.

[93] C. Bailly, J. Leymarie, A. Lehner, S. Rousseau, D. Côme, F. Corbineau, *J. Exp. Bot.* **2004**, *55*, 475.

[94] S. A. Norberg, W. Tian, E. Johnsen, M. J. Kushner, *J. Phys. D: Appl. Phys.* **2014**, *47*, 475203.

[95] G. D. Turner, R. R. Lau, D. R. Young, *J. Appl. Ecology* **1988**, *25*, 561.

[96] B. Chance, *J. Biol. Chem.* **1952**, *194*, 471.

[97] G. Arabaci, A. Usluoglu, *J. Chem.* **2012**, *2013*, 686185.

[98] O. Jun-Seok, E. J. Szili, S. Ito, S.-H. Hong, N. Gaur, H. Furuta, R. D. Short and, A. Hatta, *Plasma Med.* **2015**, *5*, 125.

[99] O. S. Degenhardt, B. Waters, A. Rebelo-Cameirao, A. Meyer, H. Brunner, N. P. Toltl, *Dissolution Technol.* **2004**, *11*, 6.

[100] V. B. Cardwell, *American Society of Agronomy and the Crop Science Society of America*. **1984**, 53–92.

[101] C. B. Rajashekar, K-H. Baek, *Am. J. Plant Sci.* **2015**, *2014*, 3572.

[102] B. Halliwell, J. M. Gutteridge, *Free Radicals in Biology and Medicine*. Oxford University Press, NY, USA **1999**.

[103] C. Bailly, H. El-Maarouf-Bouteau, F. Corbineau, *C. R. Biol.* **2008**, *331*, 806.

Biomedical applications and diagnostics of atmospheric pressure plasma

Biomedical applications and diagnostics of atmospheric pressure plasma

Z Lj Petrović[1], N Puač, S Lazović, D Maletić, K Spasić and G Malović

Institute of Physics, University of Belgrade, Pregrevica 118, 11080 Belgrade, Serbia

E-mail: zoran@ipb.ac.rs

**Abstract.** Numerous applications of non-equilibrium (cold, low temperature) plasmas require those plasmas to operate at atmospheric pressure. Achieving non-equilibrium at atmospheric pressure is difficult since the ionization growth is very fast at such a high pressure. High degree of ionization on the other hand enables transfer of energy between electrons and ions and further heating of the background neutral gas through collisions between ions and neutrals. Thus, all schemes to produce non-equilibrium plasmas revolve around some form of control of ionization growth. Diagnostics of atmospheric pressure plasmas is difficult and some of the techniques cannot be employed at all. The difficulties stem mostly from the small size. Optical emission spectroscopy and laser absorption spectroscopy require very high resolution in order to resolve the anatomy of the discharges. Mass analysis is not normally applicable for atmospheric pressure plasmas, but recently systems with triple differential pumping have been developed that allow analysis of plasma chemistry at atmospheric pressures which is essential for numerous applications. Application of such systems is, however, not free from problems. Applications in biomedicine require minimum heating of the ambient air. The gas temperature should not exceed 40 $^{\circ}$C to avoid thermal damage to the living tissues. Thus, plasmas should operate at very low powers and power control is essential. We developed unique derivative probes that allow control of power well below 1 W and studied four different sources, including dielectric barrier discharges, plasma needle, atmospheric pressure jet and micro atmospheric pressure jet. The jet operates in plasma bullet regime if proper conditions are met. Finally, we cover results on treatment of bacteria and human cells as well as treatment of plants by plasmas. Localized delivery of active species by plasmas may lead to a number of medical procedures that may also involve removal of bacteria, fungi and spores.

1. Introduction

The choice of the plasma system used for treatment is usually guided by the kind of samples that are treated and the effect these plasmas are intended to have on the samples. The desire to use plasma for in-vivo treatments have made it necessary that several requirements for plasma sources be met. Necessarily, plasmas have to operate at atmospheric pressure if they are to be used for medical treatment of living organisms. At the same time, one needs non-equilibrium plasmas in order to achieve separation of electrons on the one side, and ions and neutrals, on the other. It is an advantage that no expensive vacuum systems are needed, while, on the other hand, it is much more difficult to achieve non-equilibrium (non-thermal) mode of operation at higher pressures.

---

[1] To whom any correspondence shoul be addressed.

The sensitivity to heat of biomedical samples narrows the choice of non-thermal plasmas. There are many types of plasmas that can be generated under ambient pressure and temperature conditions suitable for treatment of sensitive samples [1, 2, 3]. The motivation is to develop new medical techniques, as plasma offers some possibilities for inducing desired processes with minimum damage to the living tissue [1, 2, 3, 4]. While the first results seemed quite impressive, including effects on tumor cells and even active tumors [5], tooth decay treatment and tooth cleaning [6], wound healing [5], treatment of fungi and spores and even treatment of ulcers and blood vessels, one can still not rule out negative effects that have not been studied over a sufficiently long time scale. Th preliminary results, however, show a large degree of selectivity.

Some of the well-known small-size atmospheric-pressure plasma sources are: plasma needle [7, 4], μAPPJ [8], plasma bullet [9], plasma torch [10] and floating electrode dielectric barrier discharge plasma [11]. Their electrode configuration, voltages and excitation frequencies are very different; some of them work at microwave frequencies, some at 13.56 MHz and others at 5-120 kHz in sine or pulse regime. Yet, all is not understood about their physics and while models are being developed mainly based on low pressure plasmas, the reliable experimental data are limited due to the limited availability of diagnostic techniques that are suited for such plasmas.

Here we will present several diagnostics techniques suited for atmospheric pressure plasmas and the operation of several different plasma systems working at atmospheric pressure. We will also summarize our results in treating living organisms and give examples of results mainly on sterilization of bacteria and biofilms.

2. Atmospheric pressure discharges – different experimental set-ups

Achieving non-equilibrium at atmospheric pressure is difficult since the ionization growth is very fast at such a high pressure. The high degree of ionization on the other hand enables transfer of energy between electrons and ions through Coulomb collisions. Furthermore, heating of the background neutral gas is achieved through collisions between ions and neutrals. Thus, all schemes to produce non-equilibrium plasmas revolve around some form of control of the ionization growth. It can be achieved either by an inhomogeneous field as in corona or by employment of a dielectric barrier which turns the field off after a space charge is deposited on the dielectric. Ionization growth limiting may also be achieved by a time-varying field. Another approach is to operate at the *pd* value corresponding to the Paschen minimum, i.e. at microscopic dimensions and high pressures. In that case, the breakdown voltage is below the threshold for streamer development and thus a glow discharge may be achieved. If the electronegative nature of the gas is increasing the breakdown and operating voltages, one may mix in an inert gas. The discharge is thus initiated in the inert gas and then the atmospheric gas is mixed to produce chemically active radicals. In most cases, however, atmospheric pressure plasmas have small dimensions making it very difficult to perform standard diagnostics.

Some of the plasma devices designed for in-vivo treatments are the μ-APPJ and the plasma needle, which operate at 13.56 MHz at atmospheric pressure. A micro-atmospheric plasma jet was developed by Schultz van der Gathen and coworkers [12]; this plasma source is interesting both for applications as well as for the study of its basic properties.

The micro-atmospheric pressure plasma jet [μ-APPJ] consists of two symmetrical electrodes of equal length (34 mm) made of stainless steel. The distance between the electrodes can be adjusted with good precision from a few mm up to several hundred micrometers. In all our experiments, the distance between the powered and the grounded electrode was 1 mm. One of the electrodes was powered by a signal generator at 13.56 MHz while the other electrode was grounded. The measurements were made at powers of 40-80 W fed by a RF power supply.

Plasma is ignited along the entire length of the electrodes (figure 1); for certain combinations of power/gas-flow parameters, effluent of plasma coming out of the cuvette can be formed. The main advantage of this design is that both the discharge volume (plasma core) and effluent region are accessible for diagnostics, such as optical emission spectroscopy (OES) and two-photon absorption
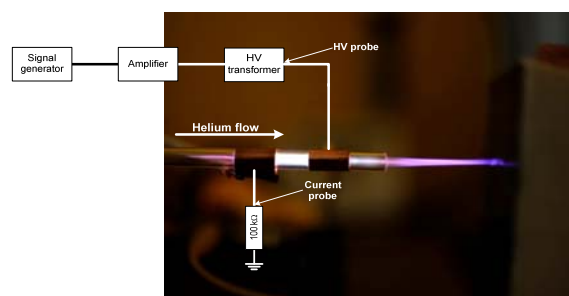
laser-induced fluorescence (TALIF) [8]. Also, the plane parallel geometry of the electrodes adds to the simplicity when it comes to modeling this type of discharge.
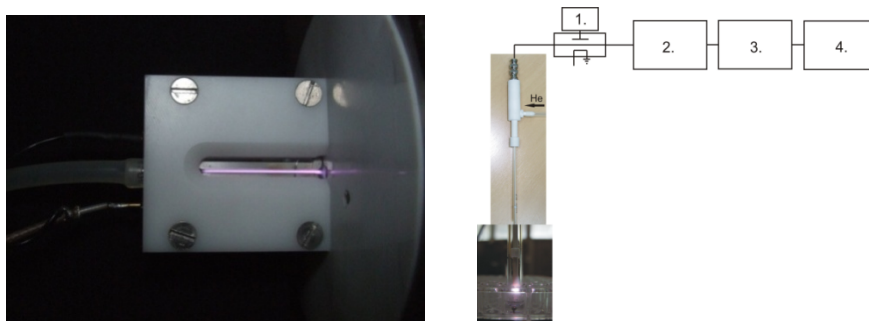
Figure 1. μ-APPJ with formed plasma and plasma needle system set-up.

Another plasma source that meets all the necessary conditions for treatment of organic materials and living tissues is the plasma needle (figure 1, picture on the right-hand side). Most importantly, in such a discharge gas the heating is minimized, while th effects on the tissue and bacteria have been clearly shown to be significant. The needle consists of a central electrode made of tungsten insulated almost to the tip by a slightly larger ceramic tube, both being placed inside a glass tube. The needle body is made of Teflon. We used helium as a buffer gas at several different flow rates. The central electrode is powered by a 13.56 MHz signal generator through an amplifier and a matching network. Both for the plasma needle and for thee μ-APPJ, we have derivative probes and a Hiden HPR60 mass/energy analyzer in order to determine the power applied to plasma and the composition of the discharge, respectively. In both of these systems, inert gas is used to reduce the breakdown voltage and achieve stable non-equilibrium plasma formation. Yet these plasmas have shown several modes of operation and further studies are required to fully understand their operation and make further optimizations.

Another type of atmospheric pressure plasma relies on mixing the inert gas carrying the plasma created by external electrodes with atmospheric gas mixture. It is the so-called plasma jet. The operating frequencies of plasma jets are in the region of several tens of kHz which are much lower frequencies then those used for the plasma needle and μ-APPJ (in MHz). It has been shown that micro jet plasma is not always continuous but often is formed by a train of fast travelling bullets which only appear to be continuous to the human eye. The atmospheric pressure plasma

Figure 2. Atmospheric plasma bullet.

jet/bullet that we constructed was made of a Pyrex glass tube with the electrodes made of a thin copper foil wrapped around the glass tube. The distance between the powered and the grounded electrode was 13.5 mm and their width was 13 mm. One of the electrodes (the left electrode, see figure 2) was grounded. The other electrode, closer to the end of the glass tube, was the powered one (see figure 2). In all experiments the buffer gas was helium. We used a signal generator connected to the custom-made amplifier to power the micro jet. The highest voltages that we could obtain from the amplifier were up to 1 kV, which was not enough to ignite the plasma. In order to the increase the applied voltages to more than 5-6 kV, we had to use an additional homemade transformer. The operating frequency was 80 kHz and the applied voltage was sinusoidal in the range of 6-10 kV$_{peak-to-peak}$. Micro jets with plasma bullets have been constructed with a range of different

geometries, frequencies and shapes of applied voltage. The effect of bullets seems to be quite universal for an optimum range of electrode sizes and flows, while the frequencies and voltage shapes vary a lot. Plasma bullets, however, still need to be fully understood and properly modelled. We will focus here on the plasma jet diagnostics, while at the same time showing some results on the sterilization achieved by a plasma needle.

3. Plasma diagnostics

It has been reported only quite recently that the plasma jets formed by the source operating at low excitation frequency is not continuous. Instead it consists of small plasma packages that are formed in positive and/or negative half cycle of the period [13]. Amazingly these little bullets are formed and travel outside the plasma jet where there is no applied electric field. The velocity of these packages are larger than the speed of the flowing feed gas by several orders of magnitude. Several theories of bullet formation have been proposed [13, 14, 15, 16, 17, 18] but to date a definite explanation of the physical mechanisms involved in creation and propagation of plasma bullet are still not fully understood.

For the current and voltage measurements, we used two commercial probes. The current and voltage waveforms when the plasma is formed and without discharge are shown in figure 3. When the plasma is off, the phase difference between the current and voltage is close to 90˚. In this case, we have a capacitive impedance of several MΩ, corresponding to a capacitance of about 0.5 pF. On the other hand, when the plasma is formed, the current signal is larger, deformed and shifted in phase overlapping more with the voltage signal. The plasma ignition changes the slopes of the V_{RMS}–I_{RMS} curves (see figure 4). The mean power calculated increases with the increase of the applied voltage; it was in the range from 1 to 8 W in all measurements.

Integral and time-resolved images of the plasma jet system were obtained by an ICCD camera. For exposure times larger than the cycle period (12.5 μs), the plasma appears to be continuous, like a plume (see figure 1 LHS picture). The length of the plasma plume is up to five centimeters, depending of the flow rate and the voltage applied. For the time-resolved images, we had to use integration on the chip because the light emission in a single shot is not sufficient to obtain clear images with gate widths less than 50 ns. This was facilitated by the high reproducibility of the pulses and the small jitter. Figure 5 shows the plasma bullet images obtained for several different flows of working gas. We can see that with the decrease in the He flow, the plasma bullet starts to be elongated, deformed and its intensity is much smaller. Eventually, bullets are not formed at the very small flows.
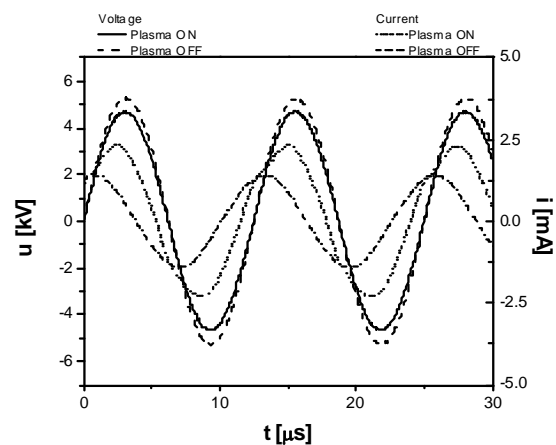
Figure 3. Current and voltage waveforms for helium flow rate of 3 slm. The dashed lines represent the case when discharge is OFF, the solid lines, when discharge is ignited [19].
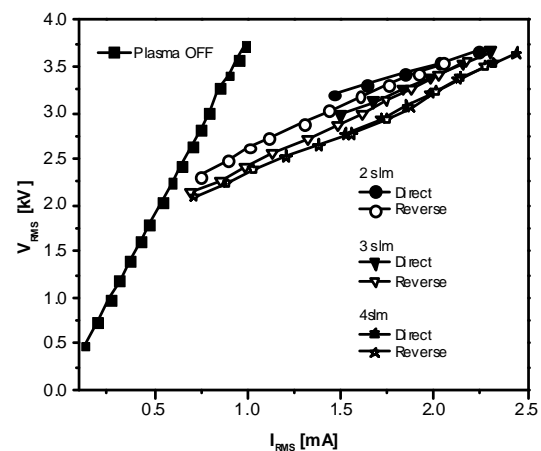
Figure 4. Current-voltage characteristics for three different flows of helium [19].
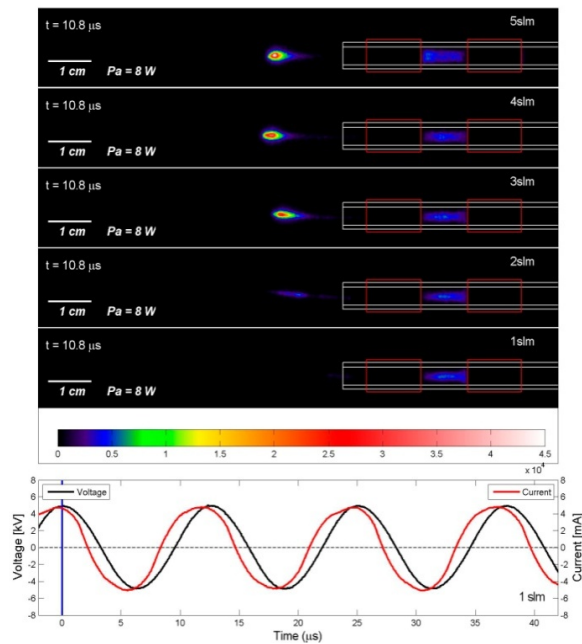
Figure 5. Plasma jet for 1, 2, 3, 4 and 5 slm of He flow. Exposure time 2 ms, gate width 25 ns, gate delay 10.8 μs [19].

Figure 6 shows the development of the plasma over the entire period of applied voltage (12.5 μs). All images are scaled to the same maximum intensity and thus can be compared. One can see that when the current and voltage signals are close to zero, the plasma is not visible. In the negative part of the current and voltage waveforms, the plasma is confined between the electrodes. During the positive part of the waveforms, the plasma is first confined between the electrodes (rising slope) and then, near the maximum of the curves, it leaves the glass tube in the form of a bullet. The dimensions of the bullet are of the order of a few millimeters. We calculated the speed of the bullet at ~20 km/s, depending on the position away from the end of the glass tube. The plasma bullet is much faster than the speed of the buffer gas flow (1 to 7 m/s). Thus we can conclude that our plasma source was not continuous, it consisted of very small plasma packages that traveled at a high speed. By varying the plasma parameters, the length and intensity of the plasma coming out of the tube can be adjusted.

For the two plasma devices operating at a much
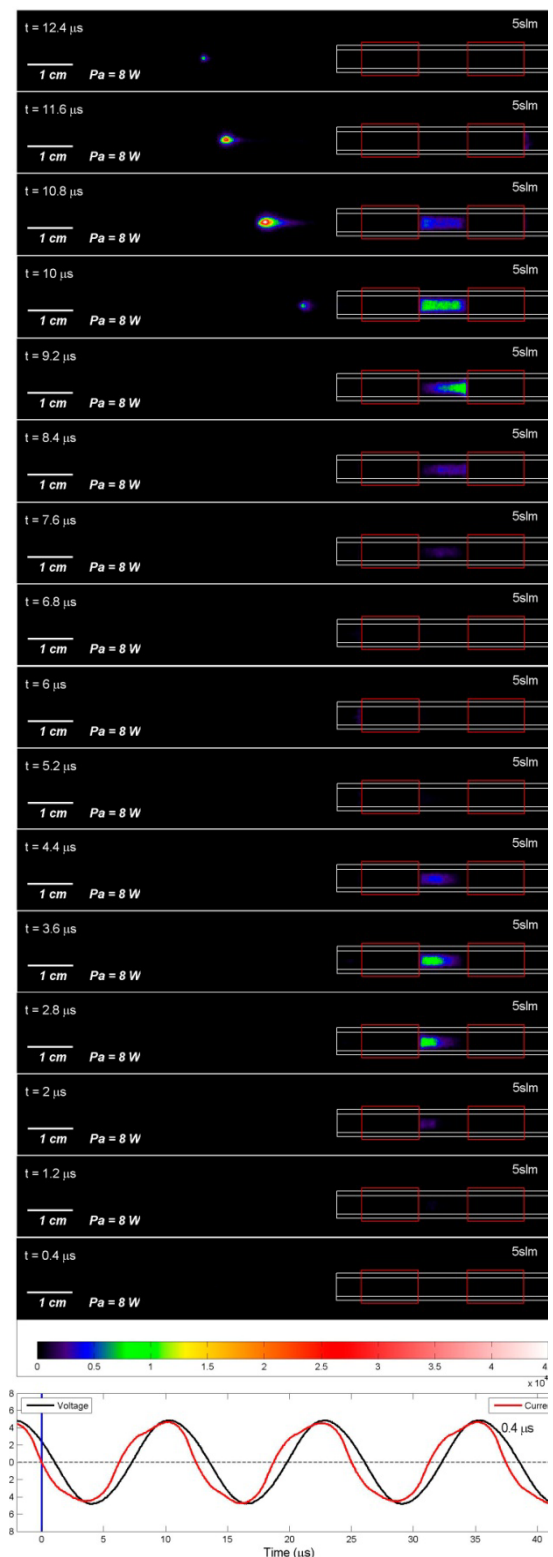
Figure 6. Plasma jet at 5 slm, exposure time 2 ms, gate width 25 ns and gate delay from 0.4 to 12.4 μs [19].

higher frequency (13.56 MHz), the diagnostics was made by using homemade derivative probes in order to determine the power transmitted to the plasma and the operation mode of the discharge. The derivative probes were very sensitive; a numerical procedure for subtracting the displacement current based on accurate calibration of the system was performed so that it was possible to measure powers of the order of 0.1 W or less even with displacement current a couple of orders of magnitude larger than the plasma current.

Besides derivative probes, we used mass spectrometry to analyze the plasma products formed by a µ-APPJ [19] and by a plasma needle [20]. Several problems occurred during the setting up of the experiment; they are described in detail elsewhere [19, 20].

The analysis of the composition of neutrals and ions was motivated by the need to check which species are formed in the discharge. These results may be used as a test of plasma chemical models, to identify radicals and ions (that may be used after acceleration to induce damage to the tissue). The performance of the mass analyzer was tested and techniques were developed to produce data without the uncertainty induced by a contribution of the ionizer to possible dissociation. It was found that the predominant ions created by the plasma are O_2^+, O^+, H_3O^+, N_2^+, N^+, NO^+, OH^+ [19]. When it comes to plasma treatment of samples of biological origin, the chemically active species that are of interest are O, metastables O and O_2, OH, N, H_2O_2 and NO.

4. Plasma sterilization

The entry point for most groups dealing with plasma medicine is a study of sterilization. The effects on bacteria may be shown quickly, although it requires expertise in biomedicine. The benefit is that direct potential applications may be developed outside the realms of strict medical regulations. Yet, in situ sterilization, for example, treatment of wounds to prevent infection, would be a much more important goal. Following preliminary work on sterilization in microwave plasma, albeit at low pressure, we reinitiated the studies of plasma sterilization as a part of our plasma medical project. So far, a plasma needle has been used to induce killing of Streptococcus mutans and Escherichia coli bacteria in the form of planktonic samples. Also, we have the plasma interaction with normal, living cells; for these experiments we used human peripheral blood mesenchymal stem cells (hPB-MSC) as a model system to predict the degree of possible damage to the cell responses [21]. Many factors are responsible for bacterial inactivation. Direct exposure of the bacterial samples to the plasma appears to be more effective than remote exposure. Another factor that determines the efficiency of the specific treatment is the type [22] of bacteria, gram positive or gram negative. Very importantly, we studied the sterilization of bacteria in planktonic samples, where bacteria are dissolved in a small amount of liquid that would otherwise give it some protection from other agents. We showed that efficient sterilization of planktonic samples is not only possible, but may be efficient depending on the initial population [21].

One of the most serious problems in the hospital environment is bacterial contamination of surfaces with methicillin-resistant Staphylococcus aureus (MRSA) responsible for significant nosocomial infections. The pathogenic contaminants form biofilms, which are difficult to treat with routine biocides. The biofilm is not just a secured shelter
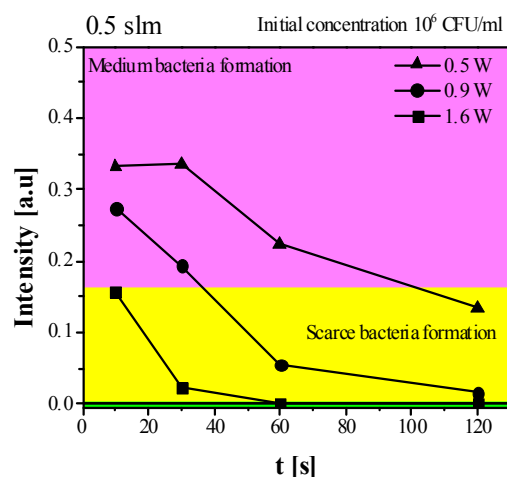
Figure 7. Treatment of MRSA biofilms of Staphylococcus aureus (ATCC 25923) by using plasma needle. Untreated sample showed STRONG bacteria formation (control intensity 0.65 a.u). Initial concentration of bacteria used was 10^6 CFU/ml.

but a defense mechanism and a nutrition depot for pathogens. We show below the preliminary results of plasma treatment of the MRSA bacteria samples in the form of a biofilm.

In figure 7, we show the optical density of bacteria samples after plasma treatment for several different treatment times (10, 30, 60 and 120 s). The initial concentration of the samples was 10^6 CFU/ml, which corresponds to a measured optical density of 0.65 a.u. The buffer gas flow was 0.5 slm, but studies were also made as a function of the flow rate. The treatment efficiency increases with the increase of the treatment time and the mean power deposited to the plasma. For the highest power and only for the shortest treatment time of 10 s, there was scarcely bacteria formation; for the longer treatment, no bacteria formation was observed after the plasma treatment and yet there was very little or no heating of the gas.

Conclusions

We reviewed shortly our studies of atmospheric pressure plasmas and their application in biomedicine. In particular, we covered new results obtained with a plasma jet showing formation of plasma bullets and their properties as a function of geometry of electrodes and gas flow. In addition, we showd some practical results of sterilization using a plasma needle. The treatment of biofilms is essential, as are the studies of treatment of fungi, spores, prions and viruses. At the same time, one needs to extend the studies to specific medical problems associated with treatment of living organisms, including humans.

As far as plasma goes, some further optimization may be made for localized accurate treatment of cells or sterilization. With good knowledge of the power deposited into the plasma and control of the radicals that are produced, together with spatial emission profiles indicating changing of the regime of operation, a sufficient control over the reproducibility of the plasma needle operation was achieved. Other sources may be sought for more refined interaction with living cells. Different applications may seek more uniform sources extended over larger areas or even more localized treatment, which is all within the reach of the present day techniques.

Acknowledgements

References

[1]   Fridman A and Kennedy L A 2004 *Plasma Phys. Eng.* (New York: Taylor and Francis)
[2]   Iza F, Kim G J A, Lee S M A, Lee J K A, Walsh A J, Zhang A Y and Kong M 2008 *Plasma Process. Polym.* **5** 322
[3]   Stoffels E, Flikweert A J, Stoffels W W, and Kroesen G M W 2002 *Plasma Sources Sci. Technol.* **11**/4 383
[4]   Puač N, Petrović Z Lj, Malović G, Đorđević A, Živković S, Giba Z and Grubišić D 2006 *J. Phys.* D: *Appl. Phys.* **39** 3514-19
[5]   Fridman G, Friedman G, Gutsol A, Shekhter A B, Vasilets V N and Fridman A 2008 *Plasma Process. Polym.* **5** 503–33
[6]   Sladek R E J, Stoffels E, Walraven R, Tielbeek P J A and Koolhoven R A 2004 *IEEE Trans. Plasma Sci.* **32**/4 1540-3
[7]   Kieft I E, v d Laan E P and Stoffels E 2004 *New J. Phys.* **6** 149
[8]   v d Gathen S V, Schaper L, Knake N, Reuter S, Niemi K, Gans T and Winter J 2008 Spatially resolved diagnostics on a microscale atmospheric pressure plasma jet *J. Phys.* D: *Appl. Phys.* **41** 194004
[9]   Shi J, Zhong F, Zhang J, Liu D W and Kong M G 2008 *Phys. Plasmas* **15** 013504
[10]   Yonson S, Coulombe S, Leveille V and Leask R L 2006 *J. Phys.* D: *Appl. Phys.* **39** 3508–13
[11]   Fridman G, Shereshevsky A, Jost M M, Brooks A D, Fridman A, Gutsol A, Vasilets V and Friedman G 2007 *Plasma Chem. Plasma Process.* **27** 163–176
[12]   v d Gathen S V, Buck V, Gans T, Knake N, Niemi K, Reuter St, Schaper L and Winter J 2007

        Contrib. Plasma Phys. **47**/7 510

[13]   Walsh J L and Kong M G 2008 *IEEE Trans. Plasma Sci.* **36** 1314

[14]   Lu X and Laroussi M 2006 *J. Appl. Phys.* **100** 063302

[15]   Walsh J L, Iza F, Janson N B, Law V J, Kong M G and Shi J 2010 *J. Phys.* D: *Appl. Phys.* **43** 075201

[16]   Zhong F, Zhang J, Liu D W and Kong M G 2008 *Phys. Plasmas* **15** 013504

[17]   Mericam-Bourdet N, Laroussi M, Begum A and Karakas E 2009 *J. Phys. D*: *Appl. Phys.* **42** 055207

[18]   Shashurin A A, Shneider M N, Dogariu A, Miles R B and Keidar M 2009 *Appl. Phys. Lett.* **94** 231504

[19]   Maletić D, Puač N, Malović G and Petrović Z Lj *unpublished*

[20]   Malović G, Puač N, Lazović S and Petrović Z Lj 2010 Mass analysis of an atmospheric pressure plasma needle discharge *Plasma Sources Sci. Technol.* **19** 034014

[21]   Lazović S, Puač N, Miletić M, Pavlica D, Jovanović M, Bugarski D, Mojsilović S, Maletić D, Malović G, Milenković P and Petrović Z Lj 2010 *New J. Phys.* **12** 083037

[22]   Stoffels E, Sakiyama Y and Graves D B 2008 *IEEE Trans. Plasma Sci.* **36**/4 1441

XXI Europhysics Conference on the

Atomic and Molecular Physics of Ionized Gases

Tuesday 10 July to
Saturday 14 July 2012

at Castelo de Santiago da Barra
Viana do Castelo, Portugal
http://escampig2012.ist.utl.pt

PROCEEDINGS

Edited by
Pedro G. C. Almeida, Luís L. Alves and Vasco Guerra

The XXI ESCAMPIG was organized by Instituto de Plasmas e Fusão Nuclear from Instituto Superior Técnico, Universidade Técnica de Lisboa, Universidade do Porto, Universidade do Minho and Universidade da Madeira, under the rules of EPS for Europhysics Conferences.

http://escampig2012.ist.utl.pt

Committees
International Scientific Committee
Jürgen Meichsner (chair), Germany
Annemie Bogaerts, BeNeLux, Baltic States and Nordic Countries
Stéphane Pasquiers, France, Andorra
Peter Hartmann, Hungary, Austria, Switzerland
Giorgio Dilecce, Italy, Greece, Israel
Vasco Guerra, Portugal
Gheorghe Dinescu, Romania, Bulgaria
Yuri Akishev, Russia, Belarus, Georgia, Ukraine, other former USSR States
Štefan Matejcik, Czech Republic, Poland, Slovakia
Mark Bowden, United Kingdom, Ireland
Dragana Maric, Serbia, Bosnia-Herz., Croatia, Montenegro, Slovenia
Francisco Gordillo-Vázquez, Spain
Local Organizing Committee
Vasco Guerra (chair), Lisboa
Pedro Almeida, Funchal, Madeira
Edgar Felizardo, Lisboa
André Janeco, Lisboa
Luís Lemos Alves, Lisboa
Mário Lino da Silva, Lisboa
Luís Marques, Braga
Carlos Daniel Pintassilgo, Porto
Rafael Saavedra, Lisboa
Miguel Santos, Lisboa

Spatial profiles of atomic oxygen concentrations in a large scale CCP reactor

S. Lazović[(*)1,2], K. Spasić[1], N. Puač[1], G. Malović[1], U. Cvelbar[2], M. Mozetič[2], Z. LJ. Petrović[1]

[1] *Institute of Physics, University of Belgrade, Pregrevica 118, 11080 Belgrade, Serbia*
[2]*Jozef Stefan Institute, Jamova 39, 1000 Ljubljana, Slovenia*
[(*)]lazovic@ipb.ac.rs

Nickel catalytic probe was used to measure atomic oxygen concentrations in a large scale cylindrical asymmetrical capacitively coupled plasma reactor. We have measured O concentrations in the main chamber of the reactor as well as in the side tube placed perpendicular to the chamber wall. The spatial profiles in these two regions differ both in magnitude (10^{19} m^{-3}vs. 10^{18} m^{-3} or even 10^{17} m^{-3}) and in the way the concentrations decrease when moving away from the powered electrode. This is explained by the different chamber wall configuration around the probe and its proximity because the grounded walls are also O atom drain due to the recombination. Working gas was air at 300 and 600 mTorr and the power was fixed at 500W.

Low temperature plasmas at sub-atmospheric pressures are an essential tool in many industrial processes due to variety of chemical reactions that can be induced and controlled while maintaining low gas temperatures. Low pressure radiofrequency plasmas are irreplaceable in the semiconductor industry but this is hardly the only field of their application [1, 2]. A large scale cylindrical asymmetrical 13.56 MHz CCP reactor was developed in our laboratory for the purpose of textile, polymer and seeds modification [3, 4]. Sensitive material treatment requires low ion energy bombardment and high concentrations of active species like O. For instance the formation of new oxygen-containing groups on the fiber surface is suggested to be due to the presence of extremely reactive atomic oxygen species in discharge during the air plasma processing and/or post-plasma chemical reactions when the activated fiber surface reacts with environmental species [5]. The asymmetric design of the reactor was chosen to provide low energies of ions bombarding the surfaces of the samples in order to avoid excessive damage of the samples.

We have used nickel catalytic probe positioned side-on to the powered electrode to measure O concentrations in the main chamber and in the small side tube (see Fig 1.).
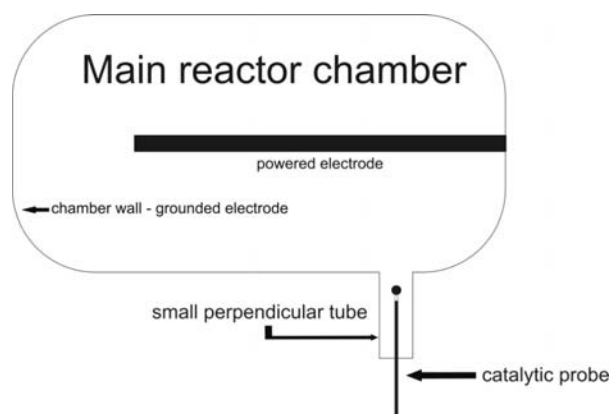
Fig. 1: Catalytic probe position in the reactor.

Detailed experimental setup details can be found elsewhere [6] as well as the design and the operation of the catalytic probe [7, 8]. Measurements are performed in air at 300 and 600 mTorr. The power was fixed at 500 W.

Spatial profiles of O concentrations are shown at Fig 2. We can see that the concentrations are higher at higher pressure and are decreasing faster in the side tube compared to the main chamber when moving away from the powered electrode. This is due to the difference in the vicinity and the area of the grounded wall which is closest to the probe at certain position.
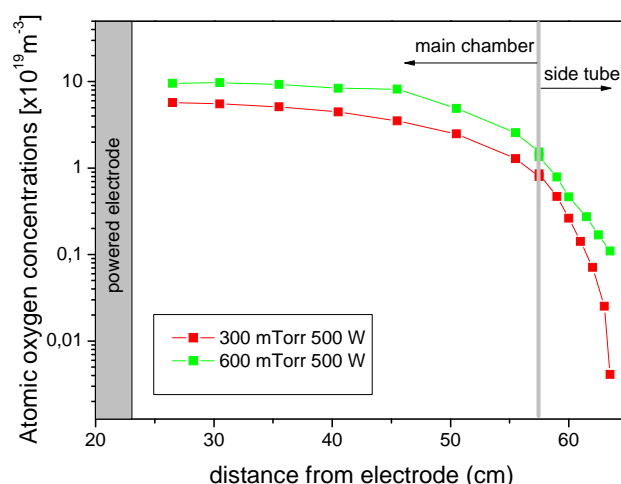
Fig. 2: Atomic oxygen spatial profiles in the main reactor chamber and in the side tube. Working gas was air at 300 and 600 mTorr and the power was fixed at 500 W.

The surface recombination of O atoms is taking place at the surface of both the nickel catalytic probe and at the chamber wall. In the tube, the wall is a stronger O atom drain both because it is closer and because the effective area is larger. By placing the sample at different distances from the powered electrode O concentrations can be controlled in the range from 10^{17} m^{-3} to 10^{19}m^{-3}. Depending on the intrinsic properties of the material being treated and on the modification effects that are desired we can tune the O concentrations at the sample surface simply by putting the sample in one of two regions of the reactor (main chamber and side tube) and adjusting its position. Adjustment can also be achieved by changing the pressure, power and gas composition.

References

[1] T. Makabe, Z.Lj. Petrović, *Plasma Electronics*, (2006) (*Taylor and Francis, New York*).

[2] M.A. Lieberman, A.J. Lichtenberg, *Principles of Plasma Discharge and Materials Processing*, (2005) (*Wiley, Hoboken*).

[3] N. Puač, Z.Lj. Petrović, M. Radetić and A. Đorđević, *Materials Science Forum*, **494** (2005) 291-296.

[4] M. Radetić, P. Jovančić, N. Puač and Z.Lj. Petrović, *Workshop on Nonequilibrium Processes in Plasma Physics and Studies of the Environment*, SPIG 2006, *Journal of Physics: Conference Series* **71** (2007) 012017.

[5] V. Ilić, Z. Šaponjić, V. Vodnik, S. Lazović, S. Dimitrijević, P. Jovančić, J. M. Nedeljković and M. Radetić, *Ind. Eng. Chem. Res.* **49** (2010) 7287–7293.

[6] S. Lazović, N. Puač, K. Spasić, G. Malović, U. Cvelbar, M. Mozetič, Z. Lj. Petrović, *30th ICPIG*, August 28th – September 2nd (2011).

[7] T.Vrlinic, C. Mille, D. Debarnot, F. Poncin-Epaillard, *Vacuum* **83** 5 (2009) 792–796.

[8] M. Mozetic, A. Vesel, U. Cvelbar, A. Ricard, *Plasma Chem Plasma P* **26** (2006) 103–117.

PROCEEDINGS OF
THE XXIIND INTERNATIONAL
CONFERENCE ON GAS DISCHARGES
AND THEIR APPLICATIONS

- VOLUME 2 -

2nd - 7th September 2018

Novi Sad, SERBIA

Serbian Academy of Sciences and Arts

&

Institute of Physics, University of Belgrade

Editors: Prof. Zoran Lj. Petrović

Dr. Nevena Puač

Dr. Saša Dujko

Dr. Nikola Škoro

EXECUTIVE MANAGMENT COMMITTEE

Dr. J.E. Jones, Chair
Prof. G.R. Jones
Prof. J.W. Spencer
Prof. K Hidaka
Dr. A.B. Murphy
Prof. D. Hong
Dr. P. Robin-Jouan

INTERNATIONAL SCIENTIFIC COMMITTEE

Dr. J.-M. Bauchire, France
Prof. Yann Cressault, France
Prof. C.M. Franck, Switzerland
Prof. K. Hidaka, Japan
Prof. G.R. Jones, UK
Dr. A.B. Murphy, Australia
Prof. G.J. Pietsch, Germany
Prof. Ph. Robin-Jouan, France
Prof. Kohki Satoh, Japan
Prof. J.W. Spencer, UK
Dr. T. Teich, Switzerland
Prof. J. -Y. Trepanier, Canada
Prof. Y. Wu, China
Dr. J. L. Walsh, UK

Dr. J.-P. Borra, France
Prof. M. Farzaneh, Canada
Prof. A. Haddad, UK
Prof. D. Hong, France
Dr. J.E. Jones, UK
Prof. Z. Lj. Petrović, Serbia
Prof. V. Rakov, USA
Prof. A. Robledo-Martinez, Mexico
Dr. M. Seeger, Switzerland
Dr. S. Stangherlin, Switzerland
Dr. Igor Timoshkin, UK
Prof. K.-D. Weltmann, Germany
Dr. J. D. Yan, UK

LOCAL ORGANIZING COMMITTEE

Prof. Zoran Lj. Petrović, Chair
Dr. Saša Dujko, Co-Chair

Dr. Nevena Puač, Co-Chair
Dr. Nikola Škoro, Secretary

Dr. Danko Bošnjaković
Dr. Dragana Marić
Kosta Spasić
Marija Puač
Nenad Selaković
Ilija Simonović

Prof. Bratislav Obradović
Dr. Gordana Malović
Jelena Sivoš
Dejan Maletić
Jasmina Atić
Vladan Simić

Panacomp Wonderland Travel

INFLUENCE OF ATMOSPHERIC PRESSURE PLASMA JET PARAMETERS ON DECONTAMINATION OF BACTERIA

A. JUROV[1,2]*, U. CVELBAR[2], Z. LJ. PETROVIĆ[3], N. ŠKORO[3], K. SPASIĆ[3], M. MODIC[2], N. HOJNIK[1,2], D. VUJOŠEVIĆ[4], V. VUKSANOVIĆ[4], AND M. ĐUROVIĆ[4]

[1] Jozef Stefan International Postgraduate School, Jamova cesta 39, 1000, Ljubljana, Slovenia
[2] Jozef Stefan Institute, Jamova cesta 39, 1000, Ljubljana, Slovenia
[3] Institute of Physics, University of Belgrade, Pregrevica 118, 11080, Belgrade, Serbia
[4] Center for Medical Microbiology, Institute of Public Health Montenegro, Džona Džeksona bb, 81000, Podgorica, Montenegro

*andrea.jurov@ijs.si

ABSTRACT

There are many new alternatives to conventional bacteria sterilisation techniques (heating, filtration, solvents, radiation), such as different plasma sources [1-4]. This research focused on non-thermal atmospheric pressure plasma jet (APPJ) because it's cost-effective, easily transportable, simple to use, and has a low operating temperature thus enabling treatment of heat sensitive surfaces.

The experiments were conducted with helium APPJ for four different typical bacteria strains (*Escherichia coli*, *Bacillus subtilis*, *Staphylococcus aureus*, and *Bacillus stearothermophilius*). The focus was on finding the most efficient discharge parameters; thus various input voltages and gas flows were tested. The analysis that was used on the jet is ICCD imaging, optical emission spectroscopy, and electrical measurements. Furthermore, the chemical analysis was done on treated medium (bacteria dispersed in saline) to detect the effectiveness of the decontamination.

1. INTRODUCTION

Improving the decontamination of the bacteria is an ongoing process and of great importance in many environments, such as hospitals. As an alternative to conventional techniques, plasma decontamination was proposed. Our choice was an atmospheric pressure plasma in a form of a single electrode jet (APPJ). Atmospheric pressure plasmas have many advantages compared to low-pressure plasmas, mostly the ability to work without the vacuum system thus reducing the cost of the process and making it possible to treat heat-sensitive materials and hard-to-reach places (e.g. corners, tubes) [5,6]. Because of that we constructed the APPJ and tested its most optimal parameters for bacteria decontamination on four types of bacteria. After finding out which powers and gas flows decontaminated bacteria, the focus shifted onto the diagnostics of the plasma source - APPJ.

2. EXPERIMENTAL SETUP

The decontamination effect of the atmospheric pressure plasma jet was investigated on four different types of spore-forming bacteria: *Bacillus stearothermophilus* ATCC No. 7953, *Bacillus subtilis* ATCC No. 6633, *Staphylococcus aureus* ATCC No. 25923, and *Escherichia coli* ATCC No. 25922, of which only the *E. coli* is Gram-negative bacteria. Bacterial cultures were grown overnight on Columbia (COS) agar plates (bioMérieux SA, Marcy l'Etoile, France) at $55^o C$ for *Bacillus stearothermophilus* and $37^o C$ for *Bacillus subtilis*, *Staphylococcus aureus* and *Escherichia coli*. Bacteria were picked up with a loop and re-suspended in sterile saline to obtain 0.5 McFarland (1-2 x 10^8 *CFU/ml*) initial bacterial suspension.

Small-size APPJ powered by a kHz signal source connected to a low-voltage DC source was used for the treatments. Measurements with the needle type APPJ were conducted with He as a working gas at a fixed distance between the jet and the sample surface (15 *mm*). Bacteria were treated for different gas flows (1 *slm* and 2 *slm*) and with several DC power supply voltages applied (3 *V*, 6 *V*, and 12 *V*). Detailed characterisation of the plasma source was performed employing optical measurements and electrical characterization.

3. RESULTS AND DISCUSSION

After preparing bacteria suspension, we treated them with Helium APPJ under different DC power supply voltages and gas flows. A surface of the suspension was fixed 15 mm under the jet nozzle, and it was fixed for all measurements. The bacteria suspension was placed in a Petri dish that was grounded.

(a)

(b)
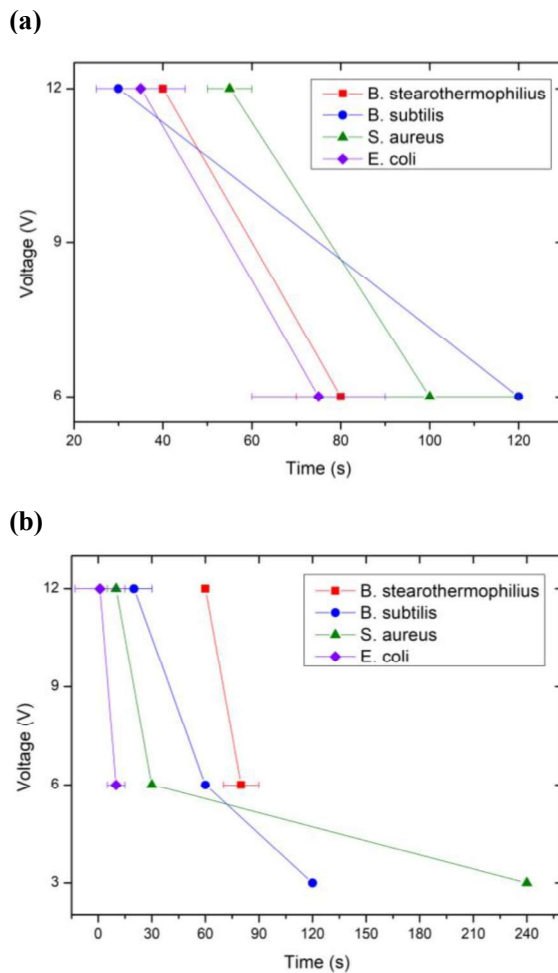
Fig. 1. Survival curves of all the bacteria for (a) 1slm and (b) 2slm

The survival curves of all the bacteria under this conditions are presented in Figure 1. These curves indicate that He APPJ with higher input power was more effective, meaning that the treatment time for decontamination is shorter for the higher power.

Once we have shown that this type of APPJ can decontaminate the bacteria, we started with the plasma source diagnostics. This was done under the same conditions as the bacteria were treated but over a Petri dish filled with distilled water (no bacteria). Petri dish was also grounded. The gas flow was 2 slm, and input power was 12 V.

The optical measurements include species detection with optical emission spectroscopy (OES) and ICCD imaging of the plasma streamer.

Figure 2 shows a complete spectrum of present species. It contains all expected species like OH, He, N and O atoms and molecules. He is present because it was used as working gas for the APPJ, and OH, N and O are present because the experiments were conducted in ambient air and in contact with distilled water. Additional spectrum was obtained, under the same conditions, where APPJ was in contact with the saline solution (not shown here). This spectrum showed no differences in comparison to the one shown in Figure 2 i.e. no existence of Na or Cl lines.
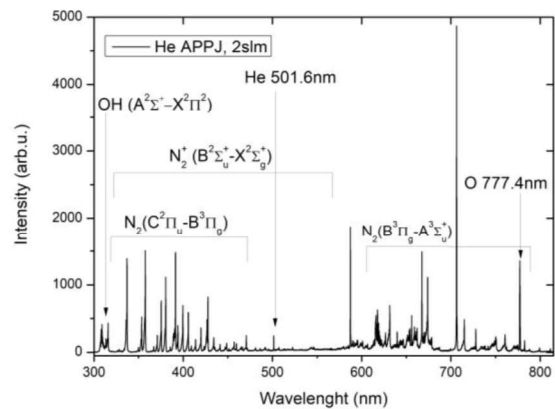
Fig. 2. OES of He APPJ (1cm from the surface of the distilled water in Petri dish (grounded))

As the second optical measurement of the APPJ we performed the ICCD imaging of the discharge. Selected images, shown in Figure 3, present length and thickness of the plasma streamer. The horizontal blue line in the images

represent the bottom of the APPJ (end of the glass tube) while the vertical orange line represents the wire electrode. It was found that the streamer reaches the surface of a distilled water for all conditions except for *1slm* and 3 *V*. Thus, in the range of these conditions, the length of the streamer depends neither on voltage nor helium flow. On the contrary, the streamer width changes with applied voltage (from 0.66 *mm* for 3 *V* up to 1.92 *mm* for 12 *V*), but again it is not dependant on the gas flow. In all conditions investigated, the brightest region of the streamer is at the electrode tip which is expected due to the high electric field. The light intensity increases as driving voltage and gas flow increase.

4. CONCLUSIONS

The decontamination effects of He APPJ were significant but dependent on the type of bacteria, exposure time, and plasma configuration (gas flow and input power). The input power of 3 *V* was not sufficient for bacteria decontamination when the gas flow was 1 *slm*; however, it was enough for decontamination of *S. aureus* and *B. subtilis* with the gas flow of 2 *slm*.

The optical emission spectrum showed that the plasma power was not sufficient enough to excite Na and Cl species, but it exhibits the intensive signature of OH, O and N species. Additional analysis will be done on specific atomic and molecular lines to observe their influence on the bacteria decontamination.

The ICCD imaging showed a spatial change of the plasma discharge and its invariance of the gas flow. Further calculations will provide us with the evaporation rate of the solution which should be taken into account for maintaining the distance from the APPJ nozzle to the surface of the bacteria solution.

REFERENCES

[1]   Ehlbeck J., Schnabel U., Polak M., Winter J., Von Woedtke T., et al., Journal of Physics D: Applied Physics, **44**, 1-33, 2011

[2]   Gadri R. B., Roth J. R., Montie T. C., Kelly-Wintenberg K., et al., Surface and Coatings Technology, **131**, 528-542, 2000

[3]   D. Vujošević, U. Cvelbar, U. Repnik, M. Modic, S. Lazović, et al., Plasma Sci. Tech., **19** 075504-075513, 2017

Fig. 3. ICCD images of discharges at different gas flows and input power. The horizontal blue line represents the bottom of the APPJ and the vertical orange line represents the wire electrode.

[4]   A. Yu. Nikiforov, X. Deng, I. Onyshchenko, D. Vujosevic, V. Vuksanovic et al, Eur. Phys. J. Appl. Phys., 75, 24710-24717, 2016

[5]   Hofmann S., *Atmospheric pressure plasma jets: characterisation and interaction with human cells and bacteria*, Eindhoven: Technische Universiteit Eindhoven, 11-30, 2013

[6]   Halfmann H., Bibinov N., Wunderlich J., Awakowicz P., 'A double Journal of Physics D: Applied Physics, **40**, 1-11, 2007

PROCEEDINGS OF
THE XXIIND INTERNATIONAL
CONFERENCE ON GAS DISCHARGES
AND THEIR APPLICATIONS

- VOLUME 2 -

2nd - 7th September 2018

Novi Sad, SERBIA

EXECUTIVE MANAGMENT COMMITTEE

Dr. J.E. Jones, Chair
Prof. G.R. Jones
Prof. J.W. Spencer
Prof. K Hidaka
Dr. A.B. Murphy
Prof. D. Hong
Dr. P. Robin-Jouan

INTERNATIONAL SCIENTIFIC COMMITTEE

Dr. J.-M. Bauchire, France
Prof. Yann Cressault, France
Prof. C.M. Franck, Switzerland
Prof. K. Hidaka, Japan
Prof. G.R. Jones, UK
Dr. A.B. Murphy, Australia
Prof. G.J. Pietsch, Germany
Prof. Ph. Robin-Jouan, France
Prof. Kohki Satoh, Japan
Prof. J.W. Spencer, UK
Dr. T. Teich, Switzerland
Prof. J. -Y. Trepanier, Canada
Prof. Y. Wu, China
Dr. J. L. Walsh, UK

Dr. J.-P. Borra, France
Prof. M. Farzaneh, Canada
Prof. A. Haddad, UK
Prof. D. Hong, France
Dr. J.E. Jones, UK
Prof. Z. Lj. Petrović, Serbia
Prof. V. Rakov, USA
Prof. A. Robledo-Martinez, Mexico
Dr. M. Seeger, Switzerland
Dr. S. Stangherlin, Switzerland
Dr. Igor Timoshkin, UK
Prof. K.-D. Weltmann, Germany
Dr. J. D. Yan, UK

LOCAL ORGANIZING COMMITTEE

Prof. Zoran Lj. Petrović, Chair
Dr. Saša Dujko, Co-Chair

Dr. Nevena Puač, Co-Chair
Dr. Nikola Škoro, Secretary

Dr. Danko Bošnjaković
Dr. Dragana Marić
Kosta Spasić
Marija Puač
Nenad Selaković
Ilija Simonović

Prof. Bratislav Obradović
Dr. Gordana Malović
Jelena Sivoš
Dejan Maletić
Jasmina Atić
Vladan Simić

Panacomp Wonderland Travel

VOLUME SCALING IN PRODUCTION OF ACTIVE OXYGEN SPECIES IN AN ASYMMETRICAL PLASMA REACTOR

K SPASIĆ*, N ŠKORO, N PUAČ, G MALOVIĆ, Lj. PETROVIĆ

Institute of Physics, University of Belgrade, Pregrevica 118, 11080 Belgrade, Serbia
*kostasp@ipb.ac.rs

ABSTRACT

Large volume plasma reactor is created as a prototype of a device for industrial scale treatment of sensitive samples. Mild and streamer free plasmas can be achieved because of strong asymmetry of electrodes. We have investigated influence of surface of grounded electrode on creation of excited oxygen species. Measurements were performed by mass-energy analyser in oxygen-argon plasma at pressures of 300 mTorr, 450 mTorr and 600 mTorr.

1. INTRODUCTION

Low pressure plasmas are extensively used over wide spectrum of industries. Their biggest advantages are ease of control in processes such are etching or deposition [1] and relatively low price of application. They are used in textile industries in colouring preparations, where they have ecological advantage over traditional wet pre-treatments [2]. Also, they can make textiles more resistant to shrinkage or even render it bactericidal [3, 4]. Low pressure plasmas have lately been widely accepted for applications in biology, mostly in treatments of seeds. It is shown that plasma treatment of seed can lead to improvement of germination rate [5, 6], can affect enzyme activity [7] and even change the speed at which sprouts are growing [8]. Certain pathogens, fungi or bacteria, may appear on surface of seed weather during long term storage or even in the field. Plasmas are proven to be very effective tool in removal of those pathogens without damage to seeds [9, 10]

Prototype of a device that is suitable for low pressure plasma treatment of temperature sensitive samples have been created in our laboratory. It is already shown to be successful in treatment of both seeds and textile [7, 11, 12].

Understanding of all discharge conditions and how they affect plasma parameters is very important in order to be able to create most effective and most energy efficient treatments. In order to gain better insight in relevant plasma chemistry, we have employed mass-energy analyser. In addition we have tested influence of surface of grounded electrode.8

2. EXPERIMENT

We have created large volume plasma reactor with asymmetric electrodes in order to provide streamer free conditions for industrial scale treatment of sensitive samples such are textiles or seeds. Cylindrically shaped discharge chamber, whose walls serve as a grounded electrode, is 2.5 m long and 1.17 m wide and it is made of stainless steel. Powered electrode, made of aluminium, is placed along the main axis of cylinder. It is 1.5 m long with diameter of 3 cm. Sample holding platform, which is also grounded, is placed 46 cm bellow powered electrode. For some measurements, additional stainless steel grounded electrode is placed around aluminium rod. It has outer diameter of 65 cm and it is grounded via contact with sample holding platform and additional contacts with chamber walls. Discharge is powered by Dressler Cesar 1310 power supply which is equipped with automatic matching box so that reflected power remains under 2% of forwarded power. It can deliver up to 1000 W at 13.56 MHz.

Gases are introduced into chamber over specially constructed home-made system which allows simultaneous control of up to 4 different gases. Desired mixture is achieved by setting up

appropriate flow of each component. In our experiments we have used mixture of 99% of oxygen and 1% of argon at pressures of 300 mTorr which was achieved with total flow of 220 sccm, 450 mTorr with flow of 400 sccm and 600 mTorr with 590 sccm. Low pressure is maintained by mechanical pump.

HIDEN EQP mass-energy analyser was placed side on into the chamber. Orifice of the device is positioned at a distance of 30 cm from powered electrode and it cannot be changed. When there was no additional grounded electrode in use mass-energy analyser protruded 25 cm from grounded wall toward powered electrode. In other case it was in level with grounded electrode.

During measurements of neutral species ionization had to be performed inside mass spectrometer. Energy of ionizing electrons can be adjusted with precision of 0.1 eV, starting from 4 eV. When mass spectra are recorded, this energy is fixed. Conversely, m/Z ratio can be fixed while measurements are performed as dependence of energy of ionizing electrons. Measurements that were performed at low RF power have low signal to noise ratio. In order to improve it 12 scans were performed for each condition.

3. RESULTS AND DISCUSION

In order to better understand plasma chemistry in our discharge and to gain better insight in processes that are taking place on surface of treated samples, we have employed mass-energy analysis as a tool to detect presence of excited species of oxygen molecules and atoms. To achieve that, special measurement method had to be applied.

$$e + O \rightarrow O^+ + 2e \ (reaction \ threshold \ 13.6 \ eV)$$
$$e + O_2 \rightarrow O_2^+ + 2e \ (reaction \ threshold \ 12.6 \ eV)$$
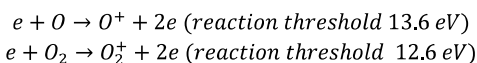
Table 1 Reaction thresholds for creating oxygen ions

Ionization of neutral species, which is necessary for their detection or any kind of manipulation, is happening inside mass spectrometer in ionization chamber by collision with ionizing electrons. These processes, presented in *Table 1*, have energy thresholds. If an atom or a molecule that is in ground state collide with an electron with energy that is below this threshold no ionization will take place and detection of these atoms or molecules will not be possible. Conversely, if some specie enters mass energy analyser in some

excited state it could be both ionized and detected after collision with an electron whose energy is below aforementioned threshold.

When discharge is turned off only ground state molecules are present and nothing is detected if energy of ionizing electrons is less than 12.6 eV. When discharge is turned on both excitation and dissociation can take place in plasma in various processes. Ionization and subsequent detection can now occur at energies that are well below threshold. Counting of excited species is performed by measuring counts for fixed ratio of m/Z at all energies up to an ionization threshold. Integrating that curve gives us number of all excited species at that m/Z that have entered mass energy analyser.
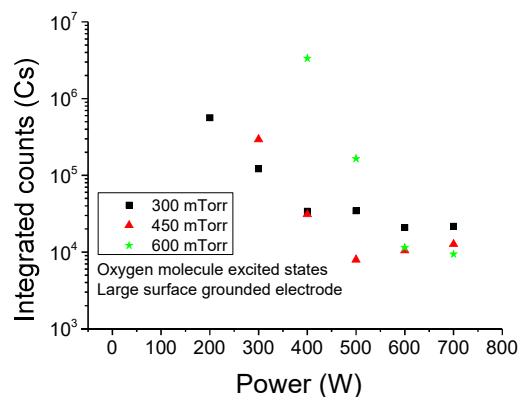
Fig. 1 Integrated counts of molecular oxygen species when larger grounded electrode was used
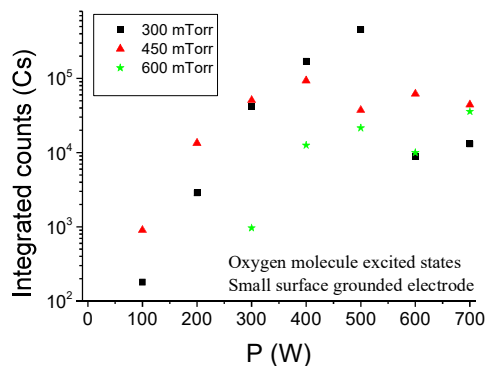
Fig. 2 Integrated counts of molecular oxygen species when smaller grounded electrode was used

Measurements were performed with grounded electrodes of two different sizes. Smaller electrode provides effective volume of plasma of $0.42 \ m^3$ while larger one stands at $1.53 \ m^3$. Integrated counts of molecular excited species are presented in *Fig. 1*. At low applied RF powers

counts were negligible. In order to detect neutral species higher powers should be applied at higher pressures. After initial detection further increase of power results in sharp decrease of excited species of molecular oxygen. This drop is most significant at the highest pressure where two orders of magnitude of reduction is observed. Behaviour like this can in part be attributed to increased dissociation of molecules at higher powers but also to increased ionization and excitation.

Excited species of molecular oxygen, when smaller grounded electrode was used, are presented in *Fig. 2*. Much lower counts were recorded in this case. Since mass spectrometer is in level with grounded electrode huge loss of excited species is taking place on surface of that electrode. At all tree pressures higher applied power caused increase in number of excited species up to a pressure dependent maximal value. Further increase of power is leading to a drop in their numbers, which is very similar to one that was exhibited when larger electrode was used.
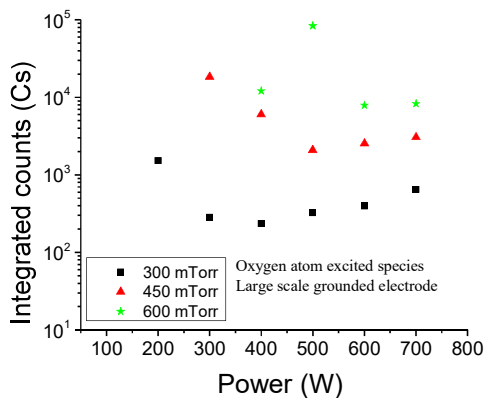
Fig. 3 Integrated counts of atomic oxygen species when larger grounded electrode was used

Integrated counts of atomic oxygen excited species, for situation when larger grounded electrode was used are shown in *Fig. 3*. Their behaviour is similar to species of molecular oxygen when larger grounded electrode was used. There is certain minimal power that is required to be applied below which no detection is taking place. This detection threshold is pressure dependent and it is higher at higher pressures. At 300 mTorr and 450 mTorr rise of applied power is causing number of excited species to, at the beginning, sharply drop to a minimum value. After that point growing trend can be observed.

Only at 600 mTorr maximal number of excited species were detected at power that is higher than detection threshold.

In *Fig. 4* we present integrated counts of excited atomic oxygen species when smaller grounded electrode was used. In contrast to behaviour with larger electrode higher counts are measured at lower pressures. Due to the fact that orifice of the mass spectrometer stands at level of the surface of grounded electrode which is depleting oxygen atoms, very low counts of excited species are measured. In addition detection was not possible at all when applied power was under 400 W. General rising trend is observed with increase of RF power but in order to create significant amount of atomic species, which would be effective in any kind of treatment one would need to apply RF powers that are beyond our technical capabilities.
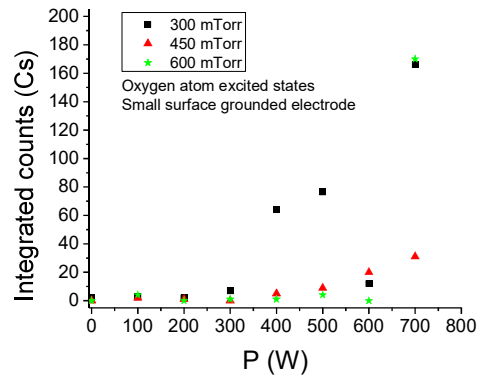
FIG. 4 Integrated counts of atomic oxygen species when smaller grounded electrode was used

4. CONCLUSIONS

We have tested influence of surface of grounded electrode in highly asymmetrical system on creation of excited species of oxygen. Measurements were performed at the same distance from powered electrode. Smaller grounded electrode is constructed as cylinder and its surface is at the same distance from powered electrode as mass-energy analyzer. Much higher production of excited species was achieved when larger grounded electrode was used.

REFERENCES

[1] T. Makabe and Z. Lj. Petrovic, PLASMA ELECTRONICS: Applications in Micro

Electronic Device Fabrication, Taylor & Francis Group, (2006)

[2] Radetic M, Jovancic P, Puac N, Petrovic ZL. Environmental impact of plasma application to textiles. InJournal of physics: conference series 2007 (Vol. 71, No. 1, p. 012017). IOP Publishing.

[3] Sun D. and Stylios G.K., Textile research journal (2004), 74, 9, 751-756.

[4] Radetic M, Jovancic P, Puac N, Petrovic, Journal of physics: conference series (2007), 71, 1, 012017

[5] Kitazaki S, Koga K, Shiratani M, Hayashi N. Growth enhancement of radish sprouts induced by low pressure O2 radio frequency discharge plasma irradiation. Japanese Journal of Applied Physics. 2012 Jan 20;51(1S):01AE01.

[6] Filatova I, Azharonok V, Gorodetskaya E, Mel'nikova L, Shedikova O, Shik A. Plasma-radiowave stimulation of plant seeds germination and inactivation of pathogenic microorganisms. Proceedings of the International Plasma Chemistry Society. 2009 Jul;19:627

[7] Puač N, Škoro N, Spasić K, Živković S, Milutinović M, Malović G, Petrović ZL, Plasma Processes and Polymers (2017), 1700082

[8] Volin JC, Denes FS, Young RA, Park SM, Crop Science (2000), 40, 6, 1706-18

[9] Nishioka T, Takai Y, Kawaradani M, Okada K, Tanimoto H, Misawa T, Kusakari S. Seed disinfection effect of atmospheric pressure plasma and low pressure plasma on Rhizoctonia solani. Biocontrol science. 2014;19(2):99-102.

[10] Schnabel U, Niquet R, Krohmann U, Winter J, Schlüter O, Weltmann KD, Ehlbeck J. Decontamination of microbiologically contaminated specimen by direct and indirect plasma treatment. Plasma Processes and Polymers. 2012 Jun 1;9(6):569-75.

[11] S. Živković, N. Puač, Z. Giba, D. Grubišić, Z.Lj, Petrović, Seed Science and Technology, 32 3 (2004) 693

[12] N. Puač, Z.Lj. Petrović, M. Radetić, A. Djordjević, Materials Science Forum 494 (2005) 494

ICPIG 2011 Conference
28th August to 2nd September 2011

- Home
- Topics
- **Committees**
- Scientific Programme
- Invited Speakers
- Awards
- Workshops
- Posters
- Proceedings
- Author index
- The Venue
- Banquet
- Conference Excursion
- Social Activities
- Travel & Visas
- Accommodation
- Local Information
- Dates & Announcements
- Registration & Fees
- Sponsors & Exhibitors
- Contact

Sponsored by

Details about sponsoring ICPIG and securing exhibition spaces are available in the *Sponsorship* section.

International Union of Pure & Applied Physics

Committees

International Scientific Committee	Local Organising Committee
Ursel Fantz (Chair), Germany	Timo Gans (Chair), University of York
Nick Braithwaite (Secretary), United Kingdom	Deborah O'Connell (co-Chair), University of York
Annemie Bogaerts, Belgium	Bill Graham (co-Chair), Queen's University Belfast
Rod Boswell, Australia	Tom Field, Queen's University Belfast
Laifa Boufendi, France	Yannis Kourakis, Queen's University Belfast
Domenico Bruno, Italy	Paul Maguire, University of Ulster
Gary Eden, US	Charlie Mahony, University of Ulster
Masaru Hori, Japan	Tomo Murakami, Tokyo Institute of Technology
Poul Michelsen, Denmark	Kari Niemi, Queen's University Belfast
Gheorge Popa, Romania	Dave Riley, Queen's University Belfast
Yi Kang Pu, China	
Milan Simek, Czech Republic	
Andrey Starostin, Russia	
Jaime de Urquijo, Mexico	

Measurements of atomic oxygen concentrations in a large scale asymmetric capacitively coupled plasma reactor by using catalytic probes

S. Lazović[1,2], N. Puač[1], K. Spasić[1], G. Malović[1], U. Cvelbar[2], M. Mozetič[2], Z. Lj. Petrović[1]

[1] Institute of Physics, Univesity of Belgrade, Pregrevica 118, 11070 Belgrade, Serbia
[2] Jozef Stefan Institute, Jamova 39, 1000 Ljubljana, Slovenia

A large scale cylindrical asymmetric capacitively coupled plasma reactor is suitable for efficient treatment of materials like polymers, textile and plant seeds. Plasma is homogeneous and stable from transitions to streamers providing uniform and safe treatment of sensitive materials. For many biomedical and textile treatment effects, role of extremely reactive atomic oxygen species is very important. Measurements were preformed using nickel catalytic probe placed side-on to the powered electrode. Concentrations of neutral oxygen atoms were measured for a range of powers given by the RF generator, at several different distances from the powered electrode, in air at two different pressures.

1. Introduction

Radiofrequency discharges are necessary for treatment of isolators and semiconductors [1]. Different kinds of conductive and non-conductive materials like microelectronics devices [2-4], biological samples [5] and textiles [6] can be treated using capacitively coupled RF plasmas. Organic samples and materials may be removed by ashing with potential applications in microelectronics and medicine.

A large scale CCP RF reactor was developed in our laboratory in order to treat cheaply and uniformly textile rolls without damaging the surface of the fibers. Homogeneous and stable plasma, without transition to streamers, capable of long term stable operation (i.e. treatments) was achieved. Detailed electrical characterization of the plasma reactor using derivative probes can provide information on the relations between external discharge properties (current and voltage waveforms, impedance) and plasma parameters (densities, energies, fluxes of charged particles). Textile samples can be placed in the chamber at several distances from the powered electrode providing various intensities of treatment. Langmuir probe measurements can provide us with ion and electron concentrations at positions were samples would be placed. These measurements show complex spatial dependences of the concentrations and are important for proper characterization of treating procedures. These measurements were part of our previous work.

Treatment and sample surface interactions are depended not only on plasma and chemistry but also on post plasma chemistry and related processes. We have used catalytic probe in order to measure concentrations of oxygen atoms.

2. Experimental setup

The discharge chamber is 2.5 m long and 1.17 m in diameter and made of stainless steel. Powered electrode is placed axially in the centre of the chamber and is 1.5 m long, 3 cm in diameter and made of aluminum. Outer chamber wall is the grounded electrode. The rest of the electrical circuit consists of RF power generator Dressler Cesar 1010 in combination with Variomatch matching network. Derivative probes, which can be used to measure the power delivered to the plasma itself are placed into a stainless steel box opposite to each other. The box is placed as close as possible to the end of the powered electrode. Low pressures are maintained using mechanical vacuum pump with a constant flow of gas air (see Fig.1).
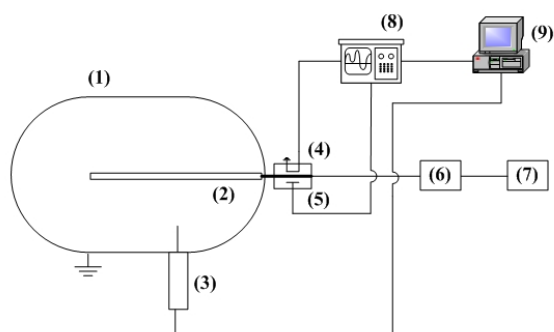
Figure 1. Experimental set-up: (1) Chamber, (2) Powered electrode, (3) Catalytic probe (4) Current probe, (5) Voltage probe, (6) Variomatch, (7) Power supply, (8) Oscilloscope, (9) Computer

Catalytic probe was mounted perpendicular to the powered electrode. The tip of the probe is in a shape of a disk made of nickel, 3 mm in diameter and

0.04 mm thick. The probe is 50 cm long and placed in a glass tube with sealed contact conductors on the other side. Digital voltmeter (Iso-Tech IDM73) connected to the computer was used to record changes of voltage signals from the probe. Voltage signal is recorded with a frequency of 2 Hz. Catalytic probe is being heated by the recombination processes of atomic oxygen at the surface of the nickel probe tip. Recorded voltage waveform corresponds to the probe temperature signal. When plasma is turned off, concentration of neutral oxygen atoms decrease. Concentrations can be calculated from the slope of that decrease.

3. Results and discussion

Plasma was ignited in air at two pressures (300 mTorr and 750 mTorr) and power was changed in range from 0 to 500 W. Probe was placed at 47.5, 42.5 and 37.5 cm from the powered electrode. Voltage signals from the catalytic probe are recorded before, during and after plasma formation. Voltage signals correspond to temperature of the probe and oxygen atom concentrations are proportional to the time derivative of temperature. When plasma is ignited, probe temperature increases (depending on how fast RF power in being increased). When a certain value of RF power is reached, temperature saturates. Pressure in the chamber increases when plasma is ignited so it is needed to adjusted the pressure to 300 or 750 mTorr. After that, plasma is turned off and temperature starts to decrease. Atomic oxygen concentrations are proportional to the slope of that decrease with the constant depending on probe mass, area, specific heat capacitance and γ coefficient for nickel as well as on thermal velocity of O atoms and dissociation energy of oxygen molecules [7].

Results at 300 mTorr for three distances are shown at Figure 2. We can see that atomic oxygen concentrations are lowest when the probe is positioned closest to chamber wall (47.5 cm). The concentration increases with the increase of power delivered to plasma. When the probe is positioned closer to the powered electrode, concentrations also increase. For shorter distances (42.5 cm and 37.5 cm) we did not cover the whole power range (0-500 W) because of intensive probe glowing due to ion bombardment of the probe surface. At 47.5 cm distance, probe was not glowing for the 0 to 200 W power range. Above this range, glowing of the probe is increasing with power. At 42.5 cm the probe was not glowing only in the 0 – 50 W power range. For the shortest distance (37.5 cm) the probe was glowing for all values of RF power. Glowing of

the probe was not noticed at 750 mTorr for 47.5 cm distance.
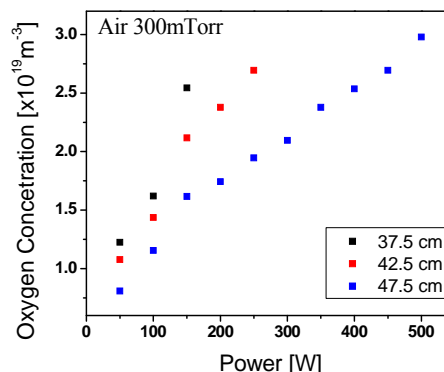
Figure 2. Atomic oxygen concentrations as a function of RF power for three different distances from the powered electrode. Air pressure was 300 mTorr

Oxygen concentrations as a function of RF power at 300 mTorr and 750 mTorr are shown at Figure 3.
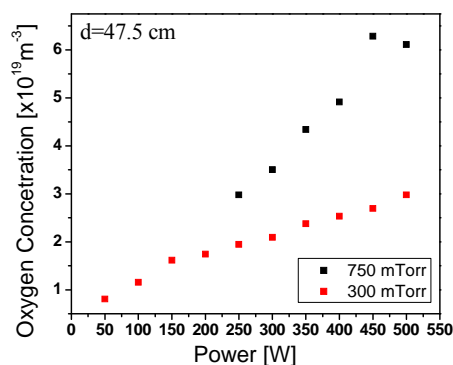
Figure 3. Atomic oxygen concentrations as a function of RF power. Distance between probe tip and the powered electrode was 47.5 cm. Chamber pressure was 300 and 750 mTorr.

For the pressure of 300 mTorr plasma is filling the whole chamber area already at several tens of watts. At 750 mTorr this happens for 250 W and higher (this is why power range at 750 mTorr goes only from 250 W to 500 W). We can see that the oxygen concentrations are higher at 750 mTorr compared to 300 mTorr and are increasing with RF power.

4. Conclusion

Neutral oxygen atom concentrations are measured in a large scale CCP plasma reactor. Discharge was generated in air at 300 mTorr and 750 mTorr. Measurements were performed at 47.5, 42.5 and 37.5 cm from the powered electrode. RF power given by the generator was varied from 0 to

500 W. This kind of plasma is suitable for treatment of different kinds of textile. Both plasma and post plasma effects at sample surface are important to study and understand for the sake of successful applications. The formation of new oxygen-containing groups on the fiber surface is suggested to be due to the presence of extremely reactive atomic oxygen species in discharge during the air plasma processing and/or post-plasma chemical reactions when the activated fiber surface reacts with environmental species [8]. Oxygen atom concentrations coming to the surface of the samples can be controlled by adjusting the pressure, distance from the powered electrode and RF power.

5. References

[1] A. Bogaerts et al. / Spectrochimica Acta Part B 57 (2002) 609–658.

[2] M.A. Lieberman, A.J. Lichtenberg, Principles of Plasma Discharge and Materials Processing, (2005) (Wiley:Hoboken).

[3] T. Makabe, Z.Lj. Petrović, Plasma Electronics, (2006) (Taylor and Francis:New York);

[4] U. Cvelbar, K. (Ken) Ostrikov and M. Mozetic, Nanotechnology 19 (2008) 405605.

[5] N. Puač, Z.Lj. Petrović, S. Živković, Z. Giba, D. Grubišić and A.R. Đorđević, Plasma Processes and Polymers, (2005) 193, (Whiley)

[6] M. Radetić, P. Jovančić, N. Puač and Z.Lj. Petrović, Workshop on Nonequilibrium Processes in Plasma Physics and Studies of the Environment, SPIG 2006, Journal of Physics: Conference Series 71 (2007) 012017

[7] M. Mozetic, U. Cvelbar, A. Vesel, A. Ricard, D. Babic and I. Poberaj, Journal of Applied Physics, 97 (2005) 103308

[8] V. Ilić, Z. Šaponjić, V. Vodnik, S. Lazović, S. Dimitrijević, P. Jovančić, J. M. Nedeljković and M. Radetić, Ind. Eng. Chem. Res. 49 (2010), 7287–7293

XXXI

INTERNATIONAL CONFERENCE OF PHENOMENA IN IONIZED GASES

JULY 14-19, 2013
GRANADA, SPAIN

e-Book of abstracts
(searchable online through
http://www.icpig2013.net/buscador/index.html)

Organized by
Spanish National Research Council (CSIC) with the participation
of the Universities of Córdoba (UCO), Country Vasc (UPV)
and Polythecnic of Madrid (UPM)

Scientific Secretariat
LOC ICPIG 2013
LOC Chair: Dr. F. J. Gordillo-Vázquez
Instituto de Astrofísica de Andalucía (IAA - CSIC)
Glorieta de la Astonomia s/n
18008 Granada, Spain
Tel: +34-958-230-642
Email: icpig2013@iaa.es
Web: www.icpig2013.net

Management Office
Department of Congresses, Conventions and Incentives
C/ Princesa 47, 4th Floor
Madrid, Spain
Tel: +34-91-204-26-00
Email: icpig2013@viajeseci.es

XXXI ICPIG
GRANADA 2013
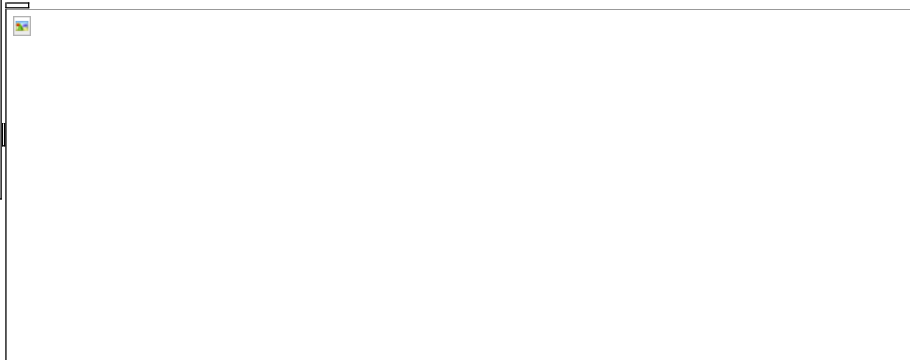
Organizing Committees

International Scientific Committee

N. Braithwaite (Chair)	UK and Ireland
Y. K. Pu (Secretary)	China, Taiwan and Korea
E. Stamate	Norway, Sweden, Finland and Denmark
S. Bhattacharjee	Australia, New Zealand, Indonesia, Polynesia, India and South Africa
E. Son	Russia and the area of the former SU
M. Kushner	USA and Canada
J. de Urquijo	Spain, Portugal, Mexico and South and Central America
M. Hori	Japan
G. Popa	Bulgaria, Romania, Serbia, Bosnia, Montenegro, Croatia and Slovenia
L. Boufendi	France and North Africa
D. Bruno	Italy, Greece and Israel
U. Fantz	Germany, Austria, Lichtenstein and Switzerland
A. Bogaerts	Belgium, Netherlands and Luxembourg
M. Simek	Poland, Hungary, Czech Republic and Slovakia

Plasma seeds treatment as a promising technique for seed germination improvement

I. Filatova[1], V. Azharonok[1], V. Lushkevich[1], A. Zhukovsky[2], G. Gadzhieva[2], K. Spasić[3], S. Živković[4], N. Puač[3], S. Lazović[3], G. Malović[3] and Z.Lj.Petrović[3]

[1] Institute of Physics NAS of Belarus, Nezavisimosti Ave. 68, 220072 Minsk, Belarus
[2]Institute of Plant Protection NAS of Belarus, Mira Str. 2, 223011 Priluki, Minsk District, Minsk Oblast, Belarus
[3]Institute of Physics, University of Belgrade, Pregrevica 118, 11080 Belgrade, Serbia
[4]Institute for Biological Research "Siniša Stanković", University of Belgrade, Bulevar despota Stefana 142, 11060 Belgrade, Serbia

An influence of RF air plasma pre-sowing treatment on seed germination of some important agricultural plants has been studied. Two plasma systems (plan-parallel and cylindrical) were used for treatment of maize, spring wheat and lupinus seeds. It is shown that the treatments contribute to seeds germination enhancement decrease and their phytosanitary conditions improvement. The modification of seed coat surface structure by plasma irradiation is investigated with scanning electron microscopy and plasma emission spectra are analyzed for possible mechanisms determination of biological effect of plasma treatment.

1. Introduction

Cold plasma treatment is widely used for activation and decontamination of surfaces. Owing to the unique plasma features this technique is applicable for modification of a wide range of thermally sensitive materials including biological tissues. Recently it has been applied successfully for treatment of plant seeds [1–7]. Low temperature plasma pre-sowing seeds treatment was shown in some cases to be ecologically safe, cheap and effective method for improvement of seed germination and their resistance to stress and diseases.

At the same time there is a lack of research explaining the mechanism of plasma bio-stimulation. Possible processes were proposed in the literature. Plasma processing subjects the seed surface to UVradiation, charged particles bombardment, radicals and chemically active molecules resulting in the formation of functional groups on the treated surface [3, 4]. Air plasma treatment changes the wetting properties of seeds due to oxidation of their surface that leads to faster germination and greater yields [8], increases the concentration of free radicals in seeds which play an important role in acceleration of the seed metabolism [9]. The possibility of delay or enhancement of germination is demonstrated by plasma-induced coating with thin films containing different macromolecular components [10, 11]. It is obvious, that plasma treatment can have a variety of effects on morphological and sowing characteristics of seeds due to the complexity of plasma interaction with organic materials and living cells [12]. Seeds are an extremely complex system too, and vitally important biological processes may be affected by the treatment in a number of different ways.

The aim of this paper is to study the efficiency of low-pressure RF air plasma treatment of seeds of some important agricultural crops for improvement of their sowing properties and to try to identify some of the main plasma agents that contribute to enhancement of germination.

2. Experimental

Seeds of spring wheat (*Triticum aestivum* L.), blue lupine (*Lupinus angustifolius*) and maize (*Zea mays* L.) were chosen for investigations. Tested species were treated with RF air plasma using two plasma systems. The first one was a planar geometry reactor operating at 5.28 MHz [5]. The electrode system consists of two identical water-cooled copper disks with the diameter of 120 mm placed in a stainless steel vacuum chamber. A supplied full specific RF power W could be changed in the range from $0.2 \, \text{W/cm}^2$ to $0.6 \, \text{W/cm}^2$ resulting in different treatment conditions. All species were treated at pressure of 500 mTorr. A Petri dish with seeds was put on the grounded (lower) electrode. Duration of the exposure was 2.5, 5, 8 and 10 min. Each Petry dish contained 50 seeds. All treatments for all experimental conditions were replicated four times. Control group was only subjected to vacuum and gas pressure P=0.5 Torr for at least 15 min. The gas temperature did not increase beyond 310°C.

The second plasma system used for pre-sowing treatment of seeds was a cylindrical CCP reactor operating at 13.56 MHz. In this system, a central, powered electrode is aluminum rod and the grounded

electrode is the wall of the chamber. A detailed description of the system can be found in [6]. The treated samples were placed in Petri dishes and put on a platform that is positioned at the bottom of the chamber. Every Petri dish housed 20 seeds with exception of maize where, due to seed size, only 10 seeds per dish were used. Total amount was 60 seeds per treatment. Spring wheat was treated at powers of 50 W and 100 W at pressure of 500 mTorr, while maize was treated at 300 mTorr with 200 W of applied RF power. Since different time of plasma exposure can cause very different results, this parameter was varied in a wide range (1min, 5min, 7min, 10min and 20 min).

The effectiveness of pre-sowing plasma seed treatments was examined by means of evaluation of the laboratory germination ability and biometric characteristics (mean root and plant length) of treated and control samples. Seeds were grown on a moist filter paper in sterile Petri dishes in a thermostat at 20° C (for wheat and lupine) and 25° C (for maize) under a light-dark regime. The seed germination and the seed infection were estimated after 7 and 10 days incubation for wheat and lupine/maize correspondingly.

Optical emission spectra (OES) were obtained with a Compact Spectrometer S100 "SOLAR LS" in the optical range from 190 to 1100 nm with an average spectral resolution of 1 nm to identify the species present in plasma during the treatment. Surface structure of the treated and untreated seeds was imaged with a high resolution scanning electron microscope (LEO 1455 VP).

3. Results and discussion

It has been found that plasma pre-treatments of seeds positively influenced their germination and biometric characteristics of sprouts. The results obtained in planar discharge are shown in Fig. 1. The plasma treatment of seeds with low germination ability (spring wheat, maize) stimulated their germination and the early stages of seedling development, while it did not affect negatively the germination of seeds with high germination ability (lupine). The seed pre-treatments for 2.5 and 5 min were the most effective for all species. The seedling of treated spring wheat was 2.1 cm higher than that in the control group (Fig. 1b). The same result was observed for maize seeds as a result of plasma treatment during 2.5 min. Large seedlings have a higher survival and growth rates than small seedlings that will provide good conditions for plant growth at the later stages of ontogenesis.

Similar results for plasma treatment of spring wheat and maize were obtained in asymmetric CCP
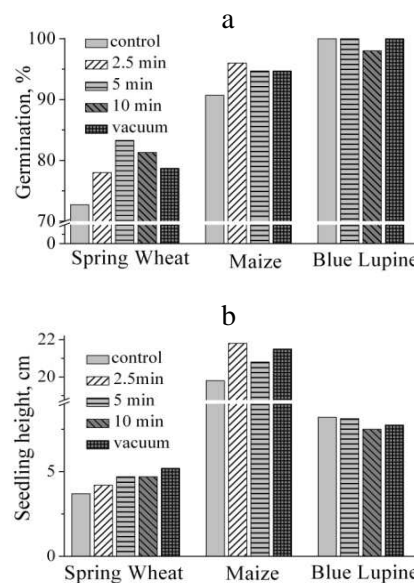
Fig. 1. Germination (a) and seedling height (b) of spring wheat, maize and blue lupine as a result of plasma and vacuum (without plasma) seed pre-treatments ($W = 0.2$ W/cm^2, $P = 500$ mTorr)

discharge. Results for spring wheat seed germination after plasma treatment at 50 and 100W are presented in Fig. 2. For both powers better results are achieved for shorter treatment times. Since the control group germination percentage is quite high the overall increase in germination percentage in treated batches is only few percent. Treatments with longer treatment times then 7 min showed a decrease in germination due to the damage of the seed inflicted by plasma bombardment. For higher power of 100 W and longer times this damage is quite high. In this case the germination percentage was reduced down to 70 %.
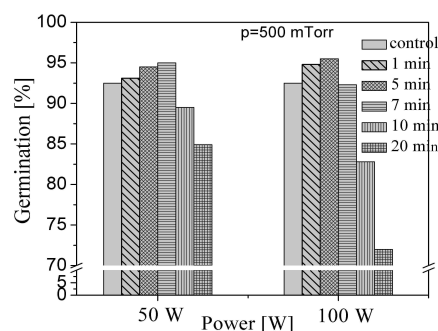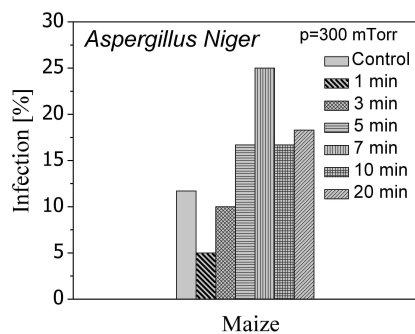

Fig. 2. Germination of spring wheat after plasma treatment in asymmetrical CCP discharge. Control represents untreated seeds. Feeding gas was air and the pressure was P = 500 mTorr

Unfortunately most of the seeds used for commercial purpose are infected with different types of fungi (belonging to the genera *Mucor*, *Fusarium*,

Alternaria etc.). Therefore, it is important to check if same plasma conditions can be used to decrease the infection of seeds.

The results for infection percentage of spring wheat are shown in Fig. 3 for both plasma systems. We can see that we are able to reduce total infection in treated wheat seeds up to 10 min of treatment. For longer treatment times (20 min) the percentage of infected seeds increases. This is most probably due to the damage of the seed coat caused by treatment. The higher damage of the seed coat further increases seed's susceptibility to infection. Plasma treatment is shown as an effective tool against *Fusarium* spp. that causes the most harmful root disease of wheat worldwide.
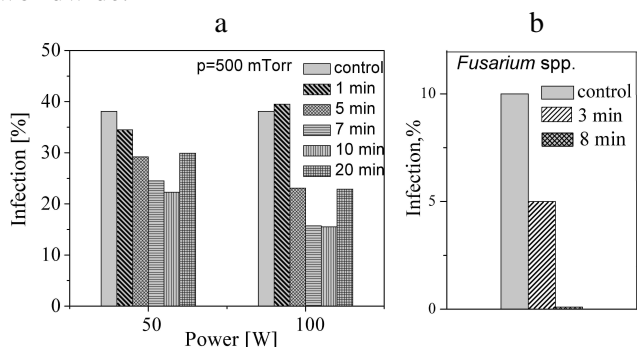
Fig. 3. Infection of spring wheat after plasma treatment in asymmetrical CCP discharge (a) and infection with *Fusarium* spp. after treatment in planar discharge (b). Control represents untreated seeds. Feeding gas was air at a pressure of $P = 500$ mTorr

Similar results are observed for maize and lupine (see Fig. 4 and 5).

Fig. 4. Infection of maize after plasma treatment in asymmetrical CCP discharge. Control represents untreated seeds. Feeding gas was air at a pressure of p = 300 mTorr. Power given by RF power supply was 200 W

For lower treatment times in asymmetrical CCP discharge we have observed a decrease of the infected seeds percentage, but with an increase in treatment times infection spreads even more than in the control

group. We can conclude that both effects (germination increase & infection decrease) can be accomplished only for lower treatment times for the present setup of the asymmetric CCP. For this pressure/power combination this interval is between 1 and 7 min of treatment. The same treatment durations (between 3 and 8 min) were the most effective against fungi and bacteria for treatment of maize and lupine seeds in planar discharge (see Fig. 5).
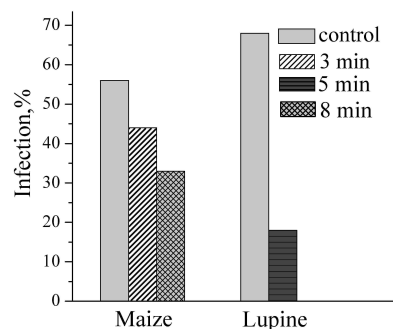
Fig. 5. Level of total infection of maize and lupine after plasma treatment in planar discharge. Control represents untreated seeds. Feeding gas was air at a pressure of P = 500 mTorr

It was revealed from the SEM images of seed coats that the surface structure of seeds changed sharply as a result of plasma treatment (Fig. 6). SEM indicated that the surface sculpture of untreated wheat seeds had a reticulate texture (Fig. 6a). The plasma treated wheat seeds had an eroded surface, with no significant ridges (Fig. 6b). The untreated lupine seed coat was formed by elongated polygonal cells (Fig. 6c).
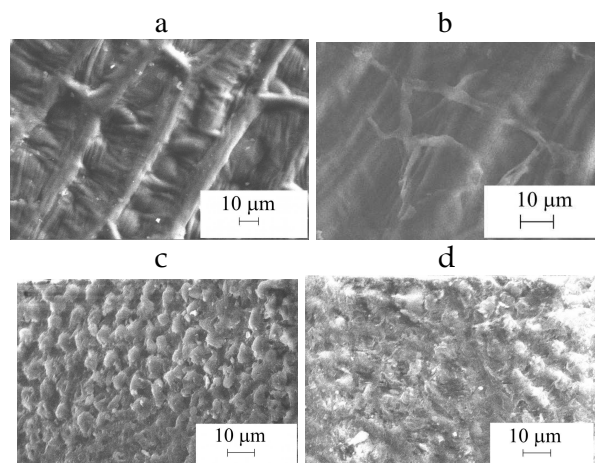
Fig. 6. Scanning electron micrograph (SEM) images of seed coat surface of wheat (a, b) (magnification = 2.00 KX) and blue lupine (c, d) (magnification = 1.00 KX) for non-treated (control) seed (a, c) and plasma treated for 5 minutes (b, d)

No well-defined cristate-papillate structure on the seed surface of lupine was observed after the plasma treatment. Similar results were obtained for another seeds which provided experimental evidence of the seed coat surface etching induced by plasma treatment [2, 3]. Study of the seed coat thicknesses after the plasma processing showed that the treatment removes effectively the very thin lipid layer that makes seeds water-repellent and probably reduces the length (and average molecular weight) of the biopolymer chains that make up the seed coat, thus enabling better water transport through the seed coat improving the germination [13].

In order to characterize the change of seed coat structure and seed germination as a function of plasma treatment conditions the OES spectra of the plasma were analyzed. The difference was observed between spectra generated by plasma without seeds and during their treatment (Fig. 7). The species identified in the spectra are neutral molecular nitrogen N_2 (bands of the first and the second positive systems), ionized molecular nitrogen N_2^+ (bands of the first negative system). When seeds are in the plasma bands of the Angstrom system of the CO molecule appear in the spectrum.
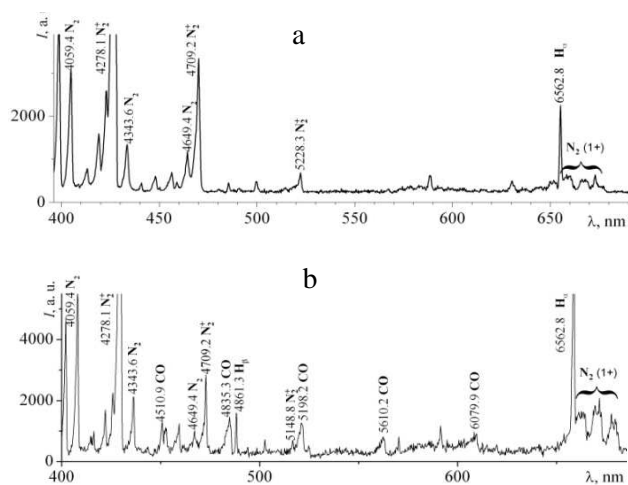
Fig. 7. Emission spectra of RF air plasma: a – pure air, b – under conditions of plasma treatment of wheat seeds

This confirms effectiveness of seed surface etching during the treatment and a possibility of formation of functional groups on treated surface that may play an important role in stimulation of seed germination [4, 5, 7].

4. Summary

This study confirms that the low temperature air plasma pre-treatment of seeds of some important agricultural crops is an effective tool for improvement of germination, shoot and root growth, providing a good fungicidal and bactericidal effect in the optimal experimental conditions that can vary for different species. SEM investigations of seeds surface have shown a significant change in its texture that is an evidence of surface etching provided by bombardment by charged particles and radicals formed in plasma. Since the seed coat for treated samples are eroded it provides a better water permeability and leads to enhancement of seed germination.

5. References

[1] A. Dubinov, E. Lazarenko, V. Selemir, IEEE Trans. Plasma Sci. **20** (2000) 180.

[2] M. Dhayal, S.Y. Lee, S.U. Park, Vacuum. **80**, No.5 (2006) 499.

[3] B. Šerá, V. Straňák, M. Šerý, M. Tichý, P. Špatenka, Plasma Science and Technology. **10**, No. 4 (2008) 506.

[4] S. Živković, N. Puač, Z. Giba, D. Grubišić, Z.Lj. Petrović, Seed Science and Technology. 32, No. 3 (2004) 693.

[5] I.I. Filatova, V.V. Azharonok, A. Shik et al., in: Plasma for Bio-Decontamination, Medicine and Food Security, ed. by Z. Machala et al., NATO Science for Peace and Security Series A: Chemistry and Biology, Springer (2012) 469.

[6] N. Puač, Z.Lj. Petrović, S. Živković, Z. Giba, D. Grubišić and A.R. Đorđević, "*Low temperature plasma treatment of dry Empress-tree seeds*", Plasma Processes and Polymers, Eds. R. d'Agostino, P. Favia, C. Oehr and M.R. Wertheimer, (Whiley: (2005) 193.

[7] M. Selcuk, L. Oksuz, P. Basaran, Bioresource Technology, **99** (2008) 5104.

[8] http:// www.ncbi.nlm.nih.gov/pmc/articles/ PMC3473364/pdf/srep00741.pdf.

[9] I.I. Filatova, V.V Azharonok, N.A. Poklonski, et al., Proc. of the VII Int. Conf. Plasma Physics and Plasma Technology, September 16-21, 2012, Minsk, Belarus, ed. by V.M. Astashinski et al., Kovcheg, Minsk (2012) 734.

[10] J.C. Volin, F.S. Denes, S.M.T. Park, R.A. Young, Crop Science. **40** (2000) 1706.

[11] R.A.M. Carvalho, A.T. Carvalho, M.L.P. da Silva et al., Quim. Nova. **28**, No. 6 (2005) 1006.

[12] B. Será, P. Spatenka, M. Serý et al., Plasma Science, IEEE Transactions on Plasma Science. **38** (2010) 2963.

[13] http://www.aff.org.au/Griesser_Plasma_ treatment_of_%20seeds_Final.pdf.

ICPIG 2015

XXXII INTERNATIONAL CONFERENCE ON PHENOMENA IN IONIZED GASES

26-31 July · IAȘI · ROMANIA

www.icpig2015.net   loc@icpig2015.net

Professor Laifa BOUFENDI
President of the ISC

Professor Gheorghe POPA
Chair of LOC

COMMITTEES

International Scientific Committee

Laifa BOUFENDI, *President of ISC* **Université d'Orléans, France**	France and North Africa
Miles TURNER Dublin City University Ireland	UK and Ireland
Yi Kang PU Tsinghua University, China	Mainland China, Taiwan and Korea
Eugen STAMATE Technical University of Denmark, Denmark	Norway, Sweden, Finland and Denmark
Sudeep BHATTACHARJEE Indian Institute of Technology, Kanpur, India	Australia, New Zealand, Indonesia, Polynesia, India and South Africa
Eduard SON Joint Institute for High temperature RAS, Russia	Russia and the area of the former SU
Mark KUSHNER University of Michigan, USA	USA and Canada
Jaime de URQUIJO **Instituto de Ciencias Físicas, UNAM, Mexico**	Spain, Portugal, Mexico and South and Central America
Masaru HORI Nagoya University, Japan	Japan
Gheorghe POPA, *LOC Chair* Alexandru Ioan Cuza University of Iasi, Romania	Bulgaria, Romania, Serbia, Bosnia, Montenegro, Croatia and Slovenia
Olga DE PASCALE CNR Institute of Inorganic Methodologies and Plasmas, Italy	Italy, Greece and Israel
Holger KERSTEN Kiel University, Germany	Germany, Austria, Lichtenstein and Switzerland
Ute EBERT Center for Mathematics and Computer Science (CWI), Amsterdam, The Netherlands	Belgium, The Netherlands and Luxembourg
Zdenko MACHALA Comenius University, Bratislava, Slovakia	Poland, Hungary, Czech Republic and Slovakia

Local Organizing Committee

Gheorghe POPA, LOC Chair	Alexandru Ioan Cuza University of Iași
Nicolae Victor ZAMFIR	IFIN-HH Bucharest
Gheorghe DINESCU	INFLPR Bucharest
Claudiu COSTIN, LOC Secretary	Alexandru Ioan Cuza University of Iași

LOC Members from Alexandru Ioan Cuza University of Iasi

Cătălin AGHEORGHIESEI	Valentin POHOAȚĂ
Silvia-Alina CHIPER	Sebastian POPESCU
Alexandra DEMETER	Ioana-Alexandra RUSU
Marius DOBROMIR	Bogdan-George RUSU
Nicoleta DUMITRAȘCU	Florentina SAMOILĂ
Roxana JIJIE	Lucel SÎRGHI
Dumitru LUCA	Teodora TESLARU
Ilarion MIHĂILĂ	Vasile TIRON
Andrei-Vasile NĂSTUȚĂ	Ionuț TOPALĂ

Characterization of a large-volume Oxygen RF discharge suitable for low-pressure treatment of sensitive samples

K. Spasić[1], N. Puač[1], N Škoro, G. Malović and Z.Lj. Petrović

[1]*Institute of Physics, Belgrade University, Pregrevica 118, 11000 Belgrade, Serbia*

We have created plasma reactor that is prototype of a commercial device for industrial applications, in order to enable large scale treatment of sensitive samples,. Strong asymmetry of electrodes and large volume are suitable for achieving streamer free and generally mild plasma. In order to optimize treatment conditions and make them as energy efficient as possible plasma characterization has to be performed. For that purpose we have used mass energy analyzer, optical emission spectrometry and actinometry in an oxygen-argon plasma at pressures of 300, 450, and 600 mTorr with applied powers between 100 and 700 W.

1. Introduction

Applications of low pressure plasmas are distributed over wide range of industries, mostly for processes such are etching and deposition. This is understandable if one bears in mind that they are easily controllable and fairly cheap to use [1]

The effect of non-equilibrium plasmas are also well-known and used in fields such are medicine and biology [2,3,4,5]. It is shown that after being exposed to gas discharges some seeds may improve their germination rate [6,7,8]. Effects can be noticeable even when seeds start to sprout since treated seedlings grow faster than those which were not treated [9]. Some seeds, usually due to bad storage conditions, can be infected with malignant bacteria and fungi that can affect their germination rate and growth. If that happens, plasma can be used for pre-saw sterilization, but discharge conditions have to be carefully set to avoid damage of seeds.

Having that in mind, a large scale plasma reactor, which can be used for treatment of sensitive samples, have been constructed in our laboratory. So far, it has been used for treatment of both seeds and textile [10,11].

Getting well acquainted with plasma chemistry and the ability to tune plasma parameters of the discharge that is used for treatments is very important in order to make it as effective and energy efficient as possible. For that purpose we have used mass-energy spectrometry, optical emission spectrometry and actinometry.

2. Experimental set-up

In order to provide a device for industrial scale treatment of sensitive samples, we have created large volume plasma reactor with asymmetric electrodes. It is 2.5 m long cylinder with the diameter of 1.17 m. Powered electrode is made of aluminum and it is placed along central axis of reactor. The cylindrical electrode is 1.5 m long and 3 cm in diameter. Chamber wall serves as a grounded electrode. Samples are placed on a flat metal platform lying at the bottom of the chamber below the powered electrode. Power is supplied via matching box at 13.56 MHz by Dressler Cesar 1310 power supply that can deliver up to 1000 W. Due to the fact that electrode surface ratio is very big we can accomplish plasma conditions that are streamer free and hence suitable for treatment of samples that cannot withstand high currents or temperatures.

Gases are introduced over two separate lines, each controlled by a flowmeter, while two mechanical pumps were used to achieve and maintain vacuum. Oxygen and argon are mixed at the ratio of 99:1. Total flows were set to 110 sccm for 300 mTorr, 200 sccm for 450 mTorr and 290 sccm for 600 mTorr.

Mass-energy analyzer, HIDEN EQP, was placed side-on into the chamber. Its orifice is positioned at a fixed distance of 30 cm from the powered electrode. Energy of ionizing electrons emanating from the hot filament, which are required for detection of neutral species, can be controlled with resolution of 0.1 eV, starting from 4 eV. Number of neutral atoms or molecules can be measured as a function of energy of these electrons.

In a single scan, measurements performed at low power have very low signal. Therefore, we had low signal to noise ratio. In order to increase precision, 12 measurements were performed for each conditionin accumulation mode resulting in a significant signal to noise improvement.

Optical emission spectra were obtained by using Oriel MS127i monochromator coupled with an ICCD camera. The spectrometer was positioned end-on, with a focusing lens collecting light along

axis of the vessel at two different levels: at the electrode level, facing the electrode tip, and at the platform level, 40 cm below the electrode. Since spectra recording times were several hundred ms, time and space integrated light emission was obtained in visual spectral range. Experimental set-up and positioning of the measurement equipment is shown in Figure 1.
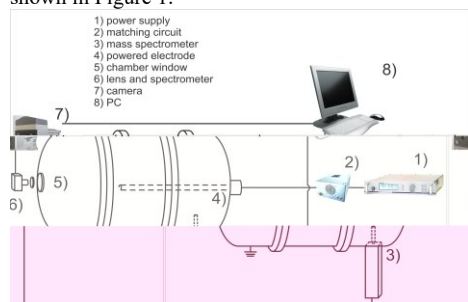
Figure 1. Experimental set-up schematics where devices are numbered as: 1) power supply, 2) matching box, 3) Mass spectrometer, 4) powered electrode, 5) chamber window, 6) lens and spectrometer, 7) camera and 8) PC.

3. Results
3.1. Mass spectroscopy

Mass spectroscopy is an indispensable tool for analyzing plasma sources. We have measured counts of oxygen molecules as a function of energy of ionizing electrons from the ionizer of the mass-energy analyzer. Measurements were performed at three different pressures: 300, 450 and 600 mTorr. Typical results are shown in **Figure 2**.

Oxygen molecules are of great interest due to their role in biochemical pathways in cells. Especially important signal molecule is O_2^- that is, among other places in cell, created at the cell membrane by ionizing O_2 metastable. In oxygen plasma we have a rich environment for this kind of reaction due to the presence of excited species and metastables. One should be aware that one of the most abundant metastables of oxygen the $O_2(a\ ^1\Delta_g)$ state has threshold energy below 1 eV and thus the extension of the signal below 5 eV of the electron energy in Fig. 2 is not surprising. With power set to 0W (plasma not ignited) we can see only those molecules which were ionized inside mass spectrometer. Only neutral oxygen molecules in ground state are present. Therefore nothing is detected below the ionization energy which is 12.3 eV [12]. When discharge is turned on, a lot of molecules are detected below the threshold energy because, when they reach mass-energy analyzer

from plasma, they are already in excited or in metastable state. Signal obtained from these molecules can be seen in Figure 2 for the electron energies below the threshold. The fact that signal below threshold decreases with increasing power probably means that the reduction is due to electron quenching of metastables and increasing electron density with power.
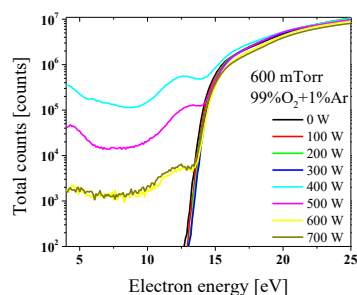
Figure 2. Counts of oxygen molecules, recorded as a function of electron energy at 600 mTorr at powers ranging from 0 to 700 W.

By integrating one curve up to the energy of 12 eV, we can get total number of molecules that are excited in the plasma and that arrived at the orifice of mass energy analyzer in excited/metastable state. We have chosen 12 eV as the limit for integration in order to be safely below the ionization threshold. Summarized results for excited and metastable oxygen molecules are shown in Figure 3.
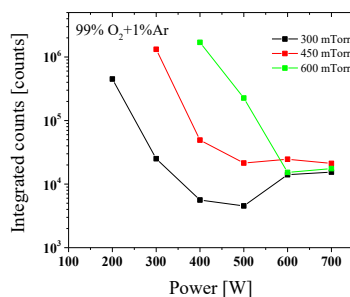
Figure 3. Counts of oxygen molecules integrated from device limit to ionization energy, recorded at various powers at pressures of 300, 450 and 600 mTorr

For all pressures that we used in these experiments plasma ignites for powers lower than 10 W. On the other hand, due to the large volume and cylindrical geometry of our reactor we have a range of power and pressure dependent conditions

when excited and metastable molecules could not be detected by mass spectrometer for present position of the orifice. In order to obtain the signal below the ionization threshold of O_2 more power has to be supplied to the system at higher pressures. Thus there appears to be a considerable loss of excited species between the active region of the plasma and the orifice of the mass analyzer especially at higher pressures. In addition there is a relative depletion towards the higher powers which may be associated by further excitation/ionization of the excited species.

We can see in Figure 3 that maximum counts are recorded at the lowest powers for each pressure. With the increase in applied power we observe the decrease in counts. At all three pressures we have a minimum that is a few orders of magnitude lower. For the highest powers there is an increase in the total counts up to the plateau that is common for all pressures.

3.2. Optical emission spectra and actinometry

In order to check the density of excited atomic oxygen species we recorded optical emission spectra of the discharge in the visual and near IR range for three different pressures and powers from 100 to 700 W. In figure 4 part of the spectrum between 740 – 850 nm is shown with characteristic atomic and molecular lines marked. The strongest lines in this wavelength range belong to O atoms produced in the discharge. Emission bend coming from oxygen molecule is also present. Additionally, due to the admixture of 1% Ar, weak Ar lines are also visible.
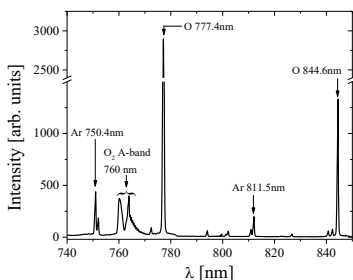
Figure 4. Part of the visual emission spectrum of O_2/Ar discharge at 200 W and 450 mTorr with characteristic oxygen and argon lines labeled in the plot

Addition of a small amount of Ar allowed us to use optical actinometry – simple and straightforward technique for determining concentration of neutral

species in low-pressure plasmas [13]. Employing this technique, ratio of the observed emission intensities for selected transitions from the upper excited atomic states of oxygen and argon can be related to the concentration ratio of ground states of these atoms.

Main assumption in actinometry is that emitter atoms are excited from the ground state in collisions with electrons. However, with atomic O lines in some cases, large extent of emission could originate from dissociative excitation and not from direct atom excitation [14]. Thus, in principle, dissociative excitation has to be taken into account as well as all other important excitation (through metastables, three-body collisions etc.) and de-excitation (spontaneous emission, quenching) channels [15,16]. In our calculations, contribution of the dissociative excitation has been included.

Using appropriate rate coefficients (k) [17], spectroscopic constants (transition probabilities, geometric constants: C(λ_{Ar}), C(λ_O)) and measured line intensities (I_O, I_{Ar}) the dissociation degree of oxygen is calculated as:

$$x = \left(\frac{N_{Ar}}{N_{O2}^0} \frac{I_O}{I_{Ar}} \gamma \frac{k_{Ar}^{dir}}{k_O^{dir}} - \frac{k_O^{dis}}{k_O^{dir}} \right) / \left(2 - \frac{k_O^{dis}}{k_O^{dir}} \right)$$

(1)

where

$$\gamma = \frac{C(\lambda_{Ar}) \lambda_O A_{Arp} \left(\sum_j A_{Oji} \right)}{C(\lambda_O) \lambda_{Ar} A_{Oj} \left(\sum_p A_{Arpq} \right)}$$
.

In numerator of equation (1) the first term represents contribution of direct excitation and the second one describes dissociative excitation channel. For calculations we used rate coefficients obtained assuming Maxwell distribution of electron energy and mean electron energy of 3 eV.
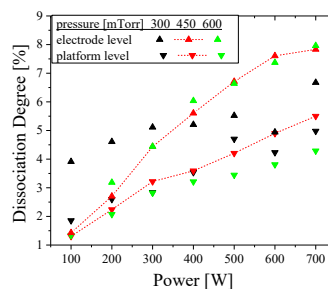
Figure 5. Dissociation degree of O_2/Ar discharge at 300, 450 and 600 mTorr calculated by using actinometry

formula and emission line intensities (O-844 nm, Ar-811 nm) obtained at two different window positions.

In figure 5 we show the extent of O_2 dissociation at three different pressures calculated by using data of oxygen 844 nm and Ar 811 nm lines obtained for two different positions of the spectrometer. The spectra were recorded for discharge conditions (pressure and power) at two windows placed at different positions with the respect to the central cylinder axis. The first one, in the center, opposite to the very bright volume around the electrode (marked as electrode level in the plot) and the other, at the platform level, close to the wall of the reactor (marked as platform level). Due to small size of the windows, emission of the lines recorded at these positions mostly originates from the volumes lengthwise the reactor facing the appropriate window.

At low powers, the dissociation degree is similar for all pressures and at both window levels. As power increases, number of dissociative products grows steadily at all pressures and for both positions. Degree of dissociation in the central region around the electrode increases much faster comparing to the degree obtained away from the electrode, at the platform level. At maximum power of 700 W the degree of dissociation reaches 8% in the region around electrode while at the platform it is around 5%. Variation of the dissociation degree for different pressures is small and almost within error bars of the technique.

From equation (1) we were able to estimate contribution of the dissociation excitation channel to the calculation of dissociation degree. For the data obtained at platform level, we estimate that dissociative excitation contributes up to 30% of the O atom emission at lowest powers while it decreases to 15% with increasing power. At the electrode level, this contribution is lower than 20% at lower powers and around 10% at the highest power.

3. Conclusion

We have used mass-energy analyzer to measure counts of oxygen molecules as a function of energy of ionizing electrons in 99% oxygen and 1% argon plasma. It is shown that the highest presence of excited and metastable oxygen molecules is obtained for minimum power in the range where signals are observable, at every pressure. Also, maximum counts are moving to higher powers at higher pressures. Optical actinometry measurements enbled us to determine dissociation degree of oxygen molecules in zone around the electrode and at the platform level. At both levels dissociation is rising with power and this increase is more pronounced near the powered electrode. The dissociation degree obtained from the space-time integrated measurements is in the range between 1 and 8 % and it has a very weak pressure dependence between 300 mTorr and 600 mTorr.

[1] T. Makabe and Z. Lj. Petrovic, *PLASMA ELECTRONICS: Applications in Micro Electronic Device Fabrication*, Taylor & Francis Group, (2006)

[2] K. Kutasi, B. Saoudi, C.D. Pintassilgo, J. Loureiro, M. Moisan, *Plasma Processes and Polymers*, **5** (2008) 840

[3] R.J. Reece, D.M. Sherman, R.B. Gadri, F. Karakaya, Z. Chen, T.C. Montie, K.W. Kimberly, and PP-Y. Tsai, *Plasma Science, IEEE Transactions on* **28** 1 (2000) 56

[4] G Fridman et al, *Plasma Processes and Polymers Special Issue: Special Issue on Plasma Medicine*, **5** 6 (2008) 503

[5] M. Laroussi, M. Kong, G. Morfill and W. Stolz, Plasma Medicine: applications of low-temperature gas plasmas in medicine and biology, *University Press, Cambridge* (2012)

[6] S. Živković, N. Puač, Z. Giba, D. Grubišić, Z.Lj. Petrović, *Seed Science and Technology*, **32** 3 (2004) 693

[7] N. Puač, Z.Lj. Petrović, S. Živković, Z. Giba, D. Grubišić and A.R. Đorđević, Low-Temperature Plasma Treatment of Dry Empress-Tree Seeds, in Plasma Processes and Polymers, *Wiley-VCH Verlag GmbH & Co. KGaA* (2005)

[8] I. Filatova, V. Azharonok, V. Lushkevich, A. Zhukovsky, G. Gadzhieva, K. Spasić, S. Živković, N. Puač, S. Lazović, G. Malović and Z.Lj.Petrović, *31st ICPIG* (2013)

[9] I. Filatova, V. Azharonok, E. Gorodetskaya, L. Mel'nikova, O. Shedikova, and A. Shik, *19th ISPC* (2009) 26

[10] S. Živković, N. Puač, Z. Giba, D. Grubišić, Z.Lj, Petrović, *Seed Science and Technology*, **32** 3 (2004) 693

[11] N. Puač, Z.Lj. Petrović, M. Radetić, A. Djordjević, *Materials Science Forum* **494** (2005) 494

[12] J. T. Gudmundsson and E. G. Thorsteinsson, *Plasma Sources Sci. Technol.* **16** (2007) 399

[13] J. W. Cobrun, M. Chen, *J. Appl. Phys.* **51** (1980) 3134

[14] H. M. Katsch, A. Tewes, E. Quandt, A. Goehlich, T. Kawetzki, H. F. Doebele, *J. Appl. Phys.* **88** (2000) 6232

[15] L. Zhongwei, L. Sen, C. Qiang, Y. Lizhen, W. Zhengduo, *Plasma Sci Technol* **13** (2011) 458

[16] S. Radovanov, B. Tomčik, Z. Lj. Petrović, B.M. Jelenković*, J. Appl. Phys.* **67** 1 (1990) 97

[17] N.C.M. Fuller, M.V. Malyshev, V.M. Donnelly and I.P. Herman, *Plasma Sources Sci. Technol.* **9** (2000) 116

treba pogledati Gudmundsson 2004 *J. Phys. D: Appl. Phys.* **37** 2073. doi:10.1088/0022-3727/37/15/005.

ICPIG 2017

XXXIII INTERNATIONAL CONFERENCE ON PHENOMENA IN IONIZED GASES

CONFERENCE PROCEEDINGS
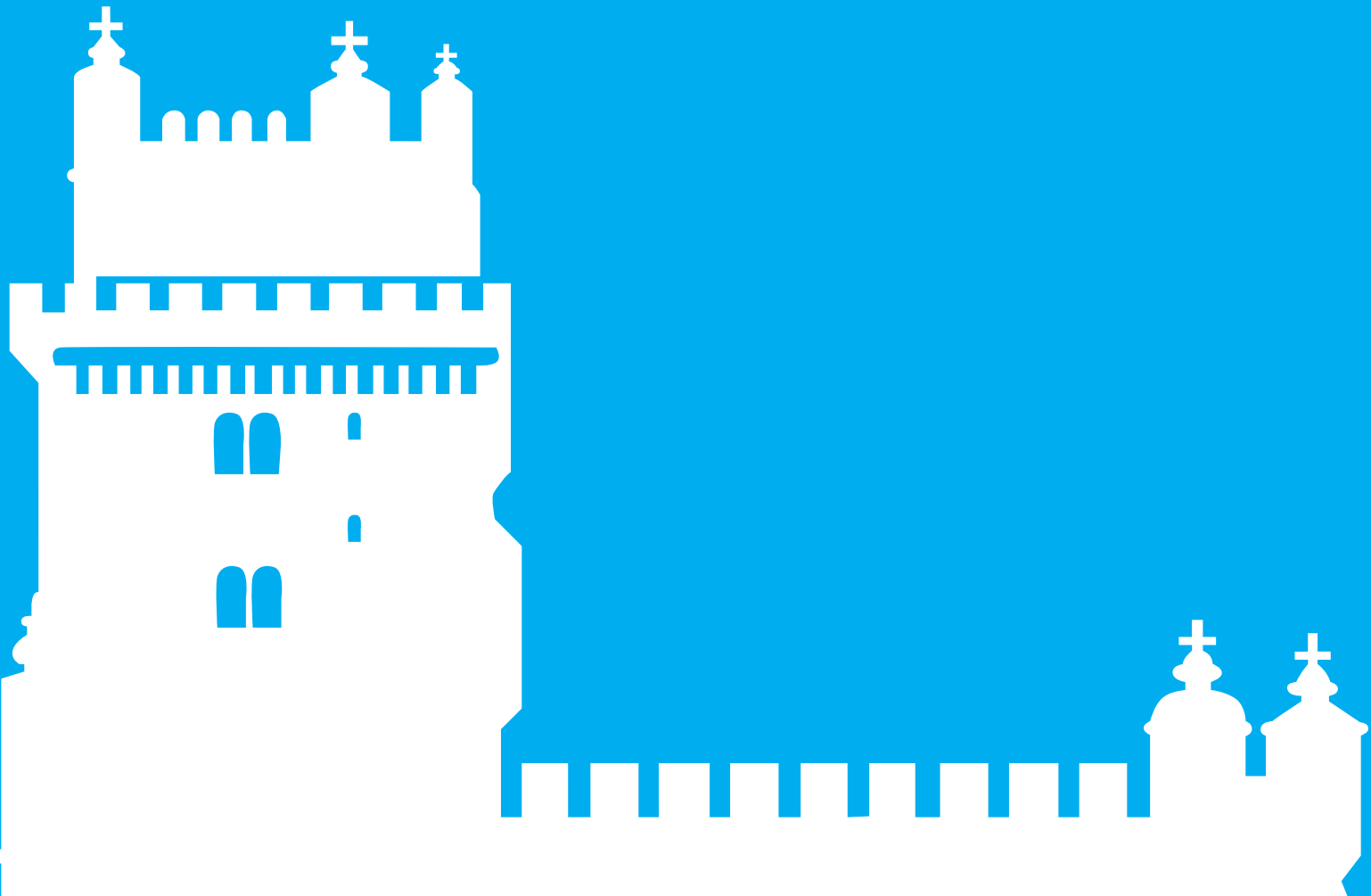
Proceedings of the

XXXIII International Conference on Phenomena in Ionized Gases

Estoril, Portugal. 9-14 July 2017

Editors:
Luís Lemos Alves
Antonio Tejero-del-Caz

The XXXIIII ICPIG (International Conference on Phenomena in Ionized Gases) has been organized by Instituto de Plasmas e Fusão Nuclear from Instituto Superior Técnico, Universidade de Lisboa, Universidade do Porto and Universidade do Minho.

The XXXIII ICPIG was organized in accordance with IUPAP principles, regarding the free circulation of scientists for international collaborations and discussions, as stated in the declaration of the International Council of Science, adopted at the 26th General Assembly in 2008 and endorsed by the 27th General Assembly in 2011. In particular, no *bona fide* scientist is excluded from participation on grounds of origin, nationality or political considerations unrelated to science.

Activity of catalase enzyme in *P. tomentosa* seeds after direct plasma treatments and treatments with plasma activated water

N. Puač[1], N. Škoro[1], K. Spasić[1], S. Živković[2], M. Milutinović[2], V. Šašić[2], G. Malović[1] and Z.Lj. Petrović[1,3]

[1] Institute of Physics, University of Belgrade, Pregrevica 118, 11080 Belgrade, Serbia
[2] Institute for Biological research "Siniša Stanković", University of Belgrade, B. despota Stefana 142, 11000 Belgrade, Serbia
[3] Serbian Academy of Sciences and Arts, Knez Mihailova 35, 11000 Belgrade, Serbia

In this abstract we report on influence of direct and indirect plasma treatments on catalase enzyme activity in *Paulownia tomentosa* seeds. The direct treatment of the seeds was performed in low-pressure RF plasma system for different treatment times. After treatments these seeds were imbibed with distilled water. The other set of *P. tomentosa* seeds was imbibed with plasma activated water (PAW). PAW was produced by using atmospheric pressure plasma source in treatments with different durations. Seeds from both sets were exposed to the same conditions and after 5 days activity of catalase enzyme was measured. In comparison to the control sample, differences in the activity was observed both regarding direct and PAW treated seeds and regarding duration of treatments.

1. Introduction

Non-equilibrium low and atmospheric pressure plasmas can be efficiently used in stimulation of seed growth, increase of germination percentage and decontamination, breaking of dormancy or increase in the length of seed sprout. We have developed several low pressure and atmospheric pressure plasma systems for treatment of seeds and plant cells [1-3]. Here we will present the results obtained in treatments of *Paulownia tomentosa* seeds by non-equilibrium plasma that operates at low and atmospheric pressures. We have determined the germination percentage and activity of catalase enzyme for all treated samples and compared it to the control samples.

2. Results and discussion

Low pressure plasma treatments of seeds were performed in the cylindrically shaped RF plasma system that operates at 13.56 MHz reactor. The seeds were then imbibed with distilled water. Unlike low pressure plasma treatments where seeds were in direct contact with plasma, in case of atmospheric pressure plasma treatments we have treated distilled water (PAW) which was then used for imbibition of seeds. After the imbibition process seeds were exposed to red light for 5 min. In Figure 1 we show activity of catalyse enzyme 5 days after imbibition of water. The catalase activity for the treated samples is increased comparing to the untreated sample. This is in accordance with the observed increase in germination percentages obtained for this samples.
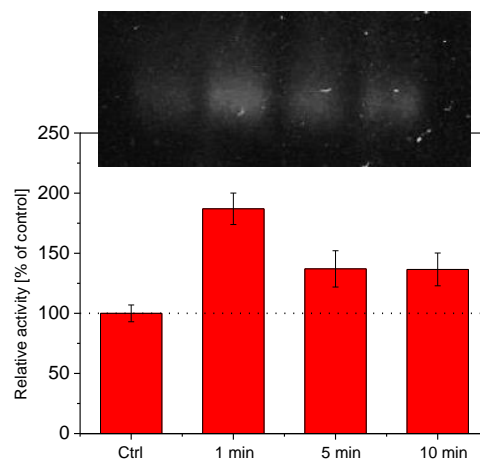
Figure 1. The activity of the catalase enzyme obtained by using native page. Data was obtained five days after the imbibition of water (distilled).

3. References

[1] N. Puač, Z.Lj. Petrović, S. Živković, Z. Giba, D. Grubišić and A.R. Đorđević, *Plasma Processes and Polymers*, Wiley-VCH Verlag GmbH & Co. (2005).

[2] N. Puač, Z.Lj. Petrović, G. Malović, A. Đorđević, S. Živković, Z. Giba and D. Grubišić, *J. Phys. D:Appl. Phys.* **39** (2006) 3514-3519.

[3] N. Puač, S. Živković, N. Selaković, M. Milutinović, J. Boljević, G. Malović and Z.Lj. Petrović, *Appl. Phys. Lett.* **104**(21) (2014) 214106.

27th Summer School and International Symposium on the Physics of Ionized Gases

August 26-29, 2014, Belgrade, Serbia

SPIG 2014

CONTRIBUTED PAPERS

&

ABSTRACTS OF INVITED LECTURES, TOPICAL INVITED LECTURES, PROGRESS REPORTS AND WORKSHOP LECTURES

Editors:
Dragana Marić
Aleksandar R. Milosavljević
Zoran Mijatović

Institute of Physics, Belgrade
University of Belgrade

Serbian Academy
of Sciences and Arts

www.spig2014.ipb.ac.rs

27th Summer School and International Symposium on the Physics of Ionized Gases

SPIG 2014

CONTRIBUTED PAPERS

&

ABSTRACTS OF INVITED LECTURES,
TOPICAL INVITED LECTURES, PROGRESS REPORTS
AND WORKSHOP LECTURES

Editors

Dragana Marić, Aleksandar R. Milosavljević and
Zoran Mijatović

Institute of Physics, Belgrade   Serbian Academy
University of Belgrade   of Sciences and Art

Belgrade, 2014

CONTRIBUTED PAPERS & ABSTRACTS OF INVITED LECTURES, TOPICAL INVITED LECTURES, PROGRESS REPORTS AND WORKSHOP LECTURES
of the 27th Summer School and International Symposium on the Physics of Ionized Gases

August 26 – 29, 2014, Belgrade, Serbia

ACKNOWLEDGEMENT

SPIG 2014

SCIENTIFIC COMMITTEE

Z. Mijatović (Chair), Serbia
S. Buckman, Australia
J. Burgdörfer, Austria
M. Danezis, Greece
Z. Donko, Hungary
V. Guerra, Portugal
M. Ivković, Serbia
D. Jovanović, Serbia
K. Lieb, Germany
I. Mančev, Serbia
D. Marić, Serbia
N. J. Mason, UK
A. R. Milosavljević, Serbia
K. Mima, Japan
Z. Mišković, Canada
B. Obradović, Serbia
G. Poparić, Serbia
L. C. Popović, Serbia
Z. Rakočević, Serbia
Y. Serruys, France
N. Simonović, Serbia
M. Škorić, Japan
M. Trtica, Serbia

ADVISORY COMMITTEE

D. Belić
N. Bibić
M. S. Dimitrijević
S. Đurović
N. Konjević
J. Labat
B. P. Marinković
M. Milosavljević
Z. LJ. Petrović
J. Purić
B. Stanić

ORGANIZING COMMITTEE

Institute of Physics Belgrade

D. Marić (Co-chair)
A. R. Milosavljević (Co-chair)
S. D. Tošić (Co-Secretary)
N. Škoro (Co-Secretary)
B. P. Marinković
M. Cvejić
J. Sivoš
K. Spasić
M. Ranković

**Serbian Academy
of Sciences and Arts**

Z. Lj. Petrović
M. Ivanović

SPIG 2014 CONFERENCE TOPICS

Section 1.
ATOMIC COLLISION PROCESSES
    1.1.   Electron and Photon Interactions with Atomic Particles
    1.2.   Heavy Particle Collisions
    1.3.   Swarms and Transport Phenomena

Section 2.
PARTICLE AND LASER BEAM INTERACTION WITH SOLIDS
    2.1.   Atomic Collisions in Solids
    2.2.   Sputtering and Deposition
    2.3.   Laser and Plasma Interaction with Surfaces

Section 3.
LOW TEMPERATURE PLASMAS
    3.1.   Plasma Spectroscopy and Other Diagnostics Methods
    3.2.   Gas Discharges
    3.3.   Plasma Applications and Devices

Section 4.
GENERAL PLASMAS
    4.1.   Fusion Plasmas
    4.2.   Astrophysical Plasmas
    4.3.   Collective Phenomena

ION ENERGY DISTRIBUTION AND LINE INTENSITIES IN ASYMMETRICAL OXYGEN RF DISCHARGE

Kosta Spasić, Nikola Škoro, Nevena Puač, Gordana Malović and
Zoran Lj. Petrović

Institute of Physics, Pregrevica 118, 11080 Belgrade, Serbia,
Belgrade University

Abstract. Asymmetric 13.56 MHz CCP plasma reactor of large area was developed for purpose of continuous plasma treatment of sensitive samples like polymers, textile and seeds. In order to maximize efficiency of plasma treatment and to get well acquainted with relevant plasma chemistry, plasma diagnostic by using mass spectrometer and optical emission recordings was performed. Supplied RF power was from 100 W to 600 W at 600 mTorr pressure of O_2 with 1% of Ar gas mixture. Distribution of O_2^+ ions had much higher counts than O^+ and for both species higher power resulted in more available high energy ions. Emission spectroscopy revealed an increase in oxygen 777 nm and argon 750 nm line intensity with the increase of power.

1. INTRODUCTION

In everlasting struggle for energetic efficiency and always needed cost reduction, numerous industries can find their solution in applications of low pressure plasmas. We have already shown some benefits for agriculture, because plasma treated seeds have higher germination rate and, in some cases, plants whose seed was treated develop significantly faster [1-3]. It is also important to emphasize possibility to use plasma as sterilization agent [1-3]. Positive effects of this technology are of great importance in textile industry [4], where they can improve quality of products and decrease ecological impact. Low pressure plasmas are used in various large scale industries, in processes like etching and deposition, where any reduction in used energy can make them more cost effective and environmentally friendly

Investigation of role of ions in plasma chemistry is of paramount importance both for general science and for industrial applications. In this paper we present measurements of ion energy distributions for singly ionized molecule and atom of oxygen (32 and 16 amu). Moreover, we have employed optical emission spectroscopy (OES) to obtain information about relevant lines of O and Ar.

2. EXPERIMENT

Large volume asymmetric CCP plasma reactor was developed as a prototype for industrial scale treatment of sensitive samples. Its asymmetric geometry allows stabile plasmas to be formed without possibility of streamer formation. Stainless steel cylindrical chamber, 2.5 m in lenght and 1.17 m in width, serves as grounded electrode, while powered electrode is 1.5 m long axially placed aluminum rod (3 cm in diameter). Power is supplied at 13.56 MHz by Dressler Cesar 1310 supply through Variomatch matching network.

Spectrally resolved emission from plasma was recorded in a part of visible spectrum (720-790 nm) through a side window positioned at level of the rod electrode. We have used monochromator Oriel MS127i with i-Star Andor ICCD camera as detector. By using a lens at the entrance slit, the spectrometer collected all light originating from the part of the plasma volume at the side-on region of the electrode. Recording time of several hundred ms contains integrated light emission from many RF periods. Two characteristic lines for atomic oxygen (777 nm) and argon (750 nm) were traced at different powers

HIDEN EQP mass spectrometer was positioned side-on and the distance of the mass spectrometer orifice from the powered electrode was 30 cm. The orifice of the mass spectrometer was at ground potential. Ion energy distribution was measured for energies between 4 and 100 eV with resolution of 0.1 eV. The working gas mixture was 99% of oxygen and 1% of argon at a pressure of 600 mTorr which is suitable for treatments. Measurements were done in the range of powers from 100 to 600 W.

3. RESULTS AND DISCUSSION

In Fig. 1 a) we have presented ion energy distributions for positive ions of molecular oxygen (O_2^+) recorded at 600 mTorr for powers 400, 500 and 600 W. For powers lower than 400 W we could not obtain valid signal of ion energy distributions. At 400 W maximum ion counts can be observed at 4 eV and after that distribution rapidly decreases 5 orders of magnitude. For this power given by RF power supply maximum of ion energy is around 20 eV. With the increase of the power we can see that ions with higher energies can be collected. For the power of 500 W maximum ion energy goes up to 70 eV and for 600 W this energy is higher than 100 eV.

Situation is somewhat similar for distribution of singly ionized atomic oxygen (O^+) shown in Fig. 1 b). However, in case of O^+ we can see two peaks present for the powers of 400 and 500 W. In case of 600 W we can only assume that there is the second peak around 100 eV since the signal started to increase at around 90 eV.

Notwithstanding that we could not obtain valid ion signal for the powers lower than 400 W, plasma was ignited for the lower powers. In order to investigate if there is some change in plasma behavior at 400 W we have performed OES and recorded oxygen and argon line intensities.
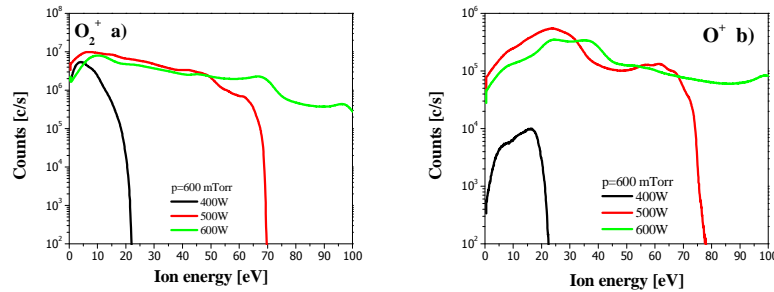
Figure 1. Ion energy distributions of O_2^+ (a) and O^+ (b), recorded at 600 mTorr for three different powers given by RF power supply.

Measurements of line intensity dependence for two oxygen and argon lines are shown in Fig. 2 for different powers (full symbols). Line intensities are relatively scaled and show similar intensities and rising tendency with power increase. For both lines the increase in intensity is larger, almost exponential, at higher powers. Additionally, the ratio between obtained line intensities is shown in the right-hand-side axis (crosses) and exhibits small increase with power. Also, interesting observation is that at 400 W there is decrease in line intensity ratio.
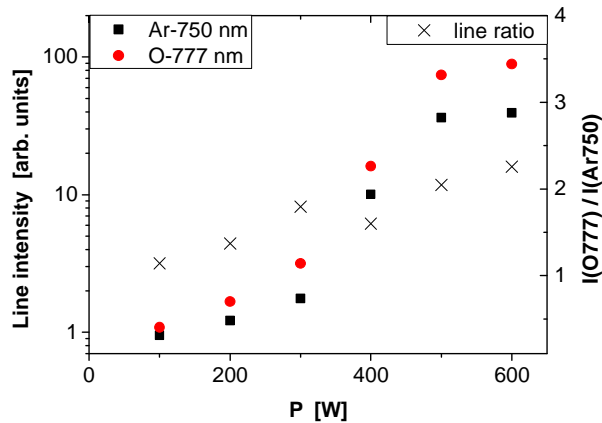
Figure 2. Left axis: oxygen 777 nm (circles) and argon 750 nm (squares) line intensities, right axis: line intensity ratio (crosses) at different powers at 600 mTorr.

Generally, in cases where emission originating from dissociative excitation is not dominant, the line intensity ratio could be used for an estimation of the dissociation extent in plasma through a method of optical actinometry [5]. However, in plasmas with low dissociation extent and where dissociative excitation channel is dominant, results of actinometry can provide only qualitative description of change in oxygen dissociation with plasma parameters

[6,7]. Thus, in this case the intensity ratio provides only general trend in dissociation of oxygen.

4. CONCLUSION

We have measured ion energy distribution and performed spectroscopic measurements of large volume asymmetric CCP plasma reactor. No valid ion signal could be detected at powers lower than 400 W, and even at that power distribution reaches minimal values at just over 20 eV. With increased RF powers, we were able to detect ions at energies higher than 100 eV. Optical emission spectroscopy, in this range of plasma parameters, could only provide us with general information that dissociation of oxygen molecules is rising with powers.

Acknowledgements

REFERENCES

[1]   I. Filatova, V. Azharonok, V. Lushkevich, A. Zhukovsky, G. Gadzhieva, K. Spasić, S. Živković, N. Puač, S. Lazović, G. Malović, Z.Lj.Petrović, "*Plasma seeds treatment as a promising technique for seed germination improvement*", (31st ICPIG, 2013).

[2]   N. Puač, Z. Lj. Petrović, S. Živković, Z. Giba, D. Grubišić, A. R. Djordjević, Plasma Process Polym, pp 193 (2005).

[3]   I. I. Filatova,V. V. Azharonok,S. V. Goncharik,V. A. Lushkevich,A. G. Zhukovsky, G. I. Gadzhieva, J Appl Spectrosc, 81 2 250 (2014).

[4]   M. Gorenšek, M. Gorjanc, V. Bukošek, J. Kovač, Z. Petrović, N. Puač, Text. Res. J. 80, 1633, (2010).

[5]   J. W. Cobrun, M. Chen, J. Appl. Phys. 51, 3134 (1980).

[6]   H. M. Katsch, A. Tewes, E. Quandt, A. Goehlich, T. Kawetzki, H. F. Doebele, J. Appl. Phys. 88 6232 (2000).

[7]   L. Zhongwei, L. Sen, C. Qiang, Y. Lizhen, W. Zhengduo,   Plasma Sci Technol, 13 458 (2011).

26th Summer School and International
Symposium on the Physics of Ionized Gases

August 27th -31st, 2012, Zrenjanin Serbia

CONTRIBUTED PAPERS

&

ABSTRACTS OF INVITED LECTURES AND PROGRESS REPORTS

Editors
M. Kuraica, Z. Mijatović

University of Novi Sad, Faculty of Sciences
Department of Physics
Novi Sad, Serbia

ISBN 978-86-7031-242-5

CONTRIBUTED PAPERS & ABSTRACTS
OF INVITED LECTURES AND PROGRESS REPORTS
of the
26th SUMMER SCHOOL AND INTERNATIONAL
SYMPOSIUM ON THE PHYSICS OF IONIZED GASES

August 27th - 31st, Zrenjanin, Serbia

Editors: Milorad Kuraica
        Zoran Mijatović

Publisher:

University of Novi Sad
Faculty of Sciences
Department of Physics
Trg Dositeja Obradovića 3
21000 Novi Sad, Serbia

© **2012 Department of Physics, Novi Sad**

Printed by:
Štamparija "Stojkov", Novi Sad, Serbia

26th SPIG

Scientific Committee

M. Kuraica (Chairmen) Serbia

S. Buckman, Australia
J. Burgdoerfer, Austria
Z. Donko, Hungary
V. Guerra, Portugal
D. Jovanović, Serbia
K. Lieb, Germany
G. Malović, Serbia
I. Mančev, Serbia
A. Milosavljević, Serbia
N. J. Mason, USA
M. Danezis, Greece
Z. Mijatović, Serbia
K. Mima, Japan
Z. Mišković, USA
G. Poparić, Serbia
L. Č. Popović, Serbia
Z. Rakočević, Serbia
Y. Serruys, France
N. Simonović, Serbia
M. Škorić, Serbia

Advisory Committee

D. Belić
N. Konjević
J. Labat
B. P. Marinković
S. Đurović
M. S. Dimitrijević
N. Bibić
M. Milosavljević
Z. Lj. Petrović
J. Purić
B. Stanić

Organizing Committee

Z. Mijatović (Chairmen)

I. Savić (Secretary)
S. Đurović
N. Cvetanović
R. Kobilarov
T. Gajo
Z. Nađ
L. Gavanski

CATALYTIC PROBE MEASUREMENTS OF ATOMIC OXYGEN CONCENTRATION IN LARGE VOLUME OXYGEN CCP

Kosta Spasić[1], Saša Lazović[1], Nevena Puač[1], Zoran Lj Petrović[1], Gordana Malović[1], Miran Mozetič[2] and Uroš Cvelbar[2]

[1]*Institute of Physics, University of Belgrade, Pregrevica 118, 11080 Belgrade, Serbia*

[2]*Jožef Stefan Institute, Jamova 39, 1000 Ljubljana, Slovenia*

e-mail: kostasp@ipb.ac.rs

Abstract. Large scale chamber with asymmetric electrodes has been developed for low pressure treatment of seeds textile and wool. Since neutrals in plasma have very active role, it is of great importance to analyze their behavior in discharges. For this paper we have used catalytic probe in order to determine concentrations and spatial profiles of atomic oxygen. This diagnostic tool has been chosen due to its low cost, simplicity and possibility of real-time use, which makes it suitable for industrial purposes.

1. INTRODUCTION

Catalytic probe is simple, yet effective tool for measuring concentration of neutral species. They are usually constructed as thermocouple and the hot end is the probe tip, where catalytic activity is taking place. Materials that can be used to construct the probe tip are nickel [1], iron [2], copper [3], silver [4] and, in extreme conditions like in fusion reactor, gold [5].This technique has been used for measurement of concentrations of atomic oxygen [1], nitrogen [6] and hydrogen [5]. They are most frequently being used for diagnostic of RF plasmas, ICP [1] as well as CCP [7] and almost exclusively in low pressure. Some applications have also been reported in microwave discharges [6]

Recent research has proved that this kind of equipment can be used for continuous data acquisition [1]. Because of this innovation, catalytic probes can now be used in industrial processes where it is not possible to frequently turn discharge on or off.

In comparison with other methods for measuring concentration of neutral species, such as optical emission, actinometry, mass spectrometry, optical absorption and chemical titration, catalytic probe comes at low price and it is simple to use. Direct interpretation of results is one of the biggest advantages of this method.

There are several issues related to catalytic probe. First of all, since recombination coefficient cannot be determined with precision higher than 30% [1], the probe itself cannot have accuracy above this mark. In some situations RF disturbances can have strong effect on measuring equipment. Even though probes are usually made to have small dimensions, their presence in discharge is still affecting plasma. When interpreting results, one should take care about the fact that probe cannot make difference whether species were excited or not when they arrived on its surface.

In our laboratory we have large scale discharge chamber in which we can have conditions similar to plasmas that are used for industrial purposes. Asymmetric geometry allows samples to be exposed to different intensity of treatment simply by adjusting their position. So far it has been used for treatment of wool [8], textile [9] and seeds [10].

Beside charged particles such as ions and electrons, neutral species have also very important role in plasma treatment. Presence of atomic oxygen in discharge can have influence on activation of surfaces of textile and seeds. Therefore, in order to have adequate treatment, it is of great importance to properly determine spatial profiles of atomic oxygen concentration inside the chamber. For this paper we have used nickel catalytic probe to measure concentration of atomic oxygen at different distances from powered electrode and different applied RF power at pressure of 450 mTorr.

2. EXPERIMENTAL SET-UP

Experimental set-up is shown on Figure 1. Our discharge chamber has cylindrical geometry. It is 2.5 m long and 1.17 m wide with walls, which are used as grounded electrode, made of stainless steel. Powered electrode is made of aluminum and it is placed axially, it is 1.5 m long and has diameter of 3 cm.

Our catalytic probe is placed side-on, perpendicular to powered electrode. Tip of it is disc made of nickel whose diameter is 1.5 mm and it is 0.04 mm thick. Since our probe is placed inside glass tube we have used Wilson seal to allow ease of movement and to secure that vacuum is maintained. Measurements were performed with MS8218 multimeter which can record data in real time.

To create and sustain our plasma we have used 13.56 MHz Dressler Cesar 1310 power supply and Variomatch matching network. Vacuum is achieved by Alcatel mechanical pump, while needle valve was used to control flow of working gas.
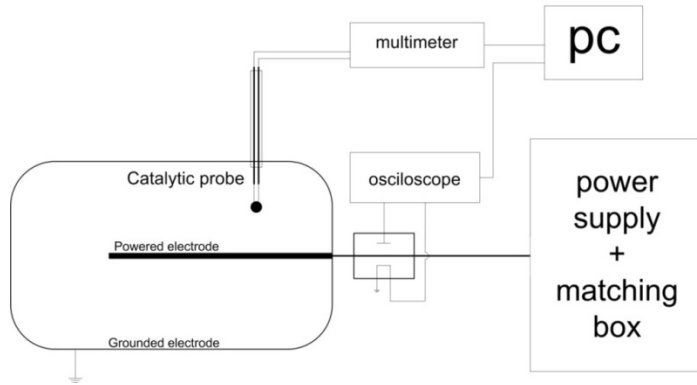
Figure 1. Experimental set-up**.**

3. RESULTS AND DISCUSSION

Typical measurements with catalytic probe require plasma to be turned off whenever data acquisition is needed. Speed of probe tip cooling when discharge is turned off provides information about power that is transferred to it when plasma is turned on. Since recombination is main cause of probe tip temperature increase, heating power can be used to derive atomic oxygen concentration [11]. It has been discovered that, for same gas and same plasma parameters, temperature time derivative of probe tip depends on maximum temperature [2]. When that dependency (shown on figure 2) is known, atomic oxygen concentration can be determined in real-time while plasma is on without interruption.
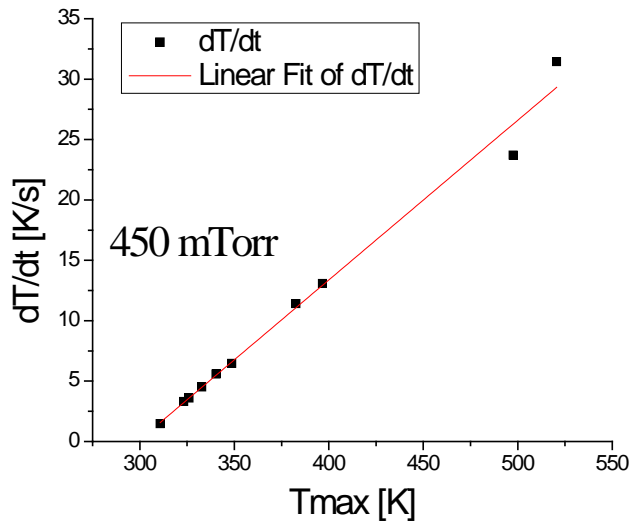
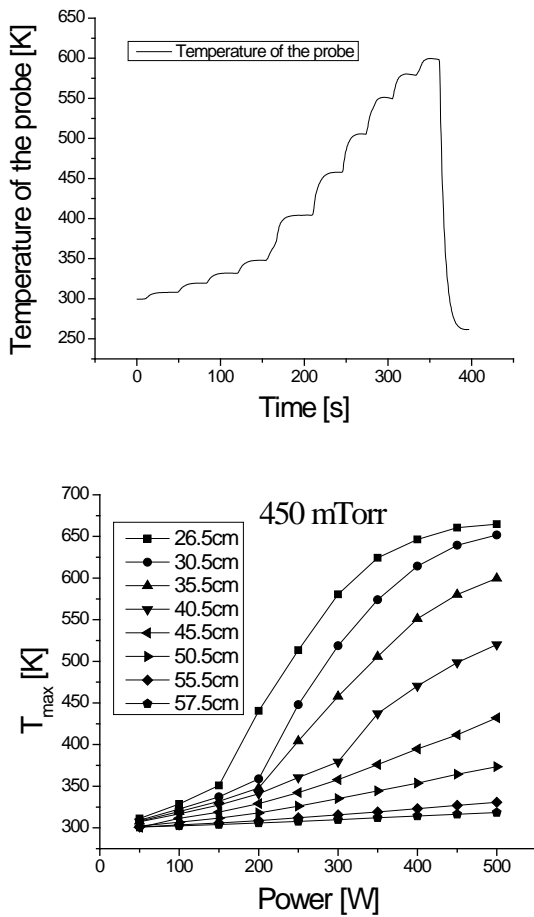**Figure 2.** Temperature time derivative versus temperature at 450m Torr.

Figure 3. Standard measured curve (left), and maximum temperatures for whole set of measurements (right).

On Figure 3, on the left hand side, we have presented one of typical measured curves. We can see that after applying certain power, temperature is starting to rise and after few seconds it reaches saturation or maximum temperature, T_{max}. Following graph on Figure 2, one can obtain temperature time derivative with known T_{max}. On the right hand side of the picture, set of maximum temperatures for different conditions is presented.

Spatial profiles of atomic oxygen concentration in large scale CCP device at 450 mTorr are shown in Figure 4. The closest distance to the powered electrode where measurements were taken was chosen according to technical capabilities and it was 26.5 cm. The most distant point was at chamber wall. Applied RF power was between 50 W and 500 W with increasing step of 50 W.
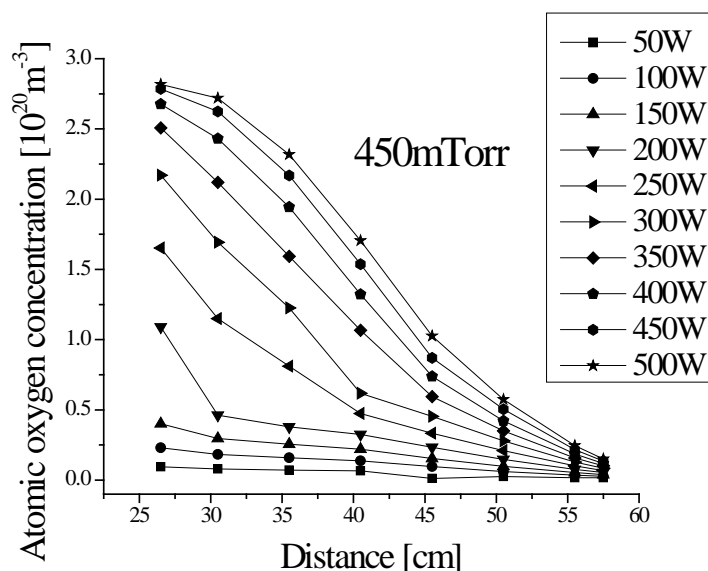
Figure 4. Spatial profiles of atomic oxygen concentration for different applied RF power at 450mTorr.

In the vicinity of the powered electrode the highest concentrations of $2.75*10^{20}$ m^{-3} were recorded. As probe was moved closer to the chamber wall concentrations were decreasing, and at the lowest point they were more than one order of magnitude lower. This big difference can be, in part, explained by very different size of electrodes. The biggest drop is between 35 cm and 45 cm. For fixed position of the probe, rising of applied RF power resulted in rise of concentration of atomic oxygen and near the chamber wall dependency is almost linear.

4. CONCLUSION

Catalytic probe was used to diagnose large volume CCP discharge at 13.56 MHz in oxygen at 450 mTorr for powers between 50 and 500 W. The highest concentrations are measured near the powered electrode, while at the chamber wall we measured concentrations that were order of magnitude lower. Higher applied power also produced higher concentrations, while dependencies lost their linearity in vicinity of the powered electrode. Since in all plasma treatments oxygen atoms play crucial role it is important to know concentrations of O atoms in order to be able to optimize the treatments. Also, knowledge of atom concentrations for different distances and different applied powers gives us opportunity to finely tune the treatments for variety of samples by just adjusting the distance from the powered electrode. It is shown that for the smaller distances from the powered electrode similar concentration of O atoms can be obtained as for greater distances, but much higher powers and this can significantly reduce the cost of treatments since same effects can be obtained for smaller power consumption

Acknowledgements

REFERENCES

[1]   I Šorli and R Ročak, J. Vac. Sci. Technol. A 18 2, 0734-2101 (2000)

[2]   M Mozetic, A. Vesel, U. Cvelbar and A. Ricard, Plasma Chem Plasma Process 26:103 (2006)

[3]   M Mozetic and U Cvelbar, Plasma Sources Sci. Technol. 18 034002 (2009)

[4]   M R. Carruth and A F Whitaker, Rev. Sci. Instrum., 61 (4) (1990),

[5]   M. Mozetic et al, Journal of Nuclear Materials 363, 1457 (2007)

[6]   F Gaboriau, U Cvelbar, M Mozetic, A Erradi and B Rouffet, J. Phys. D: Appl. Phys. 42 055204 (2009),

[7]   T. Vrlinic et al., Vacuum 83 792 (2009)

[8]   M Radetic, D Radojevic, V Ilic , D Jocic, D Povrenovic, N Puac, Z Lj. Petrovic and P Jovancic , Trends in Applied Sciences Research, 1 564 (2006)

[9]   M Radetić, P Jovančić, N Puač, Z Lj Petrović, Z Šaponjić, Textile Research Journal 79 558 (2009)

[10]   N. Puać, Z.Lj. Petrović, S. Živković, Z. Giba, D. Grubišic and A.R. Đorđević, Plasma Processes and Polymers, 203 (2005),

[11]   A Drenik, U Cvelbar, K Ostrikov and M Mozetic, J. Phys. D: Appl. Phys. 41 11520 (2008)

Radial profile of the electron energy distribution function in RF capacitive gas-discharge plasma

8 AUTHORS, INCLUDING:

Tsv K Popov
Sofia University "St. Kliment Ohridski"
58 PUBLICATIONS 221 CITATIONS

SEE PROFILE

Kosta Spasic
University of Belgrade
10 PUBLICATIONS 11 CITATIONS

SEE PROFILE

Gordana Malovic
Institute of Physics Belgrade
157 PUBLICATIONS 913 CITATIONS

SEE PROFILE

Zoran Lj Petrović
Institute of Physics Belgrade
509 PUBLICATIONS 5,521 CITATIONS

SEE PROFILE

Radial profile of the electron energy distribution function in RF capacitive gas-discharge plasma

M Dimitrova[1,5], Tsv Popov[2], N Puac[3], N Skoro[3], K Spasic[3], G Malovic[3], F M Dias[4] and Z Lj Petrovic[3]

[1]Acad. E. Djakov Institute of Electronics, Bulgarian Academy of Sciences,
 72 Tzarigradsko Chaussee, 1784 Sofia, Bulgaria
[2]Faculty of Physics, St. Kl. Ohridski University of Sofia,
 5 J. Bourchier blvd. 1164 Sofia, Bulgaria
[3]Institute of Physics, University of Belgrade, 118 Pregrevica, 11080 Belgrade, Serbia
[4]Instituto de Plasmas e Fusão Nuclear, Instituto Superior Técnico,
 Universidade de Lisboa, 1049-001 Lisboa, Portugal

E-mail: miglena.dimitrova@gmail.com

Abstract. This paper reports experimental results on low-pressure argon capacitive RF discharge (parallel-plate capacitively-coupled plasma – CCP) under different conditions, namely, gas pressure in the range $3 \div 30$ Pa and RF power in the range $10 \div 100$ W. The *IV* characteristics measured were processed by two different second-derivative probe techniques for determination of the plasma parameters and the electron energy distribution function. The radial profiles of the main plasma parameters are presented.

1. Introduction

Low-temperature (non-equilibrium) plasmas are the basis of a number of technologies, old, current and future. The success story is, of course, plasma etching, which, together with photo-lithography, is the basis for miniaturization of integrated circuits; other major applications include surface alloying, thin-film deposition, plasma displays, modification of the properties of polymers and organic materials. Recently, the most promising has seemed to be the field of plasma-based medical applications. However, non-equilibrium plasmas are difficult to describe by universal theories, so that joint efforts are needed in diagnostics and modelling in order to understand their properties and use that knowledge to control, design and optimize applications. The importance of the research is that it will facilitate applications while focusing the scientific effort on the fundamental aspects of non-equilibrium plasmas [1]. Joint experimental and modelling efforts are required to make any general, fundamental conclusions about non-equilibrium plasmas.

This paper reports experimental results on studying a capacitive low-pressure argon RF discharge for a range of conditions [2], such as gas pressure in the range $3 \div 30$ Pa and power ranging from 10 W to 100 W. The current-voltage (*IV*) characteristics obtained by a Langmuir probe were processed by two different second-derivative probe techniques [3] to determine the plasma parameters and the

---

[5] To whom any correspondence should be addressed.

electron energy distribution function (EEDF). The radial profiles of the main plasma parameters were also constructed.

2. Langmuir probe measurements in a RF capacitively coupled system

The RF system consisted of a chamber with parallel plate electrodes powered by a RF source with a driving frequency $f = 13.56$ MHz. The discharge in this experiment was ignited at an electrode distance of 0.07 m between the top powered and the bottom grounded electrode both with a diameter of 0.11 m. The transmitted RF power was measured at the source and always stayed below 1 % of transmitted power. A Hiden's ESPION Langmuir probe system with a motion stage was used to measure the *IV* characteristics. The probe tip with a diameter of 0.15 mm and a length of 10 mm was placed in the plasma with the motion stage allowing motion along the radial direction at $L = 0.02$ m above the bottom electrode. The *IV* characteristics' data were recorded using the ESPION software and then exported for further analysis.

In the "classical regime", which corresponds to our experimental conditions, the probe operates in the absence of a magnetic field and at low gas pressures in the range of 0.1 Pa to 100 Pa [4]. Then the electron probe current of the *IV* characteristic is expressed by the well-known formula [4]:

$$I_e(U) = -\frac{2\pi eS}{m^2} \int_{eU}^{\infty} (W - eU)f(W)dW ,$$ (1)

where e and m are the electron charge and mass, S is the probe area, $W = \frac{1}{2}mc^2 + eU$ is the total electron energy in the probe sheath and c is the electron velocity. Here the probe is negatively biased by a potential U_p and U is the probe potential with respect to the plasma potential U_{pl} ($U = U_p - U_{pl}$). $f(\varepsilon)$ is the isotropic electron energy probability function (EEPF) [1], normalized by:

$$\frac{4\pi\sqrt{2}}{m^{3/2}} \int_0^{\infty} f(W)\sqrt{W}dW = \int_0^{\infty} f(\varepsilon)\sqrt{\varepsilon}d\varepsilon = n .$$ (2)

The EEPF can be determined by using the Druyvesteyn's formula [5]:

$$f(\varepsilon) = \frac{2\sqrt{2m}}{e^3 S} \frac{d^2 I_e(U)}{dU^2} .$$ (3)

The second derivatives obtained from the measured *IV* characteristics were evaluated by two techniques. The first one consists in adjacent averaging, smoothing and differentiating twice the measured *IV* characteristics. The instrumental function of the differentiation technique is triangular with a half-width equal to the step of change of the probe bias [6]. The other differentiating technique is based on the convolution of data with an adaptive, differentiating filter, whose instrumental function is automatically adjusted so that noise and distortion, i.e., error, are locally kept at about the same level. Details on how noise and distortion can be readily evaluated can be found in [3], as well as in the references therein. In this work, as before, we continue using (1 + cos (…)) kind of filters for their flexibility on how the full-width-to-half-maximum (FWHM) can be adjusted to run-time, hence how readily the noise-to-error ratio can be kept constant.

Figures 1 and 2 represent examples of the EEDFs evaluated at the center of the discharge chamber at 50 W discharge power and gas pressure of 6 Pa and 27 Pa. The solid black lines present results from direct differentiation. The distortions between 0 and 10 eV cannot be explained by the influence of the differentiation method's instrumental function and the probe size [6]. A possible reason of the appearance of additional distortions is the insufficient ratio Σ between the surface area of the measuring (S_p) and reference (S_r) probes of the HIDEN probe circuit. Usually, it is accepted that it has to be:

$$\Sigma = \frac{S_r}{S_p} > \sqrt{\frac{M}{m}} \ . \tag{4}$$

Here M is the ion mass. For precise measurements, a more severe criterion for the ratio Σ must be used [7]:

$$\Sigma = \frac{S_r n_r (T_r)^{1/2}}{S_p n_p (T_p)^{1/2}} G_\alpha \geq 10^4 \ . \tag{5}$$

In this equation, T and n are the electron temperatures and densities at the positions of the measuring (p) and reference (r) probes. The factor G_α is tabulated in [7] for different probe and reference probe geometries.

On the other hand, the reference probe is flush mounted on the probe holder (close to the probe tip) with surface area not enough to satisfy the condition (5). To compensate for the insufficient ratio Σ in the second technique, an effective resistance R_{eff} was added to the probe circuit. Results with $R_{eff} = 200\Omega$ (red curve) and $R_{eff} = 500\Omega$ (blue curve) are presented in figure 1. As the effective resistance R_{eff} is increased, the EEDF evaluated approaches the Maxwellian with an electron temperature of 5 eV up to the energy of the first excited level of argon (11.56 eV). At higher energies, the EEDF deviates from Maxwellian due to the inelastic electron-atom collisions and the non-equilibrium nature of the discharge. We should point out that the distortions of the blue curve in the range $0 \div 3.5$ eV correspond to the distortions due to the instrumental function and the influence of the probe size [6].

The same considerations are related to the results recorded at a higher pressure presented in figure 2. Here, the effective resistances are $R_{eff} = 2k\Omega$ (red curve) and $R_{eff} = 5k\Omega$ (blue curve). It can be seen that the blue curve is not appropriate. The electron temperature in this regime of the discharge is 6 eV.

We have to point out that to solve the problem mentioned above, additional experiments with different reference probe areas are planned for the near future.
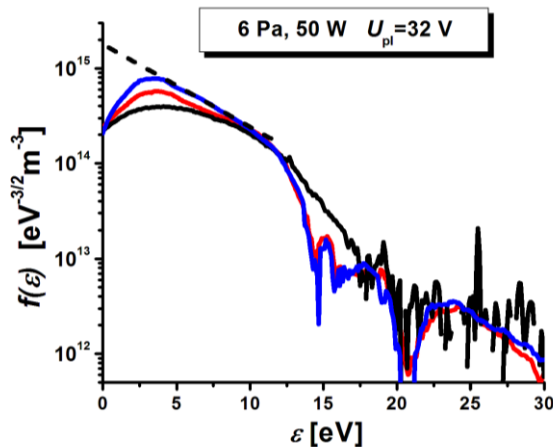

Figure 1. EEPF obtained by direct differentiation of the measured *IV* (solid black line); red curve – obtained by introducing a 200 Ω effective resistance in the probe circuit; and the blue curve, 500Ω.
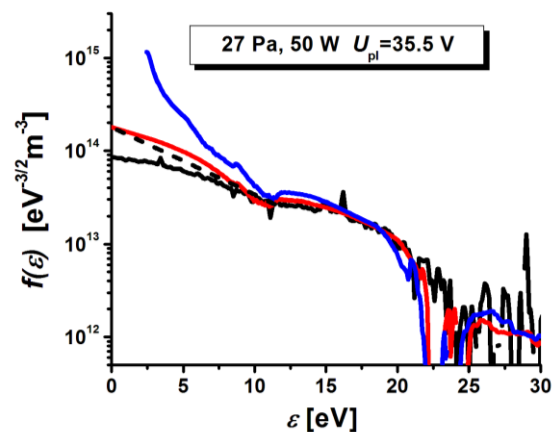
Figure 2. EEPF obtained by direct differentiation of the measured *IV* (solid black line); red curve – obtained by introducing a 2kΩ effective resistance in the probe circuit; and the blue curve, 5kΩ.

3. Experimental results

Below we present the main plasma parameters evaluated from the *IV* characteristics measured at different radial positions. The radial distributions of the plasma potential at different discharge RF power values and different gas pressures are presented in figures 3 a) and 3 b). The accuracy of the evaluation is ~10%. In figure 3, the U_{pl} is higher at the center of the discharge. This effect is more pronounced at higher gas pressures (figure 3 b)). At lower pressures, the U_{pl} is almost constant. The dashed lines indicate the size of the electrodes. As the discharge power is increased, the plasma potential values increase by about 10 V.
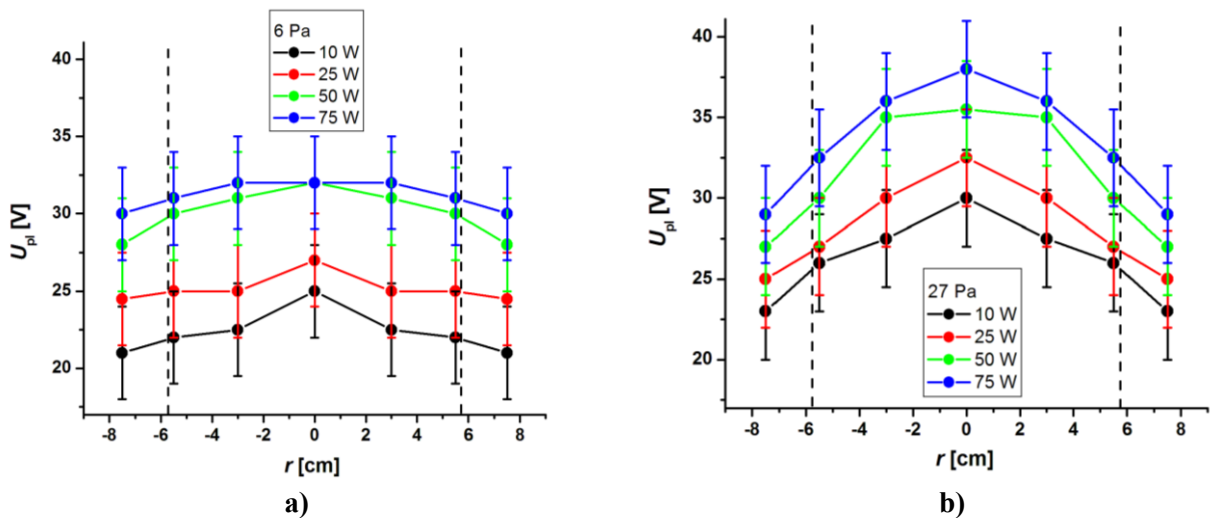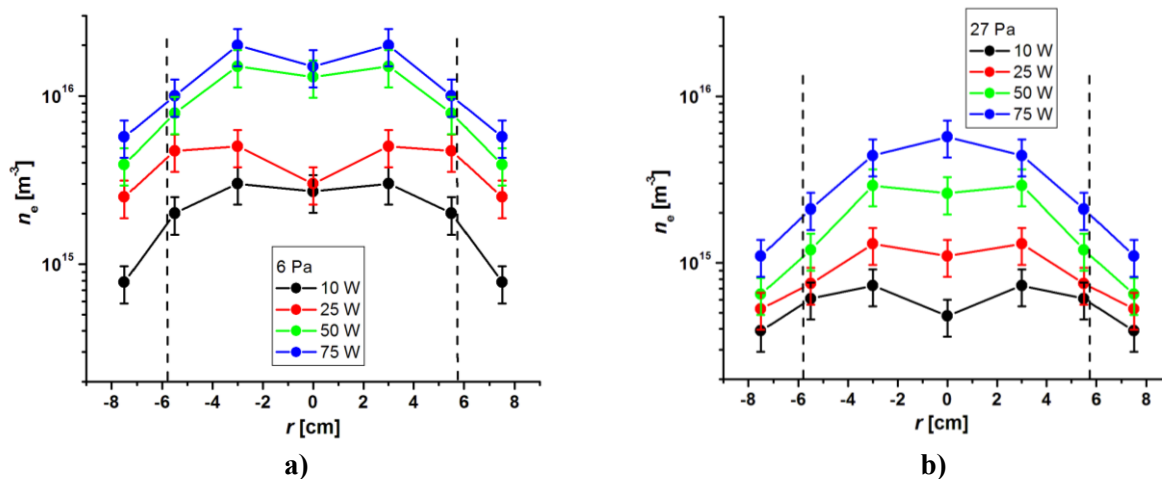

Figure 3. Radial distributions of the plasma potential at different discharge RF power values and different gas pressures.

As we mentioned, the EEPF can be approximated by a Maxwellian distribution up to the energy of the first excited level of argon. An example of the resulting electron temperatures are presented in figure 4 a), b).
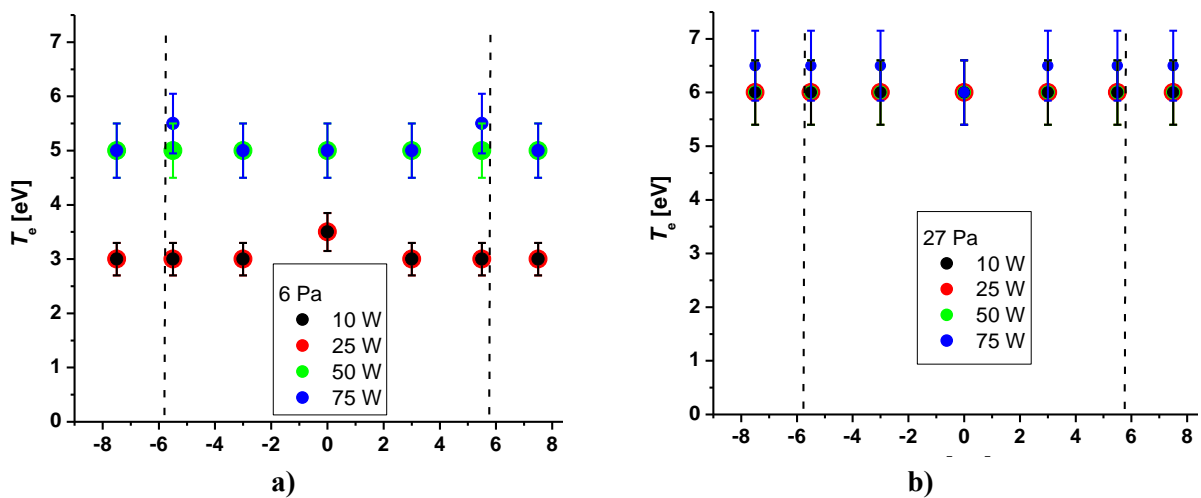
Figure 4. Radial distributions of the electron temperatures at different discharge RF power values and different gas pressures.

Figure 5 shows the corresponding radial profiles of the electron densities at different discharge RF power values and different gas pressures.

Figure 5. Radial distributions of the electron densities at different discharge RF power values and different gas pressures.

4. Conclusions

This paper reports experimental results on a capacitive low-pressure argon RF discharge at different conditions, as gas pressure in the range $3 \div 30$ Pa and RF power within $10 \div 100$ W.

The current-voltage (*IV*) characteristics measured were processed by two different second derivative probe techniques for determination of the plasma parameters and the electron energy distribution function (EEDF). The radial profiles of the plasma potential and the electron temperatures and densities at different discharge RF powers and different gas pressures are presented.

References

[1]   Godyak V A and Demidov V I 2011 *J. Phys.* D*: Appl. Phys*. **44** 233001
[2]   Godyak V A, Piejak R B and Alexandrovich B M 1992 *Plasma Sources Sci. Technol*. **1** 36-58
[3]   Dias F M and Popov Tsv K 2007 *J. Phys.: Conf. Series* **63** 012005
[4]   Demidov V I, Kolokolov N B and Kudriavtsev A A 1996 *Probe Methods of Diagnostics of Low Temperature Plasma* (Moscow: Energoatomizdat) (in Russian)
[5]   Druyvesteyn M J 1930 *Z. Phys.* **64** 781-98
[6]   Popov Tsv K, Dimitrova M, Dias F M, Tsaneva V N, Stelmashenko N A, Blamire M G and Barber Z H 2006 *J. Phys.: Conf. Series* **44** 60–9
[7]   Chang J-S 1973 *J. Phys.* D*: Appl. Phys.* **6** 1674

Република Србија
Универзитет у Београду
Физички факултет
Д.Бр.2018/8022
Датум: 10.05.2019. године

На основу члана 161 Закона о општем управном поступку и службене евиденције издаје се

УВЕРЕЊЕ

Спасић (Зоран) Коста, бр. индекса 2018/8022, рођен 11.08.1984. године, Београд, Савски венац, Република Србија, уписан школске 2018/2019. године, у статусу: самофинансирање; тип студија: докторске академске студије; студијски програм: Физика.

Према Статуту факултета студије трају (број година): три.
Рок за завршетак студија: у двоструком трајању студија.

Ово се уверење може употребити за регулисање војне обавезе, издавање визе, права на дечији додатак, породичне пензије, инвалидског додатка, добијања здравствене књижице, легитимације за повлашћену вожњу и стипендије.

Овлашћено лице факултета

РЕПУБЛИКА СРБИЈА

ФИЗИЧКИ ФАКУЛТЕТ
УНИВЕРЗИТЕТА У БЕОГРАДУ

ДИПЛОМА

О СТЕЧЕНОМ ВИСОКОМ ОБРАЗОВАЊУ

Спасић Зорана Коста

РОЂЕН-А   11-VIII-1984.   ГОДИНЕ У   БЕОГРАДУ, САВСКИ ВЕНАЦ
СРБИЈА   , УПИСАН-А 2003/2004.   ГОДИНЕ,
А ДАНА   30. ДЕЦЕМБРА 2010.   ГОДИНЕ, ЗАВРШИО-ЛА ЈЕ СТУДИЈЕ НА
ФИЗИЧКОМ ФАКУЛТЕТУ УНИВЕРЗИТЕТА У БЕОГРАДУ, НА
СТУДИЈСКОЈ ГРУПИ   ФИЗИКА
СА ОПШТИМ УСПЕХОМ 8,26 (ОСАМ И 26/100   ) У ТОКУ СТУДИЈА И
ОЦЕНОМ 10 (ДЕСЕТ   )   НА ДИПЛОМСКОМ ИСПИТУ.

НА ОСНОВУ ТОГА ИЗДАЈЕ МУ-ЈОЈ СЕ ОВА ДИПЛОМА О СТЕЧЕНОМ ВИСОКОМ
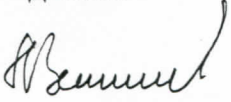ОБРАЗОВАЊУ И СТРУЧНОМ НАЗИВУ

ДИПЛОМИРАНИ ФИЗИЧАР ЗА ПРИМЕЊЕНУ ФИЗИКУ И ИНФОРМАТИКУ

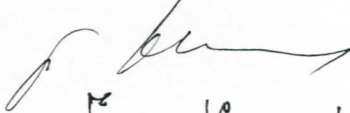РЕДНИ БРОЈ ИЗ ЕВИДЕНЦИЈЕ О ИЗДАТИМ ДИПЛОМАМА 2116/2010

У БЕОГРАДУ,   30. ДЕЦЕМБРА 2010.   ГОДИНЕ

ДЕКАН

ПРОФ. ДР Љубиша Јовковић

РЕКТОР

ПРОФ. ДР Бранко Ковачевић

УНИВЕРЗИТЕТ У БЕОГРАДУ
ФИЗИЧКИ ФАКУЛТЕТ
Бр. 41/5
10.5. 20 19 год.
БЕОГРАД СТУДЕНТСКИ ТРГ 2-12
П. ФАХ 44

ПОТВРДА

Овим се потврђује да је КОСТА СПАСИЋ, дипломирани физичар, пријавио Наставно-научном већу Физичког факултета докторску дисертацију под називом: "ДИЈАГНОСТИКА АСИМЕТРИЧНОГ И ПЛАН ПАРАЛЕЛНОГ РАДИО-ФРЕКВЕНТНОГ ПЛАЗМА СИСТЕМА У ЦИЉУ ДЕФИНИСАЊА ПЛАЗМА ХЕМИЈСКИХ ПРОЦЕСА ТОКОМ ТРЕТМАНА УЗОРАКА ОРГАНСКОГ И НЕОРГАНСКОГ ПОРЕКЛА".

Наставно-научно веће је на својој седници одржаној 27. марта 2019. године прихватило предложену тему и за ментора именовало др Невену Пуач, научног саветника Института за физику.

Београд, 19.5.2019.

ДЕКАН ФИЗИЧКОГ ФАКУЛТЕТА

Проф. др Иван Белча